Characterization of the Esp signalosome: Two hybrid histidine kinases utilize a novel signaling mechanism to regulate developmental progression in *Myxococcus xanthus*.

Dissertation

Zur Erlangung des Doktorgrades der Naturwissenschaften

(Dr. rer. nat.)

Dem Fachbereich Biologie

der Philipps-Universität Marburg

vorgelegt von

Andreas Schramm

aus Mechernich-Schaven

Marburg (Lahn), Oktober 2012

Characterization of the Esp signalosome: Two hybrid histidine kinases utilize a novel signaling mechanism to regulate developmental progression in *Myxococcus xanthus*.

Dissertation

Zur Erlangung des Doktorgrades der Naturwissenschaften

(Dr. rer. nat.)

Dem Fachbereich Biologie

der Philipps-Universität Marburg

vorgelegt von

Andreas Schramm

aus Mechernich-Schaven

Marburg (Lahn), Oktober 2012

Die Untersuchungen zur vorliegenden Arbeit wurden vom August 2009 bis Juni 2012 am Max-Planck-Institut für Terrestrische Mikrobiologie unter der Leitung von Dr. Penelope I. Higgs durchgeführt.

Vom Fachbereich Biologie der Philipps-Universität Marburg (HKZ: 1180) als Dissertation angenommen am: _____

Erstgutachter: Prof. Dr. Lotte Søgaard-Andersen
Zweitgutachter: Prof. Dr. Erhard Bremer

Weitere Mitglieder der Prüfungskommission:
Prof. Dr. Andrea Maisner
Prof. Dr. Hans-Ulrich Mösch

Tag der mündlichen Prüfung: _____

Im Zusammenhang mit der vorliegenden Promotion wurden folgende Originalpublikationen veröffentlicht:

A. Schramm, B. Lee, and P.I. Higgs, **Intra- and Interprotein Phosphorylation Between Two-Hybrid Histidine Kinases Controls *Myxococcus xanthus* Developmental Progression.** J Biol Chem, 2012. **287**(30):25060-72.

Lee B, Schramm A, Jagadeesan S, Higgs PI., **Two-Component Systems and Regulation of Developmental Progression in *Myxococcus xanthus*.** Methods Enzymol, 2010. **471**: p. 253-78.

Ich versichere, dass ich die vorliegende Dissertation unter dem Titel:

“Characterization of the Esp signalosome: Two hybrid histidine kinases utilize a novel signaling mechanism to regulate developmental progression in *Myxococcus xanthus*.“

Selbstständig und ohne unerlaubte Hilfe angefertigt und mich dabei keiner anderen als der mir ausdrücklich bezeichneten Quellen und Hilfen bedient habe. Die Dissertation wurde in der jetzigen oder einer ähnlichen Form noch bei keiner anderen Hochschule eingereicht und hat noch keinen sonstigen Prüfungszwecken gedient.

Marburg (Lahn), den _____ _____

Andreas Schramm

Für meine Eltern

ABSTRACT

Histidine-aspartate signaling systems are used by bacteria, archaea and eukarya to integrate stimuli over time and space generating coordinated, fine-tuned cellular responses. A hallmark feature is the high modularity of the signaling protein modules which can form simple ’two-component‘ systems, and also sophisticated ’multi-component’ systems. The deltaproteobacterium *Myxococcus xanthus* contains a large repertoire of signaling proteins, many of which regulate its complex multicellular developmental program. In this respect, one important systems is the Esp signaling system, consisting of the hybrid histidine protein kinase, EspA, two serine/threonine protein kinases (PktA5 and PktB8), and a putative transport protein (EspB).

In the presented study, I assign an orphan hybrid histidine protein kinase, EspC, to the Esp signaling system which negatively regulates progression through the *M. xanthus* developmental program. The genetic analysis revealed that EspC is an essential component of this system, because Δ*espA*, Δ*espC*, and Δ*espA*Δ*espC* double mutants shared an identical early developmental phenotype. Surprisingly, disruption of EspC’s auto-phosphorylation *in vivo* did not produce a mutant developmental phenotype, whereas substitution of its phospho-accepting residue within the receiver domain resulted in the null phenotype. Furthermore, it is shown that although the EspC histidine kinase could efficiently autophosphorylate *in vitro*, it did not act as a phospho-donor to its own receiver domain. Instead, both, *in vitro* and *in vivo* analyses elucidated that the phospho-donor instead is EspA’s histidine kinase. Therefore, EspA and EspC participate in a novel hybrid histidine protein kinase signaling mechanism involving both inter- and intraprotein phosphotransfer. This inter- and intraprotein phosphotransfer results in the combined phosphorylation of EspA’s and EspC’s receiver domains which represents the output of the Esp signaling system. Further genetic analyses suggested that this Esp system is regulated on the level of its phosphatase activity, likely involving the sensing domains of EspC for regulation. Finally, I uncovered that the Esp system stimulates the proteolytic turnover of MrpC, a crucial transcription factor of the developmental program, via as yet unidentified serine protease.

Altogether, these data unravel a novel signaling mechanism of His-Asp signaling systems, and thus expand the knowledge about the complexity and plasticity of these crucial signal transduction systems.

ZUSAMMENFASSUNG

Histidin-Aspartat Signaltransduktionssysteme werden von Bakterien, Archaeen sowie Eukaryoten verwendet, um Signale zu integrieren und weiter zu verarbeiten, um auf diese Weise eine koordinierte und gut abgestimmte zelluläre Antwort hervorzurufen. Ein Charakteristikum dieser Systeme sind ihre hoch modularen Signalübermittlungsmodule, welche sowohl einfache „Zweikomponentensysteme“ als auch komplexe „Multikomponentensysteme“ bilden können. Das Deltaproteobakterium *Myxococcus xanthus* besitzt eine beträchtliche Anzahl solcher Signaltransduktionsproteine, von denen viele in der Regulation seines komplexen, multizellulären Entwicklungszykluses involviert sind. Eines dieser Signaltransduktionssysteme ist das Esp-System, welches aus der Hybridhistidinkinase, EspA, zwei Serin/Threonin-kinasen (PktA5 und PktB8) und einem hypothetischen Transportprotein (EspB) besteht.

Mit der vorliegenden Studie ordne ich dem Esp-System eine weitere Hybridhistidinkinase zu, EspC, welche in der Lage ist, den Ablauf des Entwicklungsprogrammes zu verlangsamen. Die genetischen Studien zeigten auf, dass EspC eine essentielle Komponente des Esp-Systems ist, da die Deletionsmutanten Δ*espA*, Δ*espC* und auch die Doppelmutante Δ*espA*Δ*espC* den gleichen verfrühten Phänotyp bezüglich des Ablaufes des Entwicklungsprogrammes zeigen. Überraschenderweise führte das Blockieren der Autophosphorylierung von EspC *in vivo* zu keinem Defekt des Entwicklungszyklusses, wohingegen der Austausch des phosphatempfangenden Aspartats in der Empfängerdomäne von EspC den gleichen Effekt hatte, wie die vollständige Deletion von EspC. Des Weiteren wurde deutlich, dass obgleich die Kinasedomäne von EspC eine effiziente Autophosphorylierung *in vitro* zeigte, sie hingegen nicht dazu fähig war, Phosphatgruppen auf die Empfängerdomäne von EspC zu übertragen. Stattdessen konnte sowohl in *in vivo* als auch *in vitro* Analysen gezeigt werden, dass die Kinasedomäne von EspA Phosphatgruppen auf die Empfängerdomäne von EspC übertragen kann. Aus diesen Gründen postuliere ich, dass EspA und EspC einen bisher unbekannten Signaltransduktionsmechanismus verwenden, der sowohl inter- als auch intraproteinogene Phosphorylierung beinhaltet. Der Effekt dieses Mechanismus ist die Phosphorylierung beider Empfängerdomänen, der von EspA und EspC. Weitere genetische Analysen ließen zudem vermuten, dass die zelluläre Antwort des Esp-Systems auf der Ebene der Phosphataseaktivität reguliert wird, welche eventuell durch die Sensordomänen von EspC moduliert wird. Abschließend fand ich heraus, dass das Esp-System den proteolytischen

Verdau des zentralen, entwicklungsspezifischen Transkriptionsfaktors MrpC über eine noch nicht identifizierte Protease reguliert.
Zusammengefasst legen diese Daten einen neuen Signaltransduktionsmechanismus innerhalb der Histidin-Aspartat Signaltransduktionsfamilie offen und erweitern damit die Kenntnisse über die Komplexität und Plastizität dieser essentiellen Systeme.

TABLE OF CONTENT

1. INTRODUCTION

Signal transduction is a central part of life because organisms that can rapidly respond to changes in the environment have a great selective advantage. Bacteria utilize a broad variety of signaling mechanisms, such as one-component systems, second messenger signaling (*i.e.* cyclic-di-GMP signaling and cyclic-AMP signaling) and eukaryotic like protein kinases [1]. The by far most important signaling mechanisms involve histidine-aspartate (His-Asp) signaling systems (often termed two-component systems, reviewed in [2]). These systems involve histidine kinases (HK) and response regulators (RR) which are the second most abundant signaling proteins used by bacteria [3]. Even though one-component systems outnumber His-Asp signaling systems, the latter are indispensable for the perception and the response to changes in the environment. In this respect it is worth noting that HKs and RRs are not exclusively used for signal transduction by bacteria, instead they can be found in all three domains of life [4]. It is proposed that the abundance of His-Asp signaling systems is dependent on the ecological niche of the respective organism [5]. Thus, organisms that face changing environmental conditions or that have unusual and complex life styles utilize more of those signaling systems than organism that live e.g. in a static, non changing environment. Additionally, it seems that organisms which underlie complex physiological conditions more often utilize sophisticated modifications of the basic His-Asp signaling scheme (discussed below) [6].
In the last two decades a lot of progress was made towards understating the principles underlying the regulatory processes that are controlled via His-Asp signaling systems. And in the last few years several novel aspects of these signaling systems were elucidated and it became more and more evident, that His-Asp signaling systems function as highly sophisticated regulatory machines which in part are still only poorly understood.

1.1 Signal transduction via histidine – aspartate signaling (*aka* Two-component systems)

The prototypical ‘two-component’ system is comprised of a sensor histidine protein kinase (HPK) and a response regulator (RR) protein which transfer signals between each other via a phosphotransfer event (reviewed in [2], **Figure 1**). The HPK generally contains a variable sensing domain (In) and a histidine kinase region (HK). Most RRs are also composed out of

two domains, a receiver domain (REC) and a variable output domain (Out). Upon signal perception of the histidine kinase, the γ-phosphoryl group from an ATP molecule is transferred onto the HPK which then serves as a phosphoryl donor for the RR. Phosphorylation of the REC results in a conformational change in the output domain, thereby modulating the signaling state of the 'two-component' system.

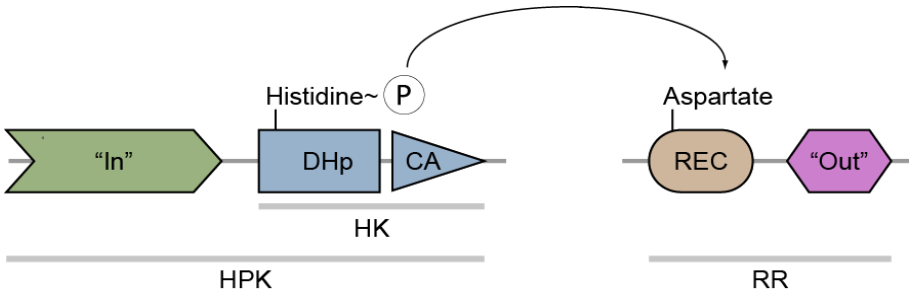

Figure 1 Scheme of a prototypical His-Asp signaling 'two-component' system. A stimulus sensed by the input domain (In) causes a change in the phosphorylation level of the histidine kinase region (HK). The phosphorylated histidine protein kinase (HPK) then donates a phosphoryl group in a linear phosphotransfer to the receiver domain (REC) of the response regulator (RR). Phosphorylation of the REC then modulates the activity of the RR output domain (Out). DHp, dimerization and histidine phosphotransfer domain; CA, histidine kinase like ATPase domain.

1.1.1 Conserved transmitter regions build the signaling core

Both, the HPK and the RR generally have a variable and a conserved protein part. The conserved parts are the actual signal transmitter regions which mediate the phosphorylation events that connect the HPK and the RR (reviewed in [2]). These transmitter regions are the HK region in the HPK and the REC domain in the RR.

The histidine kinase region is the catalytic core of the HPK

The conserved histidine protein kinase core consists of two domains, the DHp and the CA domain which are collectively referred to as histidine kinase region (HK) ([7], **Figure 2**). These two domains together conduct the initial step in the signal transduction of His-Asp phosphorelay systems, HPK autophosphorylation. Due to this functional relationship of the CA and the DHp domain, they are described together in the following section. The DHp domain is strongly conserved on the level of primary amino acid sequence [8], and has a characteristic protein fold of a two α-helix bundle [9, 10]. It mediates four major functions within a HPK. (1) DHp domains are reported to confer specificity towards its cognate RR [11, 12]. (2) They can harbor phosphatase activity to regulate the signaling state of the His-Asp signaling system [13, 14]. Because of the important implications for this study, these

two functions (1 and 2) will be introduced in later sections in more detail. (3) The DHp domains generally mediate homodimer formation of HPKs [15, 16]. Only few exceptions are known in which HPK do not form homodimers; the histidine kinases RetS and GacS of *Pseudomonas aeruginosa* and Etr1 and Etr2 from *Arabidopsis thaliana* are reported to form heterodimers instead [17-19]. (4) The by far most important function of DHp domains is their ability to autophosphorylate on a conserved histidine residue [7, 20]. There are rare exceptions known, for example the HK DivL from *C. crescentus* phosphorylates a tyrosine residues instead [21].

Autophosphorylation, the initial step in signal transduction by His-Asp phosphorelay systems, is mediated by the CA domain and generally occurs in trans [22]. Trans-phosphorylation means that the CA domain of one HK molecule phosphorylates the histidine in the second HK molecule of one dimer, and vice versa. However, trans-autophosphorylation seems not to be universal for HKs, because cis-autophosphorylation has recently been described for PhoR from *Staphylococcus aureus* and HK853 from *Thermotoga maritima* [23].

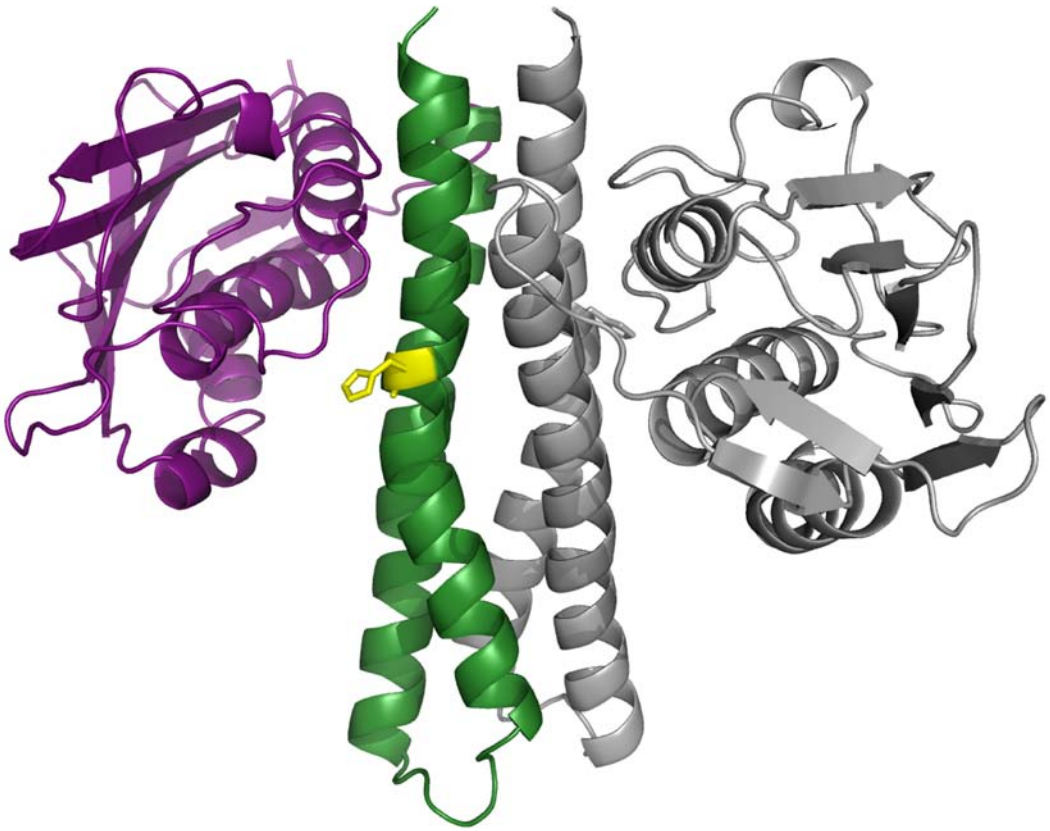

Figure 2 Molecular structure of a TMHK853 HPK dimer. One HPK molecule consists of a CA domain (purple) and a DHp domain (green). The second HPK molecule (grey) interacts with the first trough the DHp domain. The invariant histidine residue is highlighted yellow. The displayed model is based on the PDB files 3dgeA and 3dgeB [23].

The CA domain of HKs shares structural similarity to the ATPase domain of GyraseB, Hsp90 and MutL which is a $\alpha_3\beta_5$ core globular fold [24, 25]. ATP binding and subsequent hydrolysis serve as the energy source for the function of GyraseB to unwind DNA, of Hsp90 to confer *de novo* protein folding and of MutL to repair DNA [26-28]. ATP binding is mediated by specific amino acids that lie in four boxes (N, G1, F, G2) that [9, 29]. These homology boxes, together with the H-Box in the DHp domain, additionally serve for the classification of HPKs [30]. How exactly the phosphorylation of the invariant histidine residue in the DHp domain, catalyzed by the CA domain, occurs, is not yet fully understood [31]. In the few solved crystal structures of complete HK, the CA domain with bound ATP is too distal for γ-phosphoryl transfer to the invariant histidine residue in the DHp domain [16, 23, 32]. However, a recent analysis suggests a model in which conformational changes of the sensing domain(s) induce 'cracking' of the DHp α_2-helix which then allows contact between the CA domain and the invariant histidine residue [31]. An additional subject of debate is how the CA domain becomes activated; it is proposed that ligand binding via the HPK sensing domains mediates activation of the CA domain [33]. Further it is proposed that the sensing domains regulate the positioning of the CA domain with respect to the invariant His residue [34], thus allow or prevent the autophosphorylation.

The receiver domains is the catalytic core of the RR

The RR CheY from *Salmonella typhimurium* is by far the best studied RR; as it lacks any output domain, it resembles a REC domain. Its structure (and also the structure of other REC domains) is composed of a five stranded parallel β-sheet which is surrounded by five α-helices ([35], **Figure 3**). REC domains generally catalyze the transfer of a phosphoryl group from the phosphorylated histidine residue of their cognate HPK [36-38]. The site of phosphorylation within the REC, the invariant aspartate residue, resides in an acidic pocket between the tips of the α-helices [35]. Additionally, several REC domains can also use small organic phospho-molecules as phosphoryl donors, *e.g.* acetyl phosphate or carbamoyl phosphate [39]. Phosphorylation of the invariant aspartate residue subsequently induces a conformational change at the α4-β5-α5 interface of the RR [40, 41]. This conformational change either modulates the RR effectors domain interaction, for example with other proteins or the DNA [42-45], or it influences the dimerization state of two REC domains [46, 47] which then modulates the output state of the RR.

Figure 3 Molecular structure of the TMRR468 REC domain from *T. maritima*. The conserved fold of a REC domain is a five stranded parallel β-sheet which is surrounded by five α-helices. The invariant aspartate residue (yellow) lies in the center of a pocket built by the alpha helices. The structure is based on the PDB files 3dgeC [23].

1.1.2 His-Asp signaling systems are enormously versatile

As a general trend, the number of His-Asp signaling genes, is proportional to the square of the genome size [3]. Some organisms harbor hundreds of His-Asp signaling systems, most of which are totally different in their system design. A SMART architecture query [48, 49] identified more than 42 000 proteins containing a DHp domain, in the non redundant protein database (2012-10-02), and a genome survey from M.Y. Galperin revealed that more than 70 000 protein sequences contain a REC domain [50].

Linage specific expansion (LSE) and horizontal gene transfer (HGT) and are thought to be the major driving force in the evolution of His-Asp signaling systems. Interestingly, LSE is often accompanied with domain shuffling; which consequently leads to a broad variety of differently designed His-Asp signaling systems [5]. These variations often involve the N-terminal sensing domains of HPK. As depicted in **Figure 1**, a HPK often contains a sensing region, involving one or more variable sensing domains [51]. Thus it is not surprising, that a broad variety of sensing domains have been found associated with HPKs; the Microbial Signal Transduction Database lists 95 input domains (MiST2; [52]).

In addition to the variability in HPK, also RRs display a broad variability in their associated output domains, connected to the REC domain. In fact, 117 different output domains are listed in the MiST2 database [52]. These many distinct levels of diversity will be further described in the following sections.

Sensing domains

Sensing domains determine the kind of stimuli to which a His-Asp signaling system responds to. They can be grouped into three broad classes, depending on where they receive their signals. (a) Signals from the outside of the cell (Gram +) or the periplasm (Gram -), (b) signals involving sensing mechanism inside of the cytoplasmic membrane, and (c) signals from the cytoplasm [51]. Many HPK sensing domains are membrane associated; two third of all HPKs contain trans-membrane segments [3]. However, it should be noted that a trans-membrane segment in a HPK is not necessarily also a sensing domain; they might instead just be necessary to anchor the HPK in the cytoplasmic membrane. Importantly, the type of sensing domain does not necessarily reveal whether the signal is extra- or intracellular. For instance, PAS domains (introduced in more detail below) can be found in soluble HPK as well as associated with membrane bound HPK. If they are associated with membrane bound HPK, they can be located in the cytoplasm or the periplasm, thereby mediating responses to extracellular, membrane associated as well as intracellular signals [53]. In *E. coli*, only three out of the 29 HPKs lack any sensing domain [52], one of which (RcsC) is reported to receive signals from an auxiliary membrane protein [54]. The great versatility and high number of HK-associated sensing domains illustrates the importance of these domains for His-Asp signaling systems. However, the exact mechanism of how the sensing domains receive, integrate and transfer the signals within the HPK are still only poorly understood [51]. A discussion of all the characterized sensing domains would be beyond the scope of this thesis; instead, I want to focus on a description of the sensing domains that are relevant for the later sections of this study: MASE1, FHA and PAS domains.

MASE domains

MASE (membrane associated sensor) domains were identified in the course of a genome survey by Nikolskaya *et al.*, and further defined by bioinformatic prediction programs and multiple sequence alignments [55]. They can be divided into the MASE1- and the less abundant MASE2- domains; the protein family (PFAM) database lists 1 536 MASE1 domains, and 323 MASE2 domains (2012-09-19, [56]). MASE1 domains are predominantly found in bacteria, but can also be identified in few eukaryotic genomes [56]. These domains contain eight predicted transmembrane segments and are commonly associated with GGDEF, GGDEF-EAL and PAS domains. Since they were found linked to several different signal output domains, it was proposed that these evolutionary conserved

mobile domains likely contribute to the signaling in these systems [57]. Multiple sequence alignments then revealed several conserved amino acids that are assumed to be crucial for the MASE1 domain function [55], but a detailed characterization of the putative MASE1 sensing mechanism is so far lacking. M.Y. Galperin suggested that the signals may be aromatic compounds [57], controversially, there is some indirect evidence for MASE1 domains to be involved in the perception of sugars. The *E. coli* HPK UhpB which is involved in glucose-6-phosphate metabolism and transport, contains a MASE1 domain as its sole sensing domain, and a genetic analysis of UhpB showed that glucose-6-phosphate binding activates the autophosphorylation of UhpB [58]. However, detailed experimental studies of the involvement of the MASE1 domain in the glucose-6-phosphate signaling have not been made by now.

Thus far, MASE2 domains have been exclusively identified in bacteria, and the majority is found in the gammaproteobacteria [56]. These domains contain six predicted transmembrane segments and are commonly associated with adenylate cylcases and GGDEF-EAL output domains [55]. As with MASE1 domains, the function and the putative signals sensed by the MASE2 domain are unknown so far.

FHA domains

FHA (Forkhead associated) domains were originally discovered as a conserved domain that was associated with DNA binding motifs belonging to the eukaryotic group of forkhead family proteins [59]. These early identified proteins all shared one common property; they all functioned in the nucleus. Therefore, it was proposed that FHA domains mediate binding to specific nuclear components. However, it was subsequently realized that FHA domains can be additionally found in proteins which are not involved in DNA binding (*e.g.* the protein phosphatase KAPP from *A. thaliana* [60]). This observation led to the hypothesis that FHA domains do not bind one specific partner protein, but are instead involved in binding a larger group of proteins sharing a conserved binding motif. Accordingly, it was demonstrated later that protein binding by the KAPP FHA domain is mediated via interaction with a phosphorylated threonine residue in the partner protein RLK (receptor like kinase) [61]. The analysis of other FHA domain proteins revealed that this mode of interaction is universal for FHA domains [62]. Considering the structure of these FHA domains, they all share a conserved protein fold of 11 β-sheets forming a sandwich in which extended flexible loops between the sheets contain the residues that are important for the target protein interaction [63, 64].

A SMART architecture query [48, 49] of the non-redundant protein database identified 5 145 FHA domain containing proteins (2012-08-16) which can be found in all three domains of life and are distributed as follows: ~51 % in eukaryotes, ~48 % in bacteria and <1 % in archaea. Remarkably, only in 17 instances a FHA domain was associated with a HPK and, interestingly, this combination can only be found in bacteria.

PAS domains

PAS (Period Arnt Sim) domains were identified by sequence homology to the Drosophila proteins Period and Single-minded (Sim) and the vertebrate aryl hydrocarbon receptor nuclear transporter (ARNT) [65, 66]. A SMART domain architecture query [48, 49] revealed 29 283 PAS domains (2012-08-16), the vast majority (~84 %) of which could be identified in bacterial genomes. PAS domains display only a weak primary amino acid sequence conservation but all share a characteristic protein fold comprised of an antiparallel five stranded β-sheet with four α-helices flanking the sheets [67, 68]. PAS domains can sense a versatile array of signals; thereby the binding of small molecules or ions can either be a direct signal or serve as a cofactor for the perception of other signals (*e.g.* gases, light or the redox potential (reviewed in [53])).

PAS domains generally form dimers or higher order oligomers. Prokaryotic PAS domains preferentially form homo-oligomers, whereas eukaryotic PAS domains can form both homo- and hetero-oligomers [69-71]. It is thought that signal perception by PAS domains modulates the quaternary structure of the oligomers (reviewed in [68]), and these changes then modulate the output in the signaling protein [68]. Specifically, changes in the quaternary structure of the PAS-A domain in the *B. subtilis* HPK KinA was shown to regulate the kinase activity of KinA [72-74]. This theme of signal integration might be universal, since it was possible to generate an artificial fusion protein, in which a blue light sensitive PAS domain regulated a non-PAS-related output domain [72, 75].

In addition to modulation of kinase activity (*e.g.* in the *B. subtilis* HPK KinA), PAS domains have also been reported to modulate phosphatase activity of bifunctional HPKs [76]. These observations illustrate that the means by which the output of a regulatory system is modulated is dictated by the associated functional domain, rather than by the PAS domain.

Output domains

As indicated above, REC domains can be combined with a broad variety of output domains (**Figure 4**). In general, 83 % of all RR contain an output domain, and those can be grouped into more than 1 700 different domain architectures [50]. Approximately 65 % of all RR contain a DNA binding domain [50, 77]. Other common outputs are involved in RNA binding, phosphorelays, c-di-GMP signaling, protein Ser/Thr phosphorylation and protein binding [50].

Another very interesting class of RRs lack any output domain; they are called single domain (sd) RRs. sdRRs comprise the second largest group of RRs , ~17 % of all bacterial RRs and ~50 % of the archaeal RRs are sdRRs [50]. In certain archaeal genomes (*e.g. Archaeoglobus fulgidus*, *Methanococcus aeolicus*, and *Nitrosopumilus maritimus*) the number of sdRRs can reach up to 90 – 100 % [78]. For most of the sdRR it is not known how they function to mediate signal output, but for some few groups the mechanism of their function is understood. For instance, the Spo0F type sdRRs are involved in multistep phosphorelays [79, 80]. Another well characterized class are the CheY like sdRRs. In *E. coli*, CheY modulates flagella rotation by direct binding to the flagella machinery proteins FliM and FliN [40, 81]. Additionally, in *C. crescentus*, two specific sdRRs are well characterized. The sdRR DivK which regulates its own localization as well as the autophosphorylation of its cognate kinase DivJ [82], and the sdRR CpdR which recruits the protease ClpXP to the stalked cell pole during cell cycle progression [82]. Importantly, in all instances, the signal output of sdRRs is mediated by direct protein-protein interaction.

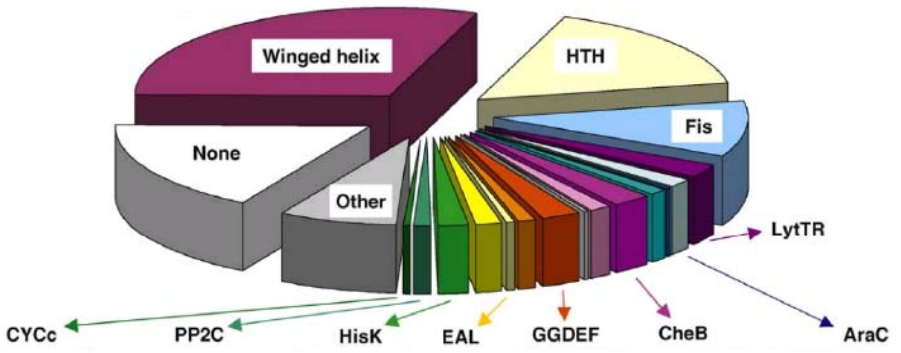

Figure 4 Distribution of output domains in RRs. RRs from 896 sequenced organisms were grouped depending on their associated output domain. Figure modified from [50].

1.1.3 Alternative system design expands the plasticity of His-Asp signaling systems

In addition to the variability of the different sensing and output domains, the plasticity of His-Asp signaling systems can be further enhanced by rearranging signal transmission modules. A common example are hybrid histidine kinases (HyHPKs), in which a REC domain is fused to a HPK. Multistep phosphorelay systems are another common variation of the "two component" paradigm. Here, the signal transmitting regions are further extended by the addition of a histidine containing phosphotransfer (HPT) protein/domain which shuttles the phosphoryl groups between a HPK/HyHPK and a terminal RR.

Multistep phosphorelays His-Asp signaling systems

HPT proteins can either be stand alone proteins, or they can be attached to a HyHPK. In a multistep phosphorelay system, many HPK can 'feed' signals via one single HPT protein to one terminal RR (Many-to-One, reviewed in [11]). Alternatively, signals from one HPK can be disseminated onto several terminal RR (One-to-Many). This integration and dissemination adds another level of plasticity to the His-Asp signaling scheme.

The first phosphorelay system was identified in *B. subtilis*, involved in the initiation of sporulation [83]. In this system, several HPKs 'feed' phosphoryl groups onto the sdRR Spo0F, these phosphoryl groups subsequently become transferred to the master regulator RR Spo0A via a HPT protein, Spo0B ([73, 83, 84], **Figure 5**).

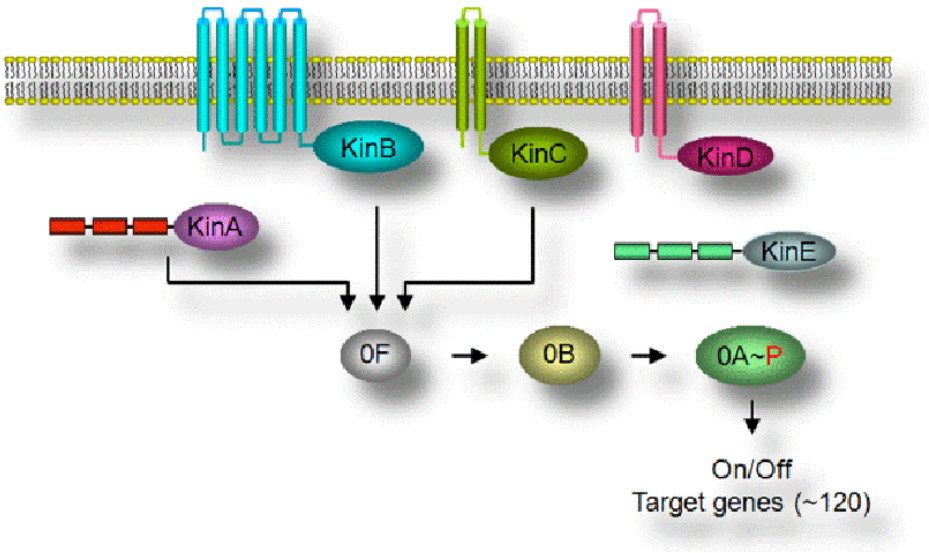

Figure 5 Scheme of the phosphorelay regulating sporulation in *B. subtilis*. The HPKs KinA, KinB and KinC together phosphorylate the sdRR Spo0F. Phosphoryl groups then are shuttled to the terminal RR Spo0A via the HPT protein Spo0B. Spo0A then controls the expression of sporulation specific genes. The scheme was made from the Fujita Lab and modified (http://bchs.uh.edu/~mfujita/index.php/research).

HPT proteins/domains structurally resemble a DHp domain dimer (four helix bundle), however, they can exist as monomers (ArcB HPT, CheA P1) as well as dimers (Spo0B) [85-87]. Generally, these proteins are difficult to identify because of their low sequence conservation [88, 89]. However, they all harbor an invariant histidine residue for phosphorylation, but do not bear kinase or phosphatase activity [90].

Multistep phosphorelay systems are thought to display more sites of regulation [2, 6, 91], which presumably enables the integration of complex signals as well as the generation of very fine tuned responses. With the example of phosphorelay systems it becomes evident that the sophisticated wiring of His-Asp signaling proteins enables the formation of complex signaling machineries.

Hybrid histidine protein kinases

HyHPKs are also a product of the inherent plasticity of His-Asp signaling systems. They resemble a HPK with a fused REC domain (**Figure 6**). In *Xanthomonas* ssp., it was shown that a HyHPK was formed by fusion of an ancestral HPK-RR pair, most probably by the loss of a stop codon [92]. HyHPKs are no rare exception of the general 'two component' scheme, a SMART domain architecture query [48, 49] revealed that out of the ~42 000 proteins contain a DHp domain, ~12 000 additionally contain a REC domain (2012-10-03). Generally, HyHPKs participate in multistep phosphorelay systems (reviewed in [2] and [78]). A well-studied example is the anaerobic redox control (Arc) system in *E. coli*. This ArcA/ArcB His-Asp phosphorelay system mediates oxygen dependent transcription [93, 94], by the regulation of a large repertoire of genes (>1 000) under anoxic and microoxic conditions [95].

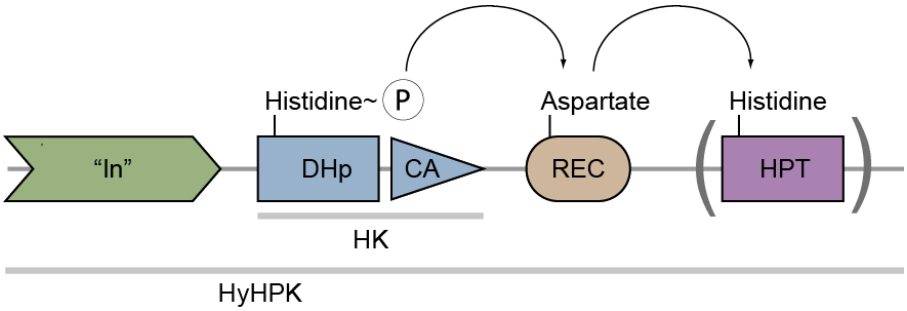

Figure 6 Scheme of a prototypical HyHPK. A stimulus sensed by the input domain (In) causes a change in the autophosphorylation level of the histidine kinase region (HK). The hybrid histidine protein kinase (HyHPK) then donates a phosphorylgroup to the internal receiver domain (REC). Often the phosphorylgroup is then further transferred to a histidine containing phosphor transfer (HPT) domain within the HyHPK which generally shuttles the phosphorylgroup to a terminal RR. The HPT region can also be located in a separate protein. DHp, dimerization and histidine phosphotransfer; CA, histidine kinase like ATPase.

Arc system signal transduction involves autophosphorylation of the invariant histidine 292 in the DHp domain, transfer to an internal aspartate 576 in the REC domain and further transfer to the histidine 717 of the HPT domain in the HyHPK ArcB [96, 97]. The phosphorylated histidine 717 ArcB then serves as phosphoryldonor for ArcA, leading to the phosphorylation of the aspartate 54. This mode of operation is the paradigm of how a HyHPK functions in His-Asp signaling systems; in fact, the majority of the analyzed HyHPK behave in this manner. The HPT protein, however, has not necessarily to be a part of the HyHPK. In the Lux system of *Vibrio harveiy* which is mediating quorum sensing, the HPT protein is present as a standalone protein (reviewed in [98]).

The REC domains in HyHPKs can act analogously to sdRRs, meaning they can mediate signal output via protein-protein interaction. One such example is the HyHPK FrzE of *M. xanthus* which is composed out of a HPT domain, a HK region and two REC domain [99]. While one REC domain mediates the phosphorylation of another RR (FrzZ), the second REC domain in FrzE, does not contribute to the phosphorylation of FrzZ, instead it fulfills a crucial regulatory function by inhibiting the HK of FrzE [99, 100]. This example illustrates that a HyHPK can not only act in phosphorelays involving a HPT protein, additionally they can directly mediate and/or modulate signal output.

1.1.4 Tuning of His-Asp signaling systems by phosphatase activity

Phosphatase activity was first described in the mid 1980s for the HK NtrB of *Escherichia coli* [13]. This study demonstrated that differential regulation of certain nitrogen responsive promoters is due to the differential activity of NtrB which switches between a phosphatase and a kinase in response to nitrogen [13, 101, 102]. Although HK mediated acyl phosphatase activity was discovered early on, the mechanism of the underlying biochemical reaction is still poorly understood and remains controversially discussed. However, it was observed early on that the CA domain contributes to the phosphatase activity of bifunctional HPKs [103-106]. For instance it was shown for the *E. coli* HPK, EnvZ, that the DHp domain possesses phosphatase activity, but full phosphatase activity was dependent on the presence of the CA domain and on the ADP concentration [103]. Interestingly, the first crystal structure of a HK_2-RR_2 complex (consisting of a dimer of the *T. maritima* HK, HK853, and a dimer of its cognate RRs, RR468), indicated that the conserved histidine residue in the *T. maritima* HK853 could plays an essential role in the phosphatase activity. This was proposed, because it lies in the optimal position to coordinate a water molecule

which might initiate hydrolysis of the phosphoryl group on the aspartic residue of the RR [23]. In contrast, several other studies demonstrated that the conserved histidine in the DHp domain of the HPK is not required for phosphatase activity [13, 107-111], although the effect of mutations in the invariant histidine residues on the phosphatase activity differed depending on which amino acid is substituted was analyzed. For example, a histidine to alanine substitution did not affect the phosphatase activity of CckA from *Caulobacter crescentus* [110], whereas in EnvZ of *E. coli* this substitution slightly reduced the phosphatase activity [108]. Interestingly, there are also reports of histidine substitution mutations that elevated phosphatase activity in certain HPK. In the HPKs VanS from *Enterococcus faecium* and NarX from *E. coli* a histidine to glutamine substitution resulted in higher phosphatase activity than in the wild type versions of the proteins [107, 111]. Therefore, the challenge is still to define the 'phosphatase site' in a HK. By comparative sequence analysis, a motif ([H]DXXXQ) has been identified that is conserved in the HisKA_3 subfamily of DHp domains and is positioned adjacent to the conserved phospho-accepting histidine ([H]) in the DHp domain ([111], **Figure 7**).

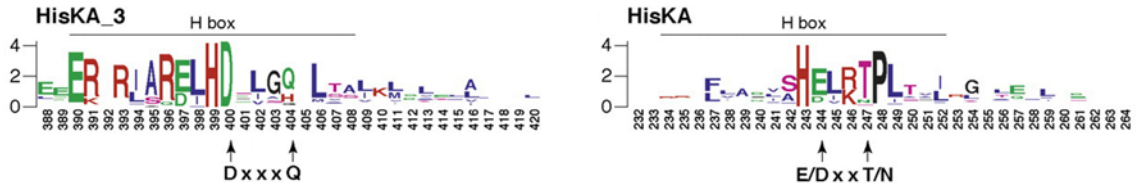

Figure 7 Sequence conservation of the H-box regions in HisKA_3 and HisKA type DHp domains. The sequence logos are modified from [111]. The HisKA_3 logo was generated from 70 different sequences. The HisKA logo shown was generated from 36 different sequences.

In the same study it was experimentally proven that the glutamine residue (Q) is essential for the phosphatase activity of NarX. The described motif is missing in the HisKA subfamily of DHp domains which comprises the biggest subclass among all DHp domains. Instead a $[H]^{E}/_{D}XX(X)^{N}/_{T}$ motif has been identified in the HisKA subfamily that is reminiscent of the EXXN motif reported for the auxiliary phosphatase, CheX from *Borrelia burgdorferi* [111, 112]. However, detailed and systematic analysis exploiting the importance and universality of this proposed phosphatase motif are so far lacking.

Not only the 'site' of phosphatase activity, but also the regulation of phosphatase activity remains to be elucidated. For the bifunctional HPK VanS, it was proposed that the oligomeric state of the HPK mediates the switch between kinase and phosphatase activity [107]; however, experimental data supporting this hypothesis is so far lacking. Interestingly, PAS domains, which often regulate the HPK kinase activity, seem also to

have regulatory function on HPK phosphatase activity in other systems. It was recently shown in *Streptococcus pneumonia* that the PAS domain of the HPK WalK regulates its phosphatase, but not kinase, activity [76].
Altogether, how exactly the phosphatase activity within bifunctional HPK functions, remains to be one of the major questions in the His-Asp signal transduction research field.

1.1.5 Specificity between histidine protein kinases and cognate response regulators

Almost all bacteria contain His-Asp signaling genes, although the number of genes encoding for these systems varies greatly; *Mycoplasma genitalium* G37 does not encode for any, *Tropheryma whipplei* str. Twist encodes for only four (2 HPKs and 2 RRs) and *Ktedonobacter racemifer* DSM 44963 encodes for 366 His-Asp signaling genes (190 HPKs, 2 HyHPKs, 167 RRs) [52]. Remarkably, unwanted 'cross talk' seems not to happen *in vivo* (reviewed in [11]), because each signaling system is generally buffered from this crosstalk. For example the HPK VanS can phosphorylate its cognate RR VanR, and a non-cognate RR PhoB; however, phosphotransfer to PhoB only occurs if PhoB's cognate kinase (PhoR) is not present. Likewise, PhoR can signal to VanR, but only if VanS is absent [107, 113, 114]. Similarly, in *E. coli*, cross-talk has been reported from the HPK CpxA to the RR OmpR, this cross-talk, however, only happens in the absence of both cognate partner proteins (the HPK EnvZ and RR CpxR); likewise, cross-talk from EnvZ to CpxR requires the absence of CpxA and OmpR [115]. These observations suggest that cognate HPK-RR pairs display strong preference towards each other so that non-cognate phosphotransfer is avoided. Additionally, these studies showed that the presence of the cognate HPK and/or the cognate RR 'buffers' against cross-talk. Importantly, cognate HPK-RR pairs also maintain this specificity in *in vitro* phosphotransfer studies, although prolonged incubation (in the range of ~1 h) allows for phosphotransfer between few non-cognate HPKs and RRs [116].
Prevention of cross-talk can also be achieved in several additional ways. Temporal and special localization differences might account for some prevention of crosstalk, but this is obviously not possibility to insulate dozens of HPK-RR pairs. It was also suggested that the stoichiometric ratio between the HPK and the RR is important to prevent crosstalk. For instance, the *E. coli* RR OmpR is present in a much higher molecular ratio than its cognate HPK EnvZ [117]. Although, slight alterations in this ratio did not perturb the robustness of the signaling system, high rates of EnvZ expression perturbed the robustness of the system

[118]. Along these lines, overproduction of the HK NtrB in a *cheA*$^{-}$ *E. coli* strain resulted in perturbed swimming behavior which suggests cross-talk between NtrB and the RR CheY [119].

Two biochemical properties have been shown to efficiently prevent cross-talk in His-Asp signaling systems. First, bifunctional HPKs remove phosphoryl groups from their cognate RR by their phosphatase activity which eliminates unwanted cross-phosphorylation (discussed below in more detail). The second and probably the most important mean of preventing cross-talk is that cognate HPK-RR pairs display an inherent specificity towards each other. During the last years, a set of amino acids, termed specificity determining residues (SDR), was identified that mediate this specificity between the two proteins [12, 120, 121], **Figure 8**). These SDR of the HPK are located directly adjacent to the invariant histidine residues in the α1-helix and also fewer residues in the α2-helix of the DHp domain. In the RR, these residues lie on the tip of the α1-helix and in the connector between the β-sheet and the α5-helix that flank the acidic pocket.

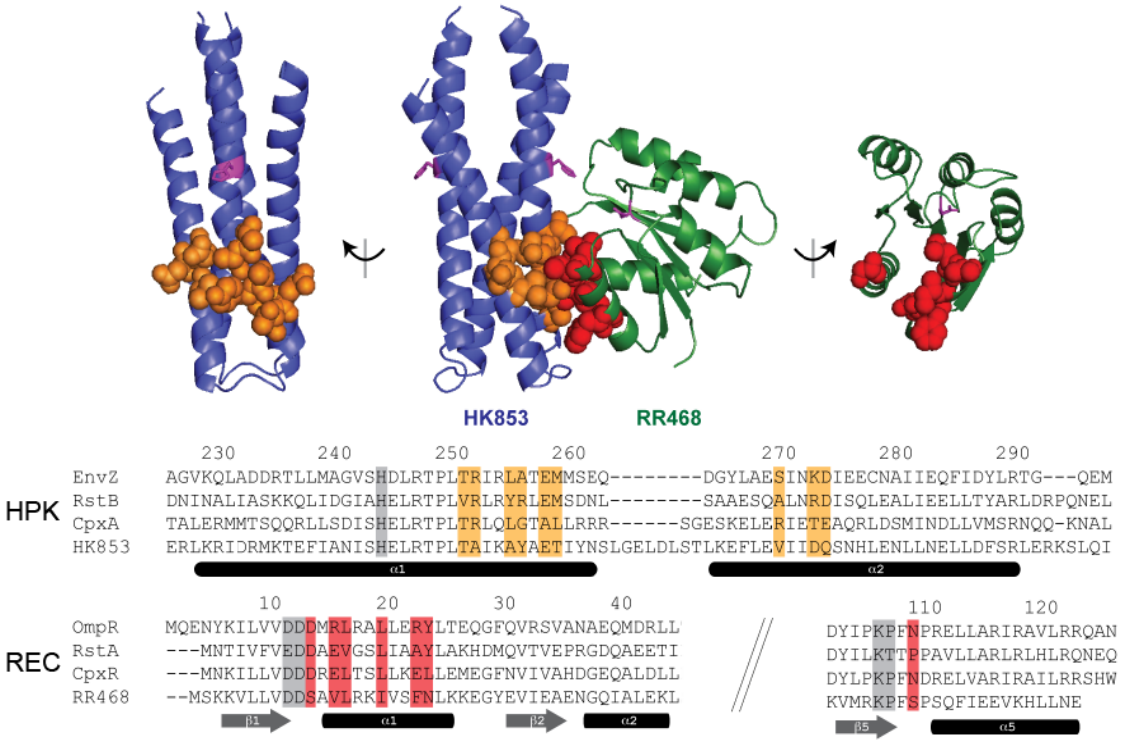

Figure 8 Specificity determining residues (SDR) mediate the specificity between cognate HPK-RR pairs. Crystal structures (top) of a DHp dimer (purple) and a REC domain (green). The putative SDR are highlighted as orange (HPK) and red (REC) spheres. Multi sequence alignments (bottom) display the relevant primary amino acid sequence regions in which the SDR are located. The SDR are highlighted in orange and red, correspondingly to the crystal structure. HPK, histidine protein kinase; REC, receiver domain. Figure modified from [121].

In HPK-RR co-crystal structures (*e.g.* the *T. maritima* HK853-RR468 or the *B. subtilis* Spo0B-Spo0F structures) these residues display near proximity to each other [23, 121]. It has been demonstrated that only few substitutions in these SDR can 'reprogram' the specificity of a HPK towards a non-cognate RR [121]. In this particular study it was shown that substitution of one or two amino acid was sufficient to reprogram the EnvZ specificity from OmpR to RstA or CpxR, respectively.

1.2 The *Myxococcus xanthus* developmental program

Myxococcus xanthus is a superior model organism to study complex and unorthodox signaling systems. One of the reasons for that is that *M. xanthus* contains a large number of signaling proteins; the ~9 Mbp genome of this deltaproteobacterium encodes for 251 non-chemosensory related His-Asp signaling proteins [122]. Interestingly, many of the His-Asp signaling genes are organized in unorthodox ways. The majority are encoded as orphan genes, meaning that they are not co-transcribed with their cognate signaling partner. Additionally, more than ~17 % of the genes are organized in complex gene clusters, meaning that more than two HK genes, RR genes or mixed HK- RR gene combinations are encoded together, suggesting complex relationships of the resulting signaling systems.
One plausible reason for the need of such complex signaling systems is that *M. xanthus* has a very complex lifestyle which relies on spatial and temporal decisions constantly being made. One part of its complex lifestyle is the formation of spore-filled multicellular fruiting bodies upon unfavorable environmental conditions (reviewed in [123]). During the developmental program, cells aggregate into mounds in which the cells differentiate into environmentally resistant spores (**Figure 9**). Interestingly, not all cells contribute to the formation of spore filled fruiting bodies, in fact a large proportion (~ 60 %) lyses during the developmental program [124, 125]. A minor proportion of the developmental cells, termed peripheral rods, remain outside of the fruiting bodies and likely represent a persister like state that can respond very quickly to newly available nutrients [126-128]. The by far best studied developmental cell fate is the formation of fruiting bodies. The whole program is initiated by RelA (ppGpp synthase) dependent accumulation of the alarmone (p)ppGpp [129, 130]. The subsequent processes are regulated by a cascade of signals that act at different times during the developmental program [131].

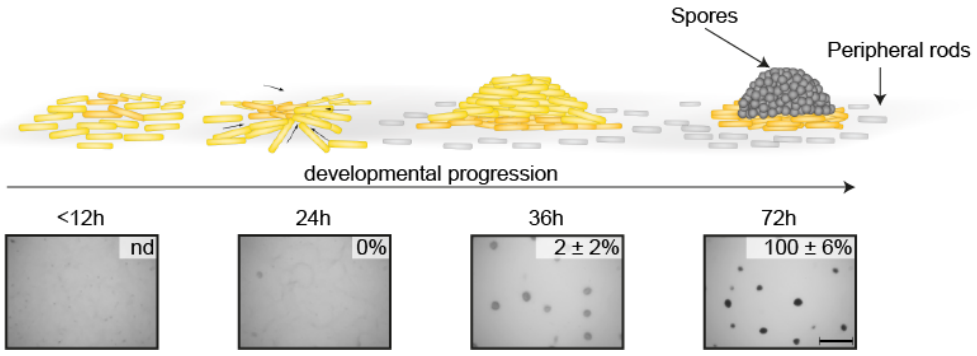

Figure 9 Schematic of the *M. xanthus* developmental program. Upon starvation, cells begin to aggregate into fruiting bodies. Exclusively inside of the fruiting bodies, the cells differentiate into environmentally resistant spores. The pictures below depict key stages at the indicated time points during the developmental program which are comparable to the stages shown in the schematic. The numbers represent the percentage of spores produced by the wild type (DZ2) strain. Scale; 0.5 mm. See text for more details.

One of these signals is the A-signal, a mixture of peptides which was initially proposed to be a quorum sensing-like mechanism [132, 133]. Five genes are identified that, upon inactivation, display an A-signal defect, *asgA*-*asgE* [134-139]. Moreover, deletion mutants in *asgA* and *asgB* show reduced level of the central transcription factor, MrpC, indicating that the A-Signaling machinery is involved in the regulation of this central regulator [140]. MrpC is a member of the CRP/FNR family of transcription factors and its essential role in the regulation of development was revealed by the analysis of *mrpC* mutants who fail to aggregate and sporulate [141]. *mrp*C is not only regulated on its transcriptional level, but also intensively on the posttranscriptional level to ensure appropriate and coordinated development. Under vegetative conditions MrpC is thought to be phosphorylated via a Ser/Thr kinases cascade (consisting of Pkn8 and Pkn14) which is thought to inactivate MrpC [142, 143]. During development, MrpC is proposed to be processed into a shorter isoform, MrpC2, which displays a higher affinity for its target DNA sequences *in vitro*, one of which is its own promoter [143]. This already indicates that MrpC activates its own transcription, thus generating a positive auto amplification loop. One of the most important targets of MrpC2 is the *fruA* gene [144]. FruA is a transcription factor which is described to be activated by a cell to cell contact dependent mechanism, the C-signaling [145, 146]. C-signal (p17) is a 17 kDa isoform of CsgA (p25) which is generated by PopC-mediated proteolysis [147-149]. C-signaling was shown to induce FruA-dependent methylation of the Frz chemosensory system which is thought to trigger the cells to migrate into aggregation centers [150, 151]. The cells in the aggregation centers then undergo cell to cell contact which leads to increased C-signaling and thus results in an auto amplification loop leading to more activated FruA. Activated FruA, in concert with MrpC2, then activates promoters of genes expressed late during development [152, 153]. One of these promoters controls the

dev locus which is necessary for sporulation inside of fruiting bodies [154, 155]. Interestingly, *devT* encodes for a protein that in turn leads to increased FruA expression [156], illustrating that the MrpC2/FruA – DevT system forms another positive auto amplification loop in the developmental program. Altogether, is it obvious that MrpC plays a central role in the coordination and regulation of development, hence it is an indispensable positive regulator of the *M. xanthus* developmental program. Further, at least two positive auto amplification loops are affiliated with MrpC, thus raising the question how MrpC is regulated in order to ensure coordinated fruiting body development.

1.3 TCS systems regulate the developmental program of *M. xanthus*

Five negative regulatory signaling systems have been identified that repress developmental progression (EspA [157, 158], EspC [159, 160], TodK [161], RedCDEF [104, 162] and Hpk30[1]). All these proteins belong to the class of His-Asp signaling systems. Interestingly, the encoding genes are organized as orphan or complex His-Asp signaling genes, suggesting complex signaling relationships. In fact, the Red signaling system utilizes a very complex four component signaling mechanism [104]. Interestingly, the majority of these negative regulators seem to act on the level of MrpC regulation; EspA is proposed to regulate the MrpC protein level [158], deletion of *todK* also leads to earlier accumulation of MrpC[2] and recent analysis of the Red systems gave initial evidence that this system is involved in regulating the phosphorylation state of MrpC[3]. Additionally, it was shown that deletion mutants of these negative regulators interfered with appropriate cell fate differentiation during the developmental program, as the progressive deletion of *espA* was accompanied by the production of spores outside of fruiting bodies which is only very rarely observed in the wild type strain [157]. Thus, we hypothesize that these negative regulatory systems counteract the positive amplification loops that are implemented in the developmental program to ensure fine tuned progression trough the developmental program.

[1] B. Lee, K. Cho, M. Glaser and P. I. Higgs, unpublished data
[2] B. Lee, PhD thesis
[3] B. Lee, X. Mei, P. I. Higgs, unpublished data

EspA and EspC are both regulating developmental progression in *M. xanthus*

The HyHPK EspA was the first of the above described negative regulators that was analyzed in more depth. EspA contains the signal transmitter modules (DHp-, CA- and REC domain) as well as three putative sensing domains, a FHA and two PAS domains (**Figure 10**A). It is co-transcribed with a putative transport protein (EspB), and it was shown that EspA acts downstream of EspB [157]. Interestingly, EspA is one of the very rare examples of a His-Asp signaling protein that contains a FHA domain [158]. It is suggested that this FHA domain mediates interaction with the two Ser/Thr kinases (PktA5 and PktB8) that are likely also involved in the regulation of the EspA signaling output [163]. Transcriptional analysis revealed that EspA is up-regulated during the developmental program [122, 158], and genetic analyses suggest that EspA functions as a classical HyHPK in which the HPK autophosphorylates and donates phosphoryl groups to the internal REC domain which then mediates repression of developmental progression [158]. This phosphorylation of the $EspA_{REC}$ was indirectly shown by phosphate release experiments, since the phosphorylated form of an $EspA_{KR}$ construct was to short lived to be detected.

How exactly EspA mediates repression of developmental progression is unknown, since the signal output of EspA was not identified. Detailed analysis of developmental marker proteins, however, revealed that MrpC, FruA and CsgA protein level were produced earlier and to higher level, additionally the FrzCD methylation was early in an *espA* mutant [158].

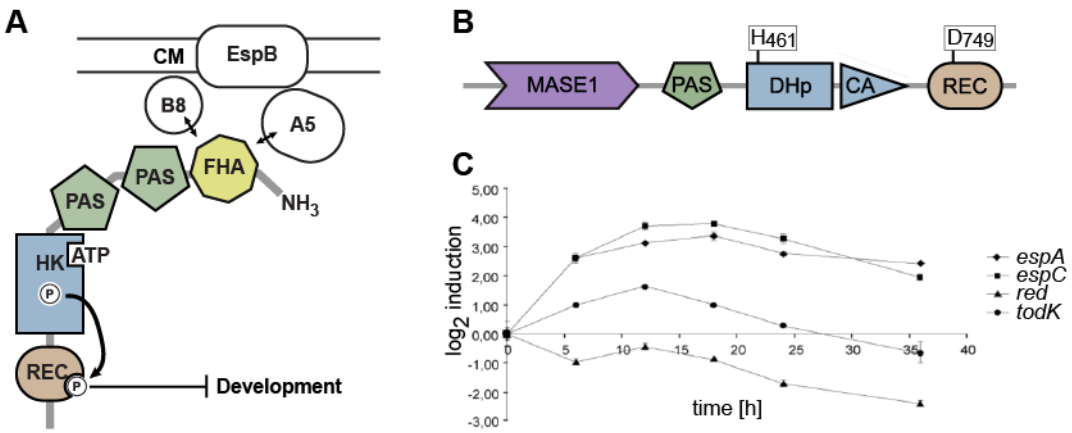

Figure 10 The two HyHPK EspA and EspC are involved in the regulation of developmental progression of *M. xanthus*. *A, Schematic of the EspA signaling complex.* EspA represses developmental progression upon phosphorylation of its REC domain. EspA is likely modulated by the EspC/PktA5/PktB8 signaling components. *B, Domain organization of EspC.* EspC is a HyHPK; it contains the conserved signal transmitter regions as well as two sensing domains: a MASE1 domain and a PAS domain. *C, Transcription analysis of negative regulators in the M. xanthus developmental program.* qPCR data was taken from B. Lee (PhD thesis). See text for details.

Interestingly, the amount of the *mrpC* transcript was not altered during the early time points of development in the *espA* mutant which suggested that EspA regulates MrpC post transcriptionally, either on the level of translation or protein stability.

The HyHPK EspC has been identified by a transposon mutagenesis screen [159] which intended to identify an output for the EspA/EspB/PktA5/PktB8 signaling module. EspC contains the conserved signal transmitter domains (HK and REC) and two sensing domains, a predicted membrane associated sensing domain (MASE1) and a PAS domain ([159], **Figure 10**B). Similar to EspA, EspC has been described to repress progression through the developmental program, as the phenotype of a Δ*espC* mutant strain was reminiscent of that of a Δ*espA* strain. Additionally, it was shown that *espC*, like *espA*, is up-regulated during developmental progression [122, 159], and both share a nearly identical expression pattern[4] ([158], **Figure 10**C). Early epistasis experiments[5] suggested that EspA and EspC may be involved in the same regulatory pathway, and prompted a thorough investigation of if and how EspC and EspA could function together in the regulation of developmental progression of *M. xanthus*.

[4] B. Lee, PhD thesis
[5] B. Lee, PhD thesis

1.4 Aim of the study

Recent advances in the His-Asp phosphorelay research revealed that these signaling proteins can be arranged into sophisticated signaling networks which is often highlighted in *M. xanthus*. The initial results about EspC suggested that it acts together with the HyHPK EspA. The aim of the presented study was to elucidate how exactly EspC functions and how it is integrated in the complex EspA/EspB/PktA5/PktB signaling system.
Specifically, the following questions were addressed:

1. **What is the molecular function of the HyHPK EspC?**

To address this question, several single substitutions mutations which are known to interfere with autophosphorylation, phosphotransfer and phosphatase activity of HPKs were generated and analyzed. Further, deletion mutants of single domains within EspC were also generated and investigated. Together, these genetic analyses were used to decipher the signaling mechanism of EspC. These achieved results were confirmed and expanded by *in vitro* biochemical characterization of autophosphorylation and phosphotransfer analyses.

2. **What is the relationship between EspA and EspC?**

During the analyses of the signaling mechanism of EspC, it became evident that EspA and EspC form one intimate signaling system. To elucidate how EspA and EspC interact, protein accumulation profiles, bioinformatic prediction of specificity determination residues, genetic and biochemical experiments were applied. Finally, biochemical phosphotransfer analysis were conducted to determine that EspA and EspC function together, utilizing a novel signaling mechanism.

3. **What is the output, and how does the Esp system regulate development?**

In order to decipher the output of the Esp system, I established an assay that allowed for the determination of the proteolytic degradation of the major transcription factor, MrpC. I identified that the Esp system regulates the degradation of MrpC, and initiated the identification of the protease which is important for this process, by applying protease inhibitor screens and a modified zymogram approach. I also addressed whether and how this proteolytic processing alters the developmental program, including the effect on the differentiation of developmental subpopulations.

2. RESULTS

2.1.1 EspA and EspC function together

Developmental phenotype analysis

To gain a better understanding about the functional relationship between EspA and EspC, the developmental phenotype of Δ*espA*, Δ*espC* and Δ*espA*Δ*espC* strains were confirmed under submerged culture conditions (**Figure 11**A). Consistent with the initial reported developmental analysis[6], the aggregation and sporulation phenotype of the Δ*espA*Δ*espC* strains was indistinguishable from each single deletion mutant strain (Δ*espA* and Δ*espC*). Aggregates could be first observed at ~24 h of development, approximately 12 h earlier than for the wild type. The production of heat and sonication resistant spores correlated with the early aggregation phenotypes. The early developing strains (Δ*espA*, Δ*espC* and Δ*espA*Δ*espC*) produced significantly more resistant spores at 36 h of development. The higher spore production rate continued throughout the period of observation ending with significantly higher amounts of spores after 72 h (~135 %, ~131 % and ~144 %).

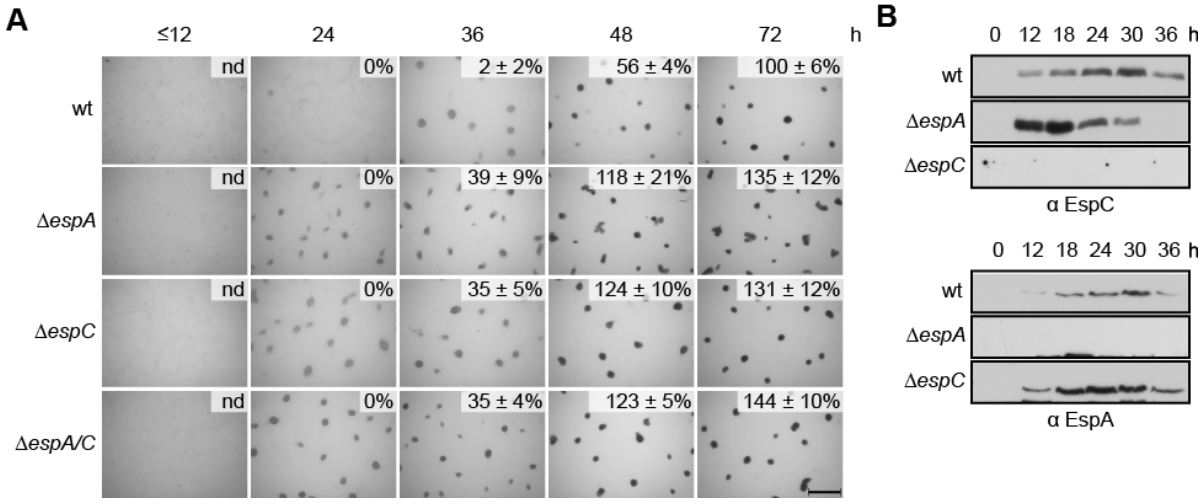

Figure 11 EspA and EspC are components of one single signaling pathway. *A, Developmental phenotypes of* esp *null mutants.* Wild type (wt; DZ2), Δ*espA* (DZ4227), Δ*espC* (PH1044) and Δ*espA* Δ*espC* (PH1047) strains were developed under submerged culture in 24-well culture dishes, and pictures were recorded at the indicated hours of development. Heat and sonication resistant spores were isolated at the indicated time points and displayed as the percent of wild type spores at 72 h. Spore numbers are the average and associated standard deviation of three biological replicates. Scale bar = 0.5 mm; nd, not determined. *B, EspA and EspC developmental protein accumulation pattern.* Anti-EspC (top) and anti-EspA (bottom) immunoblot analysis of 20 µg total protein prepared from the indicated strains developed for the indicated hours under 16 ml submerged culture format.

[6] B. Lee, PhD thesis

EspC antibody generation and immunoblot optimization

To examine whether the deletion of one *esp* gene adversely affected the protein production of the respective other *esp* gene product, the protein production of EspA and EspC were analyzed by immunoblot analysis of cell lysates prepared from wild type, Δ*espA*, or Δ*espC* stains (**Figure 11**B). The anti-EspC antibody was generated and purified against recombinant $EspC_{\Delta MASE1}$-His_6. Although, the purified antibody could detect 0.1 ng antigen by immunoblot, EspC could not be detected in developmental protein samples (data not shown). To rule out that the EspC detection failed because of EspC instability, two developmental cell samples were subjected to TCA precipitation. One of the cell samples was precipitated directly after harvesting from the petri dishes and the other sample was precipitated after 30 min incubation at RT. EspC could be detected after TCA precipitation, but it could also be detected from both protein samples (data not shown). Together, this experiment revealed that TCA precipitation is crucial for EspC detection, EspC instability, however, seems not to be responsible for the difficulties in the EspC detection. Even though EspC could be detected from TCA precipitated samples, the signal intensities were very weak (data not shown). Since proteins containing large transmembrane regions can precipitate in buffers containing SDS, the developmental protein lysates were delepidified, additionally the samples were boiled to a lesser extent. Delipidification did not enhance the EspC detection, whereas short boiling greatly enhanced EspC detection. Thus, these experiments revealed that EspC could only be detected with high signal intensities in cell lysates which were TCA precipitated and only briefly heated.

Esp protein production pattern

The anti-EspC immunosera generated in this study specifically detected a ~89 kDa band (similar to the predicted EspC molecular mass of ~88 kDa) in the wild type, but not Δ*espC*, lysates. In the time course experiments, EspC was not detected at T = 0 h, but began to accumulate at ~12 h, peaked at ~30 h, and then began to decrease. EspA showed a production pattern which was highly similar to that of EspC ([158] and **Figure 11**B). EspC and EspA were present in the Δ*espA* and Δ*espC* strains, respectively. Both proteins started to accumulate between 0 h and 12 h; peak protein production could be observed between 12 h and 18 h. Both proteins accumulated earlier in the respective other deletion backgrounds than in the wild type. As EspA was also produced in the Δ*espC* strain and vice versa the observed developmental phenotypes are no result of protein instability in the single deletion mutants. Thus, these data suggest that EspA and EspC likely act in the same signaling

pathway to regulate developmental progression. Additionally, EspA and EspC directly or indirectly repress the accumulation of the respective other protein.

2.1.2 EspA and EspC are functional homologs in the Cystobacterinaea

The genetic analysis suggests that EspA and EspC participate in one signaling pathway. Consequently, if EspA and EspC function in one obligate signaling system, they should co-occur in different bacteria that use this signaling system. Using a Reciprocal BLASTp analysis [164] in the cystobacterinaea genomes, orthologs to EspA and EspC could be identified in *Stigmatella aurantiaca* (STAUR_7060 and STAUR_0999, respectively), *Corallococcus coralloides* (COCOR_00882 and COCOR_07432, respectively) and *Myxococcus fulvus* (LILAB_04045 and LILAB_12195, respectively). Orthologs for neither protein could be identified in *Anaeromyxobacter dehalogenans*, *Haliangium ochraceum*, *Plesiocystis pacifica* or *Sorangium cellulosum*. Since EspA and EspC always were present together, this analysis suggested that EspA and EspC are functionally related proteins.

Furthermore, this analysis revealed that EspA and EspC are likely a result of a recent gene duplication event, because the close relative of *M. xanthus*, *A. dehalogenans* did not encode for either EspA or EspC. This hypothesis is supported by the observation that EspA and EspC share a high degree of primary sequence identity in their signal transmission regions (HK: 48 %, REC: 40 %, **Figure 12**A). SMART Domain architecture analysis [48, 49] of the EspA domain architecture revealed no other proteins besides the EspA orthologs (**Figure 12**C), that showed the EspA domain organization. Consistently, reciprocal BLASTp analysis using the EspA protein as query could also not identify other EspA orthologs outside of the Cystobacterinaea. Together these analyses indicate that EspA emerged within this suborder of the deltaproteobacteria. Interestingly, SMART Domain architecture analysis could identify five proteins outside of the Cystobacterinaea which displayed the same domain architecture as EspC. Conversely, reciprocal BLASTp analysis using the EspC protein as query did not identify other EspC orthologs outside of the Cystobacterinaea. This observation suggests that the proteins sharing the EspC domain architecture likely emerged by convergent evolution and are not related to the EspC orthologs found in the Cystobacterinaea.

If EspA and EspC are a result of recent gene duplication, the encoding genes are likely paralogs. However, BLASTp analysis with EspA (MXAN_0931) as a query against the protein database from *M. xanthus* DK1622 revealed three other HyHPK proteins

(MXAN_0195, MXAN_2386 and MXAN_0095) that display a higher degree of conservation towards EspA than does EspC (**Figure 12**B). This BLASTp analysis suggests that even though EspA and EspC share a high degree of primary sequence identity, they are likely not paralogous proteins. Obviously, unlike EspA and EspC, no evolutionary pressure led to the preservation of the HyHPKs MXAN_2386 and MXAN_0095 in these genomes (**Figure 12**C).

Together, these data suggest that these five proteins might be a result of recent gene duplications in the Cystobacterineae. Importantly, it revealed that EspA and EspC always co-occurred supporting the hypothesis that EspA and EspC might function together.

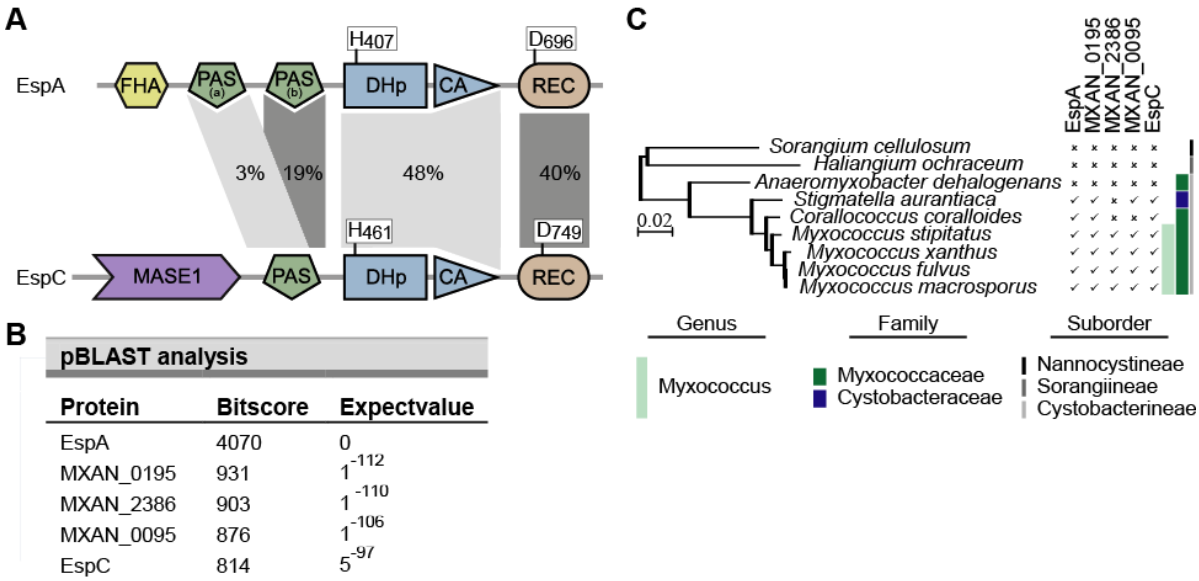

Figure 12 EspA and EspC are functional homologs. *A, Domain organization of the EspA and EspC hybrid histidine protein kinases.* Percent amino acid identity for the indicated domains is displayed in the shaded areas. The invariant histidine (H) residues in the dimerization and histidine phosphotransfer domains (DHp) and invariant aspartate (D) residues in the receiver (REC) domains are indicated. FHA, forkhead-associated domain; MASE1, predicted integral membrane sensory domain; PAS, Per Arnt Sim sensing domain (EspA contains two PAS domains, designated as PAS_a and PAS_b.); CA, ATP hydrolysis domain. *B, EspA and closely related proteins.* BLASTp result using MXAN_0931 (EspA) as a query against the *Myxococcus xanthus* DK1622 protein database. Proteins with a bitscore higher than the score of MXAN_6855 (EspC) are shown. *C, Co-occurrence of EspA homologs in different Myxococcales genomes.* The dendogram represents the relationship of members of the order Myxococcales based on their 16s rRNA [7]. The colored bars illustrate the suborder, family or genus of the respective genomes (see legend). ✔; present in the analyzed genome, x; absent in the analyzed genome.

[7] S. Huntley, unpublished data

2.1.3 EspA and EspC interact at the cytoplasmic membrane

Our hypothesis that EspA and EspC form an intimate signaling module, consequently implies that EspA and EspC must interact during the developmental program. In order to test this hypothesis T. Jeganathan performed yeast two hybrid (Y2H) analysis during her MSc research[8] under my supervision. The Y2H analysis revealed an interaction between $EspA_{HK}$ - $EspA_{HK}$ and $EspC_{HK}$ - $EspC_{HK}$, indicating that these two HyHPK form homodimers. Additionally, interaction between $EspA_{HK}$ - $EspC_{\Delta TM}$, but not between $EspA_{HK}$ - $EspC_{HK}$, could be observed, suggesting that EspA and EspC interact and this interaction seems not be mediated by the HK region.

EspC is a membrane protein, presumably anchored to the cytoplasmic membrane by the MASE1 domain

EspC is predicted to be a membrane protein, because it contains a putative membrane associated sensing domain 1 (MASE1). Further, the EspC membrane association also was predicted using the CELLO compartment localization prediction tool [165, 166] (**Figure 13**A). To confirm the EspC membrane association, EspC was analyzed by protein fractionation experiments from developmental wild type cells at different time points during the developmental program (**Figure 13**B). MrpC, a soluble transcription factor, was used as a marker protein for the cytoplasmic proteins [144]; and PilC, an inner membrane protein of the type 4 pilus machinery, was used as a marker protein for the membrane proteins [167]. As expected, PilC was found highly enriched in the membrane protein fraction at 12 h, 18 h and 24 h. At 30 h the PilC signal of the soluble- and the membrane-protein fraction did not correlate with the signal intensity of the 'whole cell' PilC signal. However, the signal intensity in the soluble protein fraction was only very weak, suggesting that this fraction is likely not contaminated with membrane proteins. The MrpC protein was not clearly detectable at 12 h of development due to its low protein level at this time point. At 18 h, 24 h and 30 h MrpC was nearly exclusively found in the soluble protein fraction. At 18 h and 24 h a contaminating band (asterisk) which runs slightly higher than MrpC appeared in the membrane associated fraction. At all time points the EspC protein was highly enriched in the membrane associated protein fraction. From this analysis it was concluded that, consistent with the bioinformatic predictions, EspC is an inner membrane protein.

[8] T. Jeganathan and A. Schramm, unpublished data

A

CELLO prediction

Compartment	Score
Cytoplasmic	0.898
Inner Membrane	**3.314**
Outer Membrane	0.443
Periplasmic	0.141
Extracellular	0.203

B

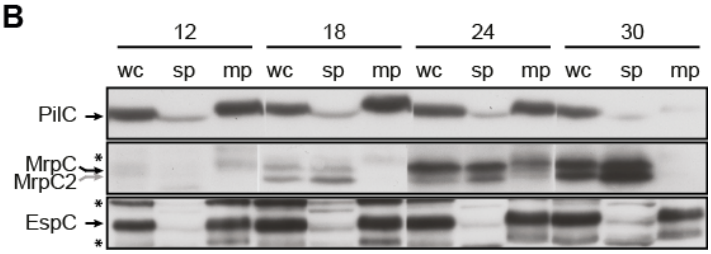

Figure 13 EspC is an inner membrane protein. *A, CELLO prediction of EspC.* EspC compartmental localization predicted by CELLO; the table lists the prediction scores for the cytoplasm, inner membrane, outer membrane, periplasm or extra cellular space. The highest score is bold. *B, Protein fractionation and EspC localization analysis.* Protein fractionations of lysates from wild type cells (wt; DZ2) harvested at 12 h, 18 , 24 h and 30 h of development under submerged culture conditions. Clarified whole cell lysates (wc) and equal sample proportions of soluble protein (sp) and membrane associated protein (mp) fractions were subjected to SDS-PAGE and analyzed by immunoblot with the indicated antibodies. PilC: inner membrane protein of the T4-Pili of *M. xanthus*, MrpC/MrpC2; soluble transcription factor and its more active isoform, EspC; hybrid histidine protein kinase; asterisk, cross reactive band.

EspC recruits EspA to the cytoplasmic membrane

EspA is a HyHPK predicted to be a cytoplasmic protein (**Figure 14**A). Interestingly, a protein fractionation experiment[9] performed by Tharshika Jeganathan during her MSc research using developed cells of the wild type, Δ*espC*, Δ*espB*, Δ*espB*Δ*espC* and Δ*espB*Δ*pknA5*Δ*pknB8* strains indicated that EspA was exclusively found to be membrane associated. This membrane association seemed to be partially dependent on the presence of EspC, because when EspC was absent in one strain (Δ*espC* or Δ*espB*Δ*espC*) a portion of EspA was then found in the soluble protein fraction (data not shown). This analysis supported the Y2H analysis and the hypothesis that EspA and EspC interact. In order to gain a better understanding of the temporal aspect of the EspA - EspC interaction, the protein fractionation experiment was performed at different time points during the developmental program (**Figure 14**B). PilC was found highly enriched in the membrane protein fraction at 12 h, 18 h, 24 h and 30 h in the wild type lysates as well as in the lysates from the Δ*espC* strain. The MrpC protein was exclusively found in the soluble protein fraction at the analyzed time points. Thus, the cell compartment fractionation by differential centrifugation was successful.

The analysis of the EspA protein revealed that, at 12 h of development, the EspA protein could be detected in the membrane protein fraction and the soluble protein fraction in nearly equal amounts in the wild type as well as the Δ*espC* lysates. At 18 h, the EspA protein was highly

[9] T. Jeganathan and A. Schramm, unpublished data

A

CELLO prediction	
Compartment	**Score**
Cytoplasmic	**3.348**
Inner Membrane	1.005
Outer Membrane	0.313
Periplasmic	0.258
Extracellular	0.075

B

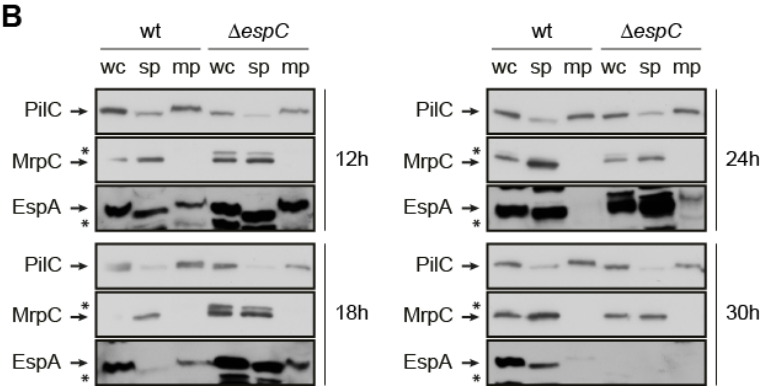

Figure 14 EspA interacts with the membrane during the developmental program. *A, CELLO prediction of EspA.* EspA compartmental localization predicted by CELLO; the table lists the prediction scores for the cytoplasm, inner membrane, outer membrane, periplasm or extra cellular space. The highest score is bold. *B, Protein fractionation and EspA localization analysis.* Cells from the wild type (wt; DZ2) and Δ*espC* (PH1044) strain were starved under submerged developmental conditions and harvested after 12 h, 18 h, 24 h and 30 h. The clearified whole cell lysate (wc) and equal sample proportions of soluble proteins (sp) and membrane associated proteins (mp), were subjected to SDS-PAGE and analyzed by immunoblot with the indicated antibodies. PilC: inner membrane protein of the T4-Pili of *M. xanthus*, MrpC; soluble transcription factor, EspA; predicted soluble hybrid histidine protein kinase, *; cross reactive protein band.

enriched in the membrane associated fraction in wild type lysates. In the Δ*espC* strain, however, a significant amount of EspA was instead found in the soluble protein fraction. At 24 h of development, EspA was found in the soluble protein fraction for both the wild type and the Δ*espC* strain. At 30 h of development, EspA could only be detected in the wild type strain and was highly enriched in the soluble protein fraction. This analysis showed that EspA was associated with the membranes at 18 h of development. Further, this membrane association was impaired in the absence of EspC. Previous observations by T. Jeganathan revealed that this association likely is not further influenced by the Esp signaling components EspB, PktA5 and PktB8. Together, these analyses suggest that EspA becomes recruited to the cytoplasmic membrane during the developmental program, and this membrane association is directly or indirectly mediated by EspC.

2.2 The Esp system signals via an unique intra- and inter- phosphorylation event

EspA is shown to transfer phosphoryl groups from its HK to its REC [158]. To further confirm this observation a double substitution mutant substituting both invariant phosphor-accepting residues to alanines was generated and analyzed (**Figure 15**A). Similar as reported previously for each single substitution (*espA*$_{H407A}$ and *espA*$_{D696A}$), the double substitution mutant (*espA*$_{H407A,D696A}$) displayed a phenotype indistinguishable from the

Δ*espA* strain (**Figure 11**A). Aggregation and production of resistant spores was observed ~12 h earlier than for the wild type. All strains (Δ*espA*, $espA_{H407A}$, $espA_{D696A}$ and $espA_{H407A,D696A}$) produced significantly more resistant spores at 36 h of development compared to wild type; the higher spore production rate continued throughout the period of observation ending with significantly higher amounts of spores after 72 h (~135 %, ~139 %, ~149 % and 144 %). The observation that the $espA_{H407A,D696A}$ strain shared the phenotype of the individual single substitution mutants further supports the model that EspA mediated repression of developmental progression is dependent on phosphoryl transfer from the EspA HK to the EspA REC [158].

2.2.1 EspC D749, but not H461, is important for regulation of development

To better understand the EspC function in these regulatory processes, alanine substitution mutants of the invariant phosphor-accepting residues, histidine 461 and aspartate 749, were analyzed ($espC_{H461A}$, $espC_{D749A}$ and $espC_{H461A,D749A}$; **Figure 15**B). Similar as to the corresponding mutations in *espA*, the $espC_{D749A}$ and $espC_{H461A,D749A}$ strains displayed an early developmental phenotype identical to all the early mutants described so far (Δ*espA*, Δ*espC*, Δ*espA* Δ*espC*, $espA_{H407A,}$ $espA_{D696A}$ and $espA_{H407A,D696A}$; **Figure 11**A, **Figure 15**A and B). Aggregation and production of spores was observed ~12 h earlier than in the wild type. Moreover, these mutant strains produced significantly more resistant spores at 36 h and 48 h, resulting in significantly higher amounts of spores after 72 h than the wild type (~128 % and 122 %).

Surprisingly, the substitution of the invariant phospho-accepting histidine residue 461 ($espC_{H461A}$) did not result in an early developmental phenotype. Aggregation and spore production were indistinguishable from that of the wild type: Aggregates were formed at ~30 h of development, together with the onset of spore formation. Furthermore, at later time points the spore production rate was similar to the production rate of the wild type.

To exclude that the substitution mutations negatively affected the protein stability of the respective strain which in turn would also lead to an early developmental phenotype, the protein accumulation pattern of EspA and EspC were analyzed by immunoblot. None of the analyzed point mutants resulted in protein instability of EspC or EspA (**Figure 15**C). Both proteins analyzed (EspA and EspC) showed a gradual increase in protein level with peak expression between 24 h and 36 h, and a decreased protein level at 36 h of development in the wild type and the $espC_{H461A}$ strains. The early mutants ($espC_{D749A}$ and $espC_{H461A,D749A}$) showed a much steeper increase of EspC protein between 12 h and 18 h of development.

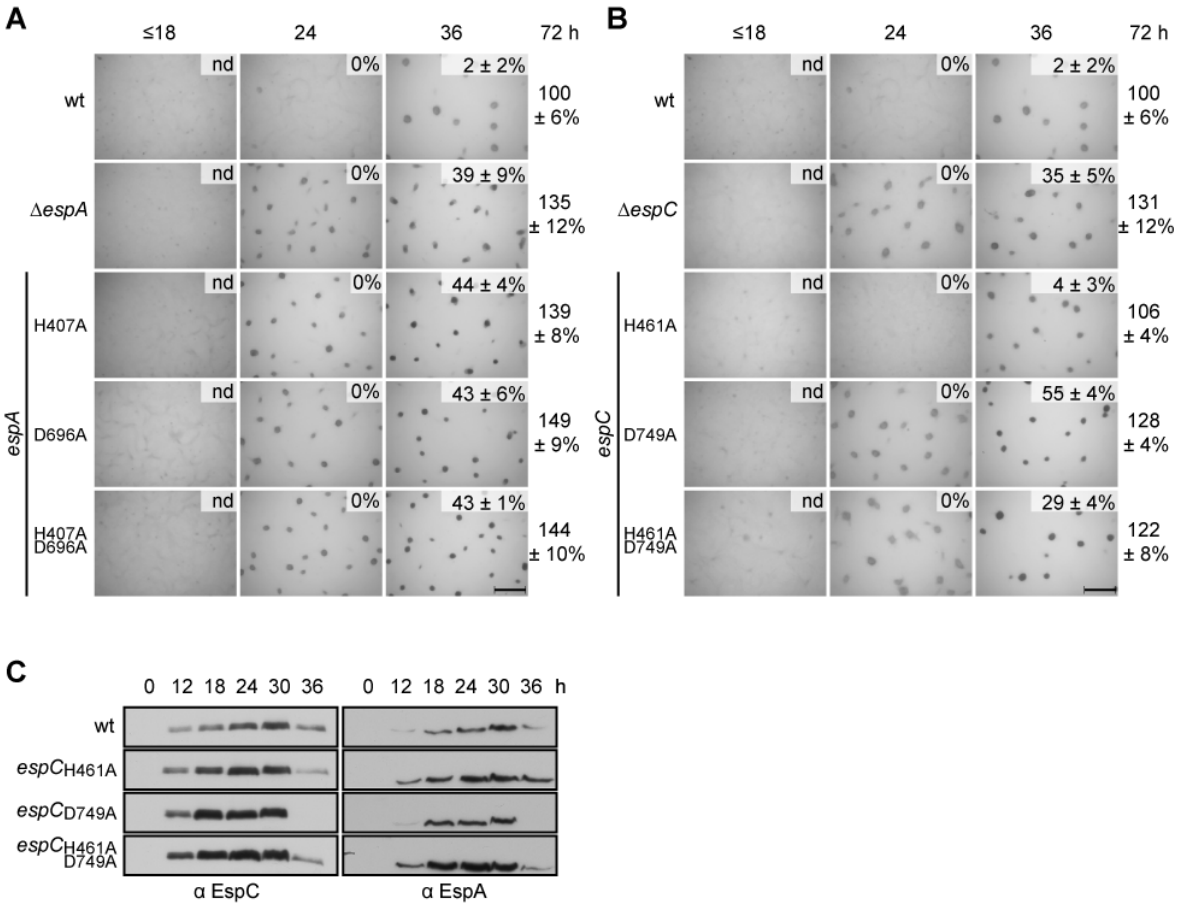

Figure 15 $EspC_{REC}$~P, but not $EspC_{HK}$ autophosphorylation, is required for regulation of development. *A, Developmental phenotypes of* espA *signal transmission point mutants.* Wild type (wt; DZ2), Δ*espA* (DZ4227), $espA_{H407A}$ (PH1008), $espA_{D696A}$ (PH1009) and $espA_{H407A,D696A}$ (PH1029) strains were developed under submerged culture in 24-well culture dishes, and pictures were recorded at the indicated hours of development. Heat and sonication resistant spores were isolated at the indicated time points and displayed as the percent of wild type spores at 72 hours. Spore numbers are the average and associated standard deviation of three biological replicates. Scale bar = 0.5 mm; nd, not determined. *B, Developmental phenotypes of* espC *signal transmission point mutants.* Wild type (wt; DZ2), Δ*espC* (PH1044), $espC_{H461A}$ (PH1026), $espC_{D749A}$ (PH1027) and $espC_{H461A,D749A}$ (PH1028) strains were analyzed as in A. *C, EspC and EspA developmental protein accumulation patterns.* Anti-EspC (left) and anti-EspA (right) immunoblot analysis of cell lysates prepared from the indicated strains developed for the indicated hours under 16 ml submerged culture format.

At 36 h of development, the protein levels also decreased for these early strains. Furthermore, the production of EspA was also earlier in these strains. Together with the analysis of the developmental phenotypes of the different strains, these results suggest that EspC represses developmental progression upon phosphorylation of the invariant aspartate 749 in the EspC REC domain. Additionally, phosphorylation of the EspC REC seems to, directly or indirectly, influence the protein production level of both EspA and EspC. Surprisingly, the EspC HK does not contribute to regulation of development which suggests that it does not donate a phosphoryl group to the EspC REC. This can be explained by the following two possibilities: $EspC_{HK}$ is incapable of autophosphorylation or $EspC_{HK}$ is incapable of donating a phosphoryl group to $EspC_{REC}$.

2.2.2 EspC HK autophosphorylates on the invariant histidine 461 *in vitro*

To test if the EspC HK is capable of autophosphorylation *in vitro*, $EspC_{HK}$-His_6 protein was overproduced, purified and tested for autophosphorylation by incubation with radioactive [γ^{32}P]-ATP (**Figure 16**A). Since I was unable to find conditions in which the $EspC_{HK}$-His_6 recombinant protein resulted in soluble protein production, the protein was refolded from inclusion bodies (section 4.4.4). After 60 min of co-incubation of $EspC_{HK}$-His_6 and [γ^{32}P]-ATP, a radioactive signal could be detected using the wild type version of $EspC_{HK}$ but not using a mutated version were the phosphor-accepting histidine 461 was substituted to alanine. In order to determine whether EspC has a autophosphorylation behaviour which is comparable to that of EspA, a comparable version of the EspA HK region was generated and analyzed for autophosphorylation. Although the $EspA_{HK}$-His_6 protein could be over produced as a soluble protein, it was subsequently denatured and refolded, to be consistent with the analysis of the $EspC_{HK}$-His_6 protein. As reported previously, using an amino-terminally GST tagged $EspA_{HK\text{-}REC}$ protein [158], the $EspA_{HK}$-His_6 was capable of autophosphorylation on its invariant histidine residue 407 (**Figure 16**A). However, the radioactive signal detected after 60 min of autophosphorylation was stronger using the $EspA_{HK}$-His_6 version instead of a GST-$EspA_{HK}$ protein[10]. For subsequent phosphotransfer experiments it was important to know the time of maximal phosphorylation of the two proteins. In order to compare the *in vitro* autophosphorylation rates of $EspA_{HK}$ and $EspC_{HK}$, the [^{32}P] incorporation by $EspC_{HK}$-His_6 and $EspA_{HK}$-His_6 was monitored over a time course of 60 min (**Figure 16** B and C). A [^{32}P]-label could be detected on both $EspC_{HK}$-His_6 and $EspA_{HK}$-His_6 after less than 1 min of incubation. Interestingly, the signal increased more rapidly on $EspC_{HK}$-His_6 peaking between 10 min and 30 min of incubation, followed by a gradual decrease between 30 and 60 min of incubation. In contrast, $EspA_{HK}$-His_6 displayed a more gradual increase of signal intensity with its maximum at 60 min of co-incubation; afterwards, the signal intensity remained constant (data not shown). It should be noted that autophosphorylation characteristic displayed in **Figure 16**C are relative signal intensities normalized to the maximum signal intensity of each kinase construct. At 60 min, the $EspC_{HK}$-His_6 signal intensity was approximately 2.5 fold higher than the $EspA_{HK}$-His_6 signal intensity.

[10] T. Jeganathan and A. Schramm, unpublished data

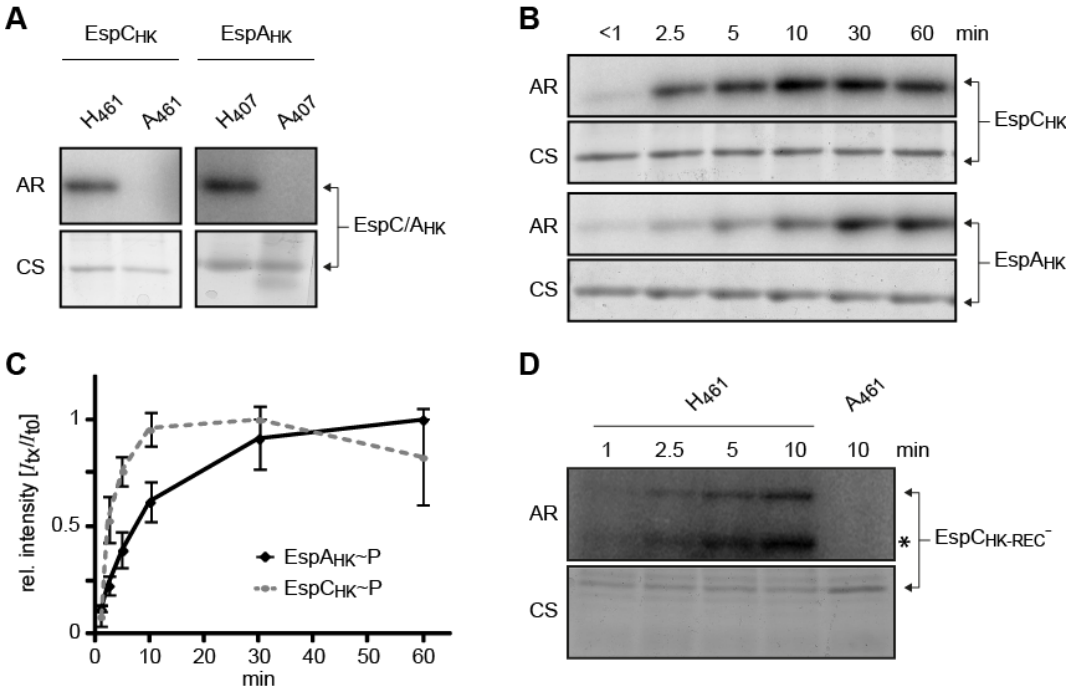

Figure 16 EspC$_{HK}$ and EspC$_{HK-REC}$ autophosphorylate *in vitro*. *A,* In vitro *autophosphorylation of EspA$_{HK}$-His$_6$, EspC$_{HK}$-His$_6$, EspA$_{HK\ H407A}$-His$_6$ and EspC$_{HK\ H461A}$-His$_6$.* 10 µM of each recombinant protein was incubated in the presence of [γ^{32}P]ATP for 60 min, quenched, resolved by SDS-PAGE, and the radiolabel was detected by exposure to a Storage Phospho Screen (AR). Total protein was subsequently detected by Coomassie stain (CS). *B, Relative* in vitro *autophosphorylation rates of EspC and EspA kinase regions.* 10 µM EspA$_{HK}$-His$_6$ or EspC$_{HK}$-His$_6$ were incubated in the presence of [γ^{32}P]-ATP; aliquots were removed at the indicated time points and analyzed as above. *C, Quantification of EspC (dashed line) and EspA (solid line) HK autophosphorylation in B.* Relative signal intensities of the bands from three independent time course experiments were quantified and normalized to the maximal signal intensity of each protein. The average relative signal intensity and the associated standard deviation from each time point was plotted. *D,* In vitro *autophosphorylation of EspC$_{HK-REC}$-His$_6$ and EspC$_{HK-REC\ H461A}$-His$_6$.* 7 µM EspC$_{HK-REC}$-His$_6$ or EspC$_{HK-REC\ H461A}$-His$_6$ were incubated in the presence of [γ^{32}P]ATP; aliquots were removed at the indicated time points and analyzed as in A.

In order to determine whether the EspC$_{REC}$ inhibits the EspC$_{HK}$ autophosphorylation behavior, the autophosphorylation of an EspC$_{HK-REC}$-His$_6$ construct was additionally tested (**Figure 16**D). The EspC$_{HK-REC}$ construct showed increasing autophosphorylation over the 10 min of co-incubation with [γ^{32}P]-ATP which was specific to the histidine 461. In addition to the EspC$_{HK-REC}$ phospho-labeled protein a second, more intense radioactive signal could be detected. In the corresponding Commassie-stained gel, a smear appeared at the comparable molecular mass, indicating that this radioactive signal might be produced from a degradation product of the EspC$_{HK-REC}$ construct, probably still remaining the intact HK region. Taken together, these analyses indicate that: a) the recombinantly produced and refolded EspC$_{HK}$-His$_6$, EspC$_{HK-REC}$-His$_6$ and EspA$_{HK}$-His$_6$ proteins were capable of autophosphorylation *in vitro*, despite the observation that EspC$_{HK}$ function seems not to be important for developmental regulation *in vivo*. b) EspC$_{HK}$ autophosphorylation occurs on

the predicted invariant phospho-accepting histidine 461. c) Both proteins exhibited an autophosphorylation consistent with those of other recombinant HK proteins [168, 169], indicating that $EspC_{HK}$ is likely physiologically active.

2.2.3 $EspC_{HK}$ does not donate phosphoryl groups to $EspC_{REC}$

Since $EspC_{HK}$ autophosphorylates *in vitro*, I next examined phosphotransfer from $EspC_{HK}$ to $EspC_{REC}$ (**Figure 17**A). Either $EspC_{HK}$-His_6 or $EspC_{HK\ H461A}$-His_6 were incubated with [γ^{32}P]-ATP for 30 min and then buffer was added to achieve a final concentration of 10 µM kinase (lane 1 and 2). As expected, only $EspC_{HK}$-His_6 could be labeled radioactively. The signal intensity measured from three independent experiments was quantified and the value for $EspC_{HK}$-His_6 incubated only with buffer served as the input reference and was set to 100 % (**Figure 17**B, lane 1). When 10 µM $EspC_{REC}$-His_6 was added instead of buffer, no labeling could be detected on the receiver domain after two minutes of co-incubation with either $EspC_{HK}$-His_6 or $EspC_{HK\ H461A}$-His_6 (**Figure 17**A, lane 3 and 4, respectively). Only an insignificant signal loss from $EspC_{HK}$ could be measured (**Figure 17**A and B, lane 3). Extended incubation for five minutes also did not result in phosphorylation of $EspC_{REC}$ (data not shown). As expected, no phosphoryltransfer could be detected if $EspC_{REC\ D749A}$-His_6 was incubated with $EspC_{HK}$-His_6 (lane 5). These observations support the previous genetic analyses suggesting that $EspC_{HK}$ likely does not donate phosphoryl groups to $EspC_{REC}$.

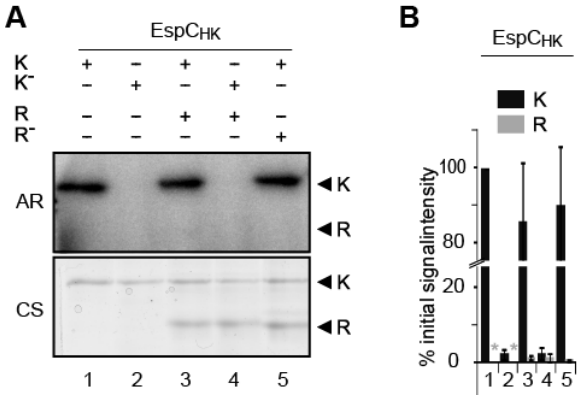

Figure 17 $EspC_{HK}$ does not donate phosphory groups to $EspC_{REC}$. *A,* In vitro *phosphotransfer from autophosphorylated $EspC_{HK}$ to $EspC_{REC}$*. $EspC_{HK}$-His_6 (K) or $EspC_{HK\ H461A}$-His_6 (K^-) were first incubated in the presence of [γ^{32}P]ATP for 30 min, and then incubated with either buffer or equimolar amounts (10 µM) of $EspC_{REC}$-His_6 (R) or $EspC_{REC\ D749A}$-His_6 (R-) for two min. +: indicated component present; -: indicated component absent. The samples were quenched with 2x LSB, resolved by SDS-PAGE and radiolabel was detected by exposure to a Storage Phospho Screen (AR). Total protein was subsequently detected by Coomassie stain (CS). *B, Quantification of the relative signal intensities*. Signal intensities of radiolabeled $EspC_{HK}$ (K, black bars), and $EspC_{REC}$ (R, gray bars) are shown as the average and associated standard deviation of three independent replicates of the reactions represented in A. Intensity values were normalized to the respective autophosphorylation control (lanes 1). *; not determined.

2.2.4 Putative specificity determining residues support the $EspA_{HK}$-$EspC_{REC}$ inter protein phosphorylation hypothesis

The *in vitro* experiments demonstrated that $EspC_{HK}$ can autophosphorylate, but it is unable to donate phosphoryl groups to $EspC_{REC}$. Additionally, the genetic analysis revealed that the EspC kinase function has no effect for the developmental regulation. Since the genetic analysis further indicated that EspA and EspC participate in one signaling pathway, I hypothesize that $EspA_{HK}$ instead might act as a phosphoryl donor for $EspC_{REC}$ which displays a novel yet undescribed signaling mechanism of His-Asp signaling systems. Consequently, this hypothesis implies that EspA has specificity determining residues (SDR) which allow interaction with both cognate RECs, $EspA_{REC}$ and $EspC_{REC}$.

In order to support the hypothesis that $EspA_{HK}$ can donate phosphoryl groups to both RECs, I mapped the putative SDR residues in $EspA_{REC}$, $EspC_{REC}$, $EspA_{HK}$ and $EspC_{HK}$ based on previous SDR analysis for canonical two component systems [12, 120, 121]. Based on my hypothesis, I predicted the SDR residues in the REC domains to be conserved between $EspA_{REC}$ and $EspC_{REC}$. Conversly, in the DHp domains I predict these residues to differ between $EspA_{HK}$ and $EspC_{HK}$, because $EspC_{HK}$ was unable to donate phosphoryl groups to its own receiver *in vitro*.

The *in silico* evolutionary analysis already revealed that EspA and EspC are not paralogs (section 2.1.2). Using a BLASTp analysis, six HK regions and five REC domains could be identified that displayed a higher bit-score towards EspA, than EspC did (**Table 1**). Since crosstalk between unrelated TCS systems only rarely occurs [11], I rationalized that these other His-Asp phosphorelay proteins do not phosphorylate $EspA_{REC}$ nor $EspC_{REC}$. Therefore, despite their higher REC sequence conservation, the SDR regions should be sufficiently diverged and could serve as an excellent negative control group. In order to identify the SDR for the $EspA_{HK}$ the control group sequences were aligned against $EspA_{HK}$ and $EspC_{HK}$ from *M. xanthus*, *Corallococcus coralloides* and *Stigmatella aurantiaca* (designated as: Mx_EspA, Cc_EspA, Sa_EspA and Mx_EspC, Cc_EspC, Sa_EspC, respectively). Additionally, the HK sequences were aligned against EnvZ from *E. coli* (**Figure 18**A), for which the SDRs have previously been mapped.

Table 1 HK regions and REC domains identified and used for the SDR analysis

KINASE REGION			
Gene product	**bit score**	**expect value**	**two component system type**
MXAN_3974	613	$7e^{-76}$	HyHPK
MXAN_0195	614	$8e^{-75}$	HyHPK
MXAN_0928	542	$8e^{-69}$	classic
MXAN_7206	568	$8e^{-68}$	HyHPK
MXAN_0095	556	$2e^{-67}$	HyHPK
MXAN_2386	552	$7e^{-67}$	HyHPK
RECEIVER DOMAINS			
MXAN_2386	276	$6e^{-31}$	HyHPK
MXAN_7206	249	$4e^{-27}$	HyHPK
MXAN_0095	245	$1e^{-26}$	HyHPK
MXAN_0314	239	$6e^{-26}$	HyHPK
MXAN_2763	229	$8e^{-25}$	HyHPK

The putative SDR region in $EspA_{DHp}$ is composed of two stretches of amino acids at the positions 21-27 and 64-68 in the alignment (**Figure 18**A). These regions are highly conserved in Mx_EspA, Cc_EspA and Sa_EspA, consistent with a role as SDR for a cognate REC; for simplicity, these two regions are termed 'specificity consensus'. The Mx_EspC_{HK}, Cc_EspC_{HK} and Sa_EspC_{HK} SDR residues are diverged from the EspA specificity consensus at the positions 25-27, 64 and 66, because non-conservative substitutions are present at these possitions. Interestingly, Mx_EspC, Cc_EspC and Sa_EspC showed non-conservative substitutions in the putative SDR region at the positions 21, 25, 64 and 66 between each other; the SDR region diverged significantly between the EspC orthologs suggesting no evolutionary pressure preserving this region. Moreover, positions 25-27 and 66 in the control group DHp domains also displayed very low conservation, with conservative substitutions only at the positions 26 and 27 in MXAN_3974, MXAN_0195 and MXAN_0928. Together, these data suggest that in $EspC_{DHp}$, the SDR diverged between the EspC orthologs and also from the EspA specificity consensus. Finally, these analyses imply that the core residues in $EspA_{HK}$ which determine specificity towards $EspA_{REC}$ and $EspC_{REC}$ are at positions 25-27, and 64 (**Figure 18**; asterisks), because these residues are diverged in both the EspC orthologs and the control group proteins. This is consistent with the hypothesis that EspA, but not EspC or the control group HKs, can phosphorylate $EspA_{REC}$ and $EspC_{REC}$.

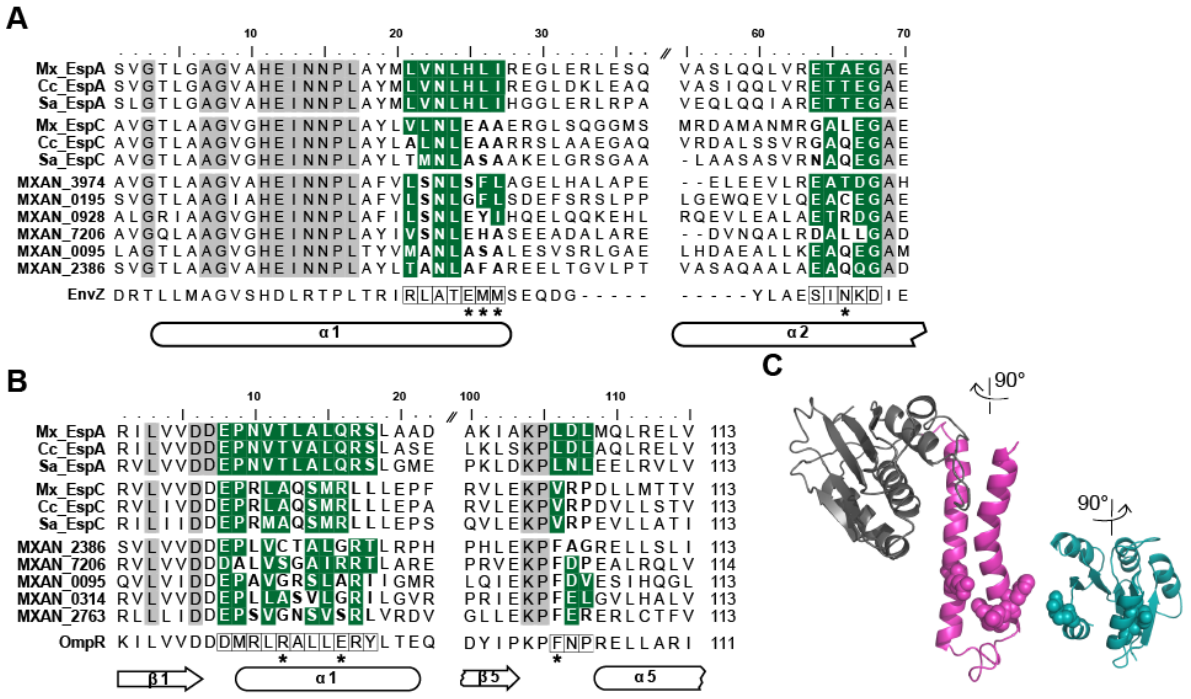

Figure 18 The diverged putative SDR residues in $EspC_{HK}$ might not allow for phosphotransfer to $EspC_{REC}$. *A, Depiction of the putative DHp SDR.* Multiple sequence alignments of the DHp protein sequences from EspA and EspC in *M. Xanthus*, *Stigmatella aurantiaca* (Sa_EspA: STIAU_9475 and Sa_EspC: STIAU _0700, respectively), *Corallococcus coralloides* (Cc_EspA: COCOR_00882 and Cc_EspC; COCOR_07432, respectively), the control group proteins of *M. xanthus* and *E. coli* $EnvZ_{DHp}$ were generated using ClustalX [170]. Previously identified SDR residues [12, 120, 121] are boxed in the EnvZ sequence. Highly conservative residues (PAM250 score > 1) [171] are shaded green. Putative SDR residues for the Esp system are marked by asterisks. *B, Depiction of the putative REC SDR.* Multiple sequence alignments of the REC protein sequences from EspA and EspC in *M. Xanthus, S. aurantiaca* (Sa_EspA: STIAU_9475 and Sa_EspC: STIAU _0700, respectively), *C. coralloides* (Cc_EspA: COCOR_00882 and Cc_EspC; COCOR_07432, respectively), the control group of *M. xanthus* REC domains and *E. coli* $OmpR_{REC}$ as above. *C, Homology model of $EspA_{HK}$ and $EspC_{REC}$.* The $EspA_{HK}$ and the $EspC_{REC}$ were modeled on the $(HK853)_2$-$(RR468)_2$ co-crystal structure (PDB: 3dgeA and 3dgeC) from *T. maritime* [23]. The $EspA_{HK}$ (left) is depicted grey (CA domain) and purple (DHp domain). The $EspC_{REC}$ domain (right) is depicted teal. Both domains were rotated ~ 90° outwards, to gain a better view on the contact interface. The putative SDR residues found in *A* and *B* are highlighted by spheres.

Putative SDR residues have likewise also been mapped in $EspA_{REC}$ and $EspC_{REC}$ using OmpR from *E. coli* as reference sequence (**Figure 18**B). If $EspA_{HK}$ can phosphorylate both, its own and EspCs receiver domain, the SDR should be conserved in $EspA_{REC}$ and $EspC_{REC}$. The putative specificity region of the REC domains is composed of two amino acid regions from positions 8 - 18 and positions 106 - 108 in the alignment. Again, the putative SDR region in the analyzed REC domains is nearly perfectly conserved in Mx_EspA, Cc_EspA and Sa_EspA. The respective regions in the Mx_EspC, Cc_EspC and Sa_EspC REC also display perfect identity towards each other. Unlike to the SDR region in the $EspC_{HK}$ orthologs, the REC SDR region seems not to have freedom to diverge. However, compared to the consensus from the EspA REC, some residues are non-

conservative substitutions (positions 10, 13, 17, 18, 107 and 108). Since it has been shown that residues in this region do not have an equivalent impact on the specificity determination [121], I compared the conservative substitutions of the EspC REC domains to that of the control group. Assuming that the control group proteins do not accept phosphoryl groups from $EspA_{HK}$, only residues that are conservative in EspC but not in the control group seem to be potential candidates for SDR between $EspA_{HK}$ and $EspC_{REC}$. The amino acids at the positions 12, 156 and 116 fulfill the above criteria, and thus they likely represent the core residues in $EspA_{REC}$ and $EspC_{REC}$ mediating specificity towards $EspA_{HK}$. Together, these analyses support our hypothesis that $EspA_{HK}$ might be the phosphoryl donor for both receiver domains in EspA and EspC. These results are also consistent with the observation that the $EspC_{HK}$ did not act as a phosphoryl donor to its own receiver domain because, the SDR were conserved in the $EspC_{REC}$ but not in the SDR of the $EspC_{DHp}$ domains of the EspC orthologs.

2.2.5 $EspA_{HK}$ donates phosphoryl groups to $EspC_{REC}$ *in vitro*

To test the hypothesis that $EspA_{HK}$ acts as a phosphoryl donor for $EspC_{REC}$, phosphotransfer between $EspA_{HK}$ and $EspC_{REC}$ was examined (**Figure 19**A). Either $EspA_{HK}$-His_6 or $EspA_{HK\ H407A}$-His_6 was incubated with [γ^{32}P]-ATP for 30 min and then buffer was added to achieve a final concentration of 10 µM kinase (lane 1 and 2). As expected, only $EspA_{HK}$-His_6 could be labeled radioactively. The measured average signal intensity from three independent experiments were expressed relative to the buffer only control, set to 100 % (**Figure 19**B, lane 1).

After the addition of $EspC_{REC}$-His_6 to $EspA_{HK}$-His_6, 8 (± 1) % of the initial signal intensity could be detected on the $EspC_{REC}$ (**Figure 19**A and B, lane 3); simultaneously the remaining label intensity on $EspC_{HK}$ showed a stark reduction to 16 (± 5) % (**Figure 19**B, lane 3). Incubating $EspA_{HK\ H407A}$-His_6 together with $EspC_{REC}$-His_6, or $EspA_{HK}$ together with $EspC_{REC\ D749}$-His_6, did not result in phosphorylation of $EspC_{REC}$ (**Figure 19**A and B, lane 4 and 5). These results indicate that $EspA_{HK}$ is capable of donating phosphoryl groups to $EspC_{REC}$ *in vitro*. Interestingly, extended incubation of $EspA_{HK}$-His_6 with $EspC_{REC}$-His_6 led to a decreased signal intensity on $EspC_{REC}$ (**Figure 19**C), suggesting that the $EspA_{HK}$ may additionally act as a phosphatase on $EspC_{REC}$.

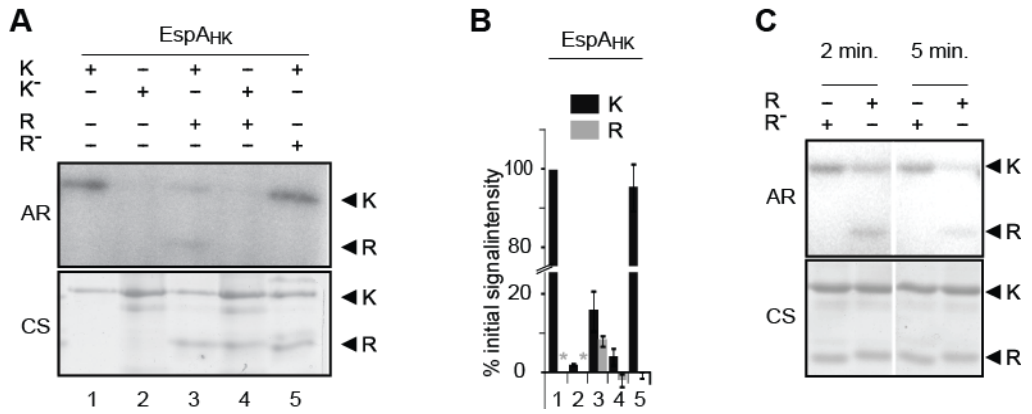

Figure 19 EspA$_{HK}$ efficiently phosphorylates EspC$_{REC}$. *A,* In vitro *phosphotransfer from autophosphorylated EspA$_{HK}$ to EspC$_{REC}$.* EspA$_{HK}$-His$_6$ (K) or EspA$_{HK\ H407A}$-His$_6$ (K$^-$) were first incubated in the presence of [γ^{32}P]ATP for 30 min, and then incubated with either buffer or equimolar amounts (10 µM) of EspC$_{REC}$-His$_6$ (R) or EspC$_{REC\ D749A}$-His$_6$ (R-) for two min. +: indicated component present; -: indicated component absent. The samples were quenched with 2x LSB, resolved by SDS-PAGE and radiolabel was detected by exposure to a Storage Phospho Screen (AR). Total protein was subsequently detected by Coomassie stain (CS). *B, Quantification of the relative signal intensities.* Signal intensities of radiolabeled EspA$_{HK}$ (K, black bars), and EspC$_{REC}$ (R, gray bars) are shown as the average and associated standard deviation of three independent replicates of the reactions represented in A. Intensity values were normalized to the respective autophosphorylation control (lanes 1). *; not determined *C, Time dependent* in vitro *phosphotransfer from autophosphorylated EspA$_{HK}$ to EspC$_{REC}$.* EspA$_{HK}$-His$_6$ were first incubated in the presence of [γ^{32}P]ATP for 30 min, and then incubated with equimolar (10 µM) EspC$_{REC}$-His$_6$ (R) or EspC$_{REC\ D749A}$-His$_6$ (R-) for two and five min as indicated. +: indicated component present; -: indicated component absent.

2.3 Regulatory mechanism of the Esp system

2.3.1 Phosphatase activity is a regulatory strategy of the Esp system

Since the genetic and biochemical analysis suggest that the EspC$_{HK}$ does not contribute to the phosphorylation of the EspC$_{REC}$, I wanted to assign a function for the EspC$_{HK}$. Many HPK are bifunctional, meaning they also possess phosphatase activity on their cognate RR. A phosphatase motif was proposed ([H]$^{E}/_{D}$XX$^{T}/_{N}$) which is located directly adjacent to the invariant histidine residue in DHp domains which is reminiscent to a motif in CheX and CheZ necessary for phosphatase function [111, 172]. Both Esp HyHPKs share this putative phosphatase motif (**Figure 23**A and **Figure 20**A). Although my genetic analysis did not show a phenotype for the *espC*$_{H461A}$ mutant, phosphatase activity, however, might not be assayed by this genetic analysis, because it has been reported that substitution of the phospho-accepting histidine residue does not necessarily impair phosphatase activity [108, 110]. Furthermore, the *in vitro* phosphotransfer experiments suggested that EspA could act as a phosphatase on EspC$_{REC}$ (section 2.2.5). Together, these observations strongly suggest

that EspA and EspC could act as phosphatases to regulate the Esp system *in vivo*. Thus, the following experiments were set out to examine whether phosphatase activities of EspA and EspC play an important role in regulation of developmental progression.

Disruption of the putative EspC phosphatase motif results in a wild type phenotype

In order to analyze whether the $EspC_{HK}$ might also act as a phosphatase to regulate the signaling state of the Esp system, single amino acid substitutions in the proposed phosphatase motif of EspC were generated. Since I demonstrated that phosphorylation of the $EspC_{REC}$ mediates repression of developmental progression, I predicted that mutants which no longer possess phosphatase activity to display a delayed developmental phenotype. A $espC_{N465Y}$ mutant strain, bearing a substitution in the phosphatase motif, displayed a wild type phenotype (**Figure 20**B), suggesting that either phosphatase activity was not disrupted in this mutant, phosphatase activity is not important in EspC dependent control of developmental progression, or phosphatase activity cannot be assayed with our developmental phenotype analysis. Since it was reported that the effect on the phosphatase activity is strongly dependent on the disruptive substitution which is analyzed [108-111], four additional substitution mutations ($espC_{E462A}$, $espC_{N465E}$, $espC_{N465R}$ and $espC_{N465C}$) were generated and tested (**Figure 21**A). None of these additional mutations in the phosphatase motif displayed the predicted delayed developmental phenotype. In all the analyzed mutations, the aggregation phenotype as well as the spore production pattern was indistinguishable from that of the wild type strain. Additionally, these strains showed an EspC protein production pattern similar as to the wild type, although the overall protein level were reduced (**Figure 20**C and **Figure 21**B). When these mutations were combined with an $espC_{D749A}$ mutation (resulting in the following strains: $espC_{N465Y,D749A}$, $espC_{E462A,D749A}$, $espC_{N465E,D749A}$, $espC_{N465R,D749A}$, $espC_{N465C,D749A}$), the early developmental phenotype of the e.g. $espC_{D749A}$ mutant strain was restored (**Figure 20**B and **Figure 21**A). Interestingly, in these double substitution mutants, the EspC protein levels were restored to level similar to the $espC_{D749A}$ strain (**Figure 20**C), suggesting that the reduced protein level in the strains containing a substitution in the phosphatase motif only, is likely not a result of protein instability caused by the substitution.

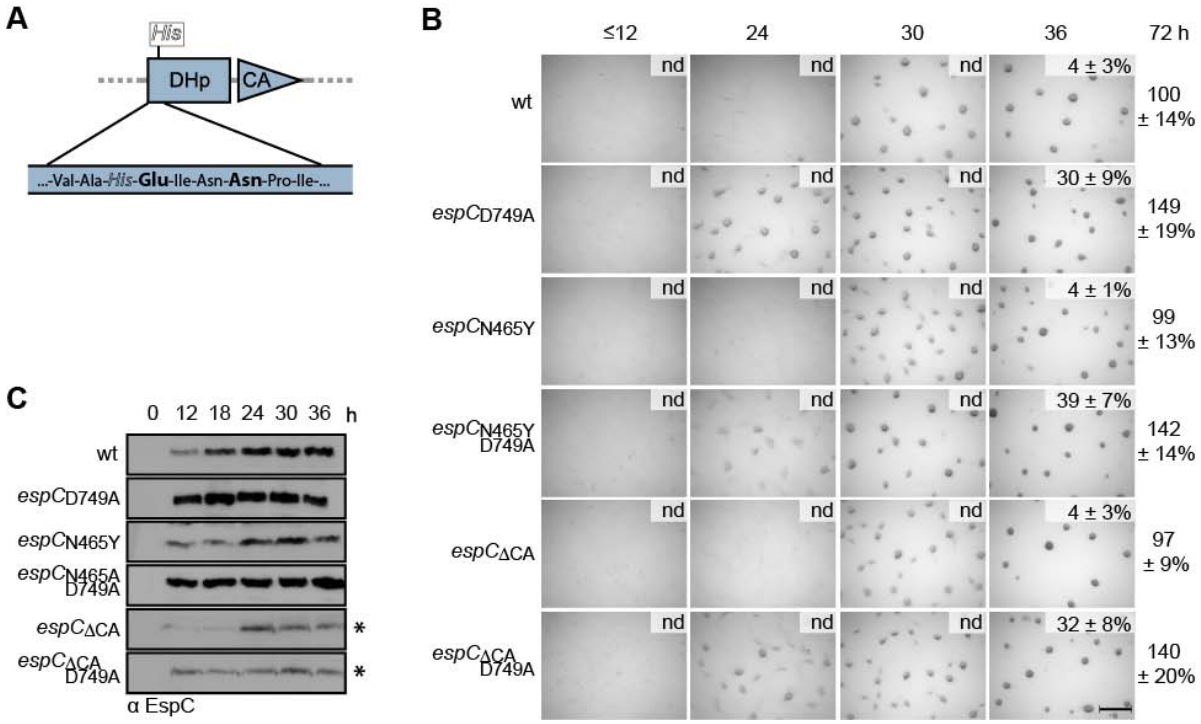

Figure 20 Disruption of the putative phosphatase motif in EspC does not effects developmental progression. *A, Putative phosphatase motif within the DHp domains of EspC.* The amino acid sequence surrounding the putative phosphatase motif $[H]^{E}/_{D}XX^{T}/_{N}$ [111] in EspC is displayed magnified from the scheme of a HK region. The invariant histidine residue is drawn italicized; the putative phosphatase residues are drawn as bold. *B, Developmental phenotypes of* espC *phosphatase-motif mutants.* Wild type (wt; DZ2), *espC*$_{D749A}$ (PH1027), *espC*$_{N465Y}$ (PH1034), *espC* $_{N465Y,D749A}$ (PH1035), *espC*$_{\Delta CA}$ (PH1032) and *espC*$_{\Delta CA,D749A}$ (PH1033) strains were developed under submerged culture in 24-well culture dishes, and pictures were recorded at the indicated hours of development. Heat and sonication resistant spores were isolated at the indicated time points and displayed as the percent of wild type spores at 72 h. Spore numbers are the average and associated standard deviation of three biological replicates. Scale bar = 0.5 mm; nd, not determined. *C, EspC developmental protein accumulation patterns.* Anti-EspC immunoblot analysis of cell lysates prepared from the indicated strains developed for the indicated hours using a 16 ml submerged culture format. *: 2.5 times longer exposure required.

To further assess whether EspC functions as a phosphatase, the CA domain of EspC was deleted, since it was reported that the CA domain of histidine kinases support efficient phosphatase activity [103-106]. Deletion of the CA domain in EspC (*espC*$_{\Delta CA}$) also resulted in a developmental phenotype indistinguishable from the wild type; in the *espC*$_{\Delta CA,D749A}$ double mutant the early developmental phenotype could be restored (**Figure 20**B). The protein accumulation pattern of the *espC*$_{\Delta CA}$ and the *espC*$_{\Delta CA,D749A}$ strains were similar to that of the wild type and *espC*$_{D749A}$ strains, respectively. However, the overall signal intensity obtained from the EspC$_{\Delta CA}$ and EspC$_{\Delta CA,D749A}$ immunoblots were strongly reduced. In this case, the reduction was likely caused by the loss of immunogenic epitopes in the deletion protein, as the deletion of the CA domain removed 28 % of the antigenic amino acids from EspC$_{\Delta MASE1}$ which was used for antibody production. Together, these analyses revealed that under the applied experimental conditions, disruption of the putative

phosphatase motif in EspC or deletion of the CA domain in EspC did not alter the regulation of developmental progression by the Esp system.

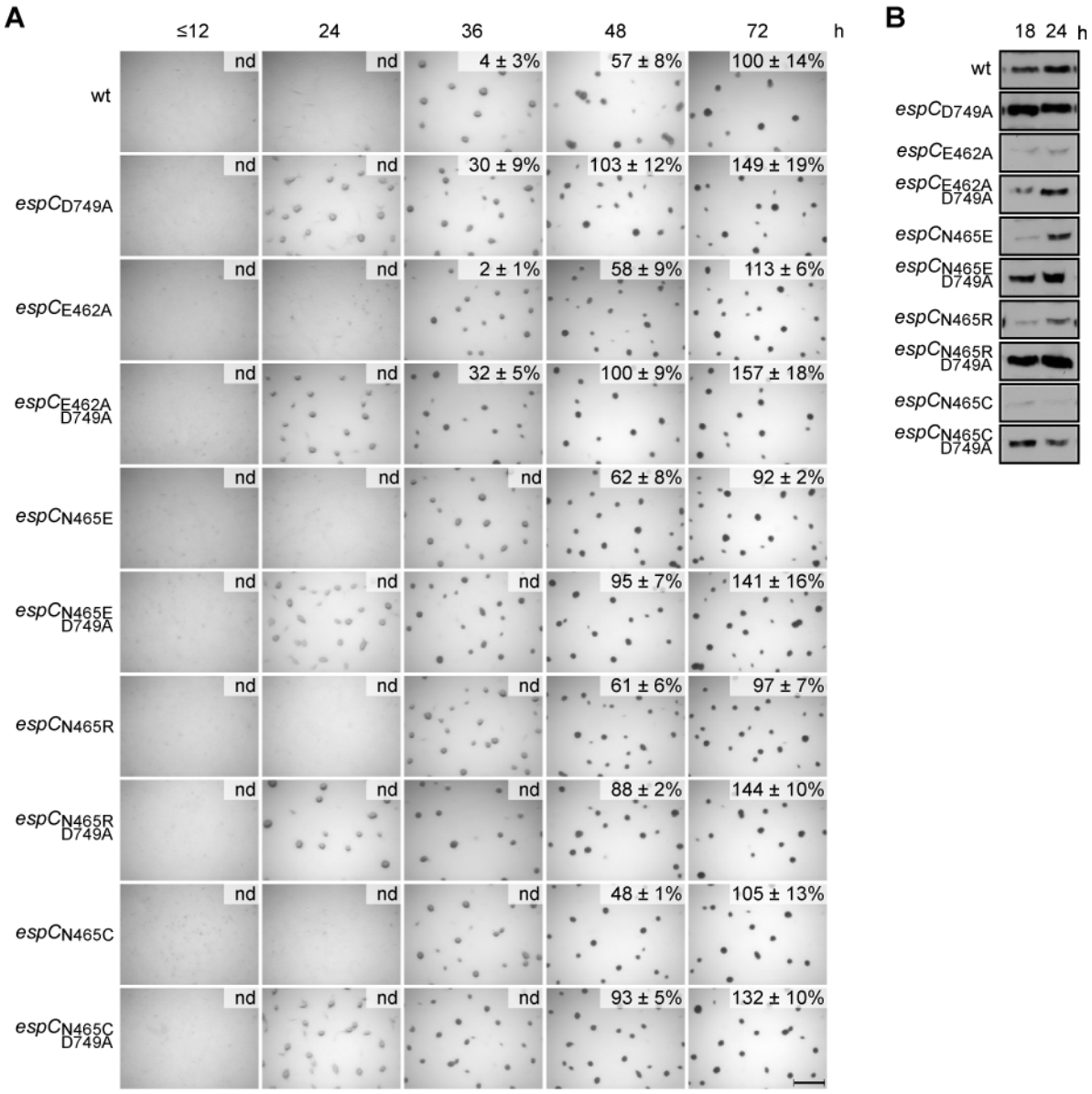

Figure 21 Disruption of the putative phosphatase motif in EspC does not effects developmental progression. *A, Developmental phenotypes of further* espC *and* espA *phosphatase-motif mutants.* Wild type (wt; DZ2), *espC*$_{D749A}$ (PH1027), *espC*$_{E462A}$ (PH1042), *espC* $_{E462A,D749A}$ (PH1043), *espC*$_{N465E}$ (PH1036), *espC* $_{N465E,D749A}$ (PH1037), *espC*$_{N465R}$ (PH1038), *espC* $_{N465R,D749A}$ (PH1039), *espC*$_{N465C}$ (PH1040), *espC* $_{N465C,D749A}$ (PH1041) strains were developed under submerged culture in 24-well culture dishes, and pictures were recorded at the indicated hours of development. Heat and sonication resistant spores were isolated at the indicated time points and displayed as the percent of wild type spores at 72 h. Spore numbers are the average and associated standard deviation of three biological replicates. Scale bar = 0.5 mm; nd, not determined. *B, EspC developmental protein accumulation patterns.* Anti-EspC immunoblot analysis of cell lysates prepared from the indicated strains developed for 18 h and 24 h using a 16 ml submerged culture format.

The $[H]^{E}/_{D}XX^{T}/_{N}$ phosphatase motif and the CA domain are not the only determinants of phosphatase activity in bifunctional HPKs. It has also been shown that the invariant histidine residue is involved in phosphatase activity, although it is not absolutely required [107, 108, 110, 111, 169]. Interestingly, substitution of the invariant phospho-accepting histidine to a glutamine was reported to increase phosphatase activity in the HPKs VanS and NarX [107, 111]. Therefore, a histidine to glutamine substitution was also tested for EspC (**Figure 22**A). The *espC*$_{H461Q}$ strain showed an intermediate phenotype in which aggregation was observed earlier than in the wild type but later than in the *espC*$_{D749A}$ mutant strain. Aggregation was observed at 27 h of development and the spore production pattern was also intermediate between the wild type and the *espC*$_{D749A}$ strain at 36 h and 48 h. However, after 72 h of development ~92 % of wild type spores were detected in the *espC*$_{H461Q}$ strain.

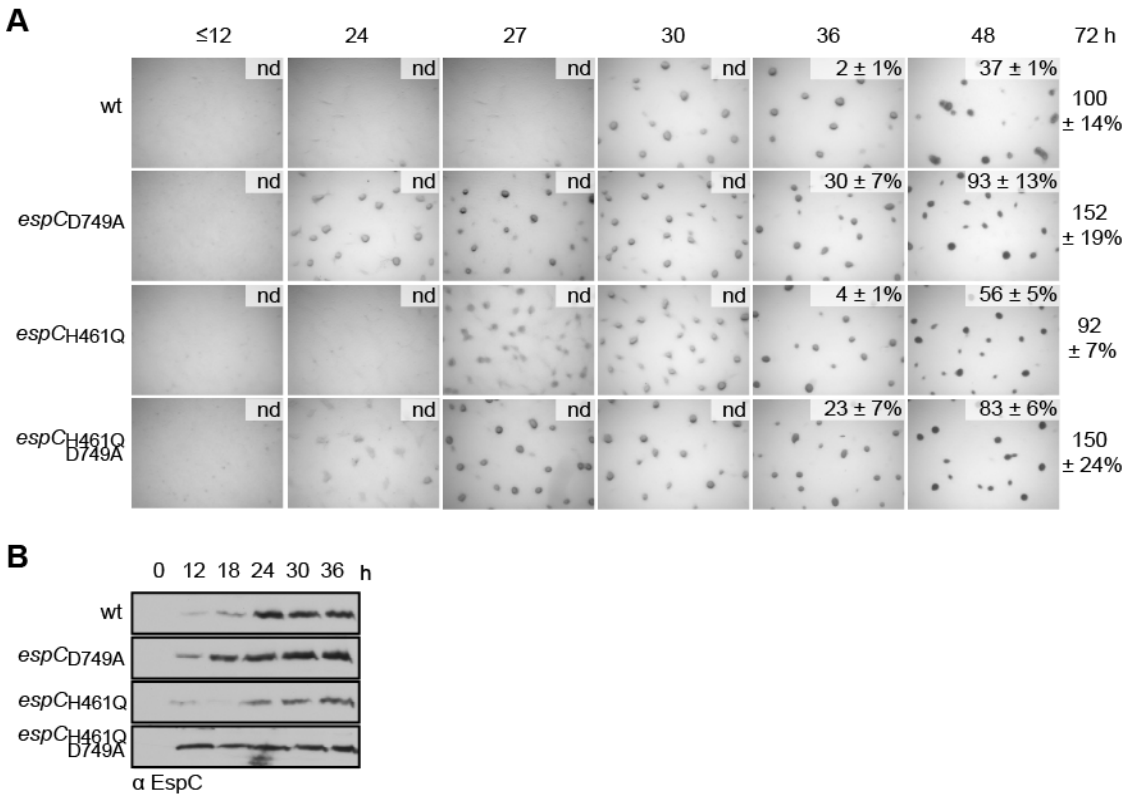

Figure 22 A histidine to glutamine substitution in EspC displayed a putative phosphatase^{+} phenotype. *A, Developmental phenotypes of* espC$_{H461Q}$ and espC$_{H461Q,\ D749A}$ *strains.* Wild type (wt; DZ2), *espC*$_{D749A}$ (PH1027), *espC*$_{H461Q}$ (PH1068) and *espC* $_{H461Q,D749A}$ (PH1069) strains were developed under submerged culture in 24-well culture dishes, and pictures were recorded at the indicated hours of development. Heat and sonication resistant spores were isolated at the indicated time points and displayed as the percent of wild type spores at 72 h. Spore numbers are the average and associated standard deviation of three biological replicates. Scale bar = 0.5 mm; nd, not determined. *B, EspC developmental protein accumulation patterns.* Anti-EspC immunoblot analysis of cell lysates prepared from the indicated strains developed for the indicated hours using a 16 ml submerged culture format.

Simultaneous substitution of the phospho-accepting aspartate residue 749 (*espC* $_{H461Q,D749A}$) restored the early developmental phenotype. The EspC protein production of the *espC*$_{H461Q}$ strain was reduced compared to the wild type, however, the *espC*$_{H461Q, D749A}$ strain showed the same early and steeper EspC protein accumulation as the *espC*$_{D749A}$ strain (**Figure 22**B). As the *espC*$_{H461Q, D749A}$ mutant immunoblot analysis showed early and high EspC protein accumulation, I consider it unlikely that the histidine to glutamine substitution negatively influenced the protein stability of EspC. Therefore, the intermediate early developmental phenotype of the *espC*$_{H461Q}$ strain is likely due to differential signaling in EspC rather than due to partial protein instability. Together, this analysis suggests that a histidine to glutamine substitution in EspC might activate or turn on the putative EspC phosphatase activity.

EspA acts as a phosphatase in the Esp system

Since I showed that EspA phosphorylates the EspC$_{REC}$, I was also interested to determine whether EspA additionally functions as a phosphatase on the Esp system. A substitution mutation in the EspA putative phosphatase motif (*espA*$_{N411D}$) displayed a delayed developmental phenotype (**Figure 23**B).

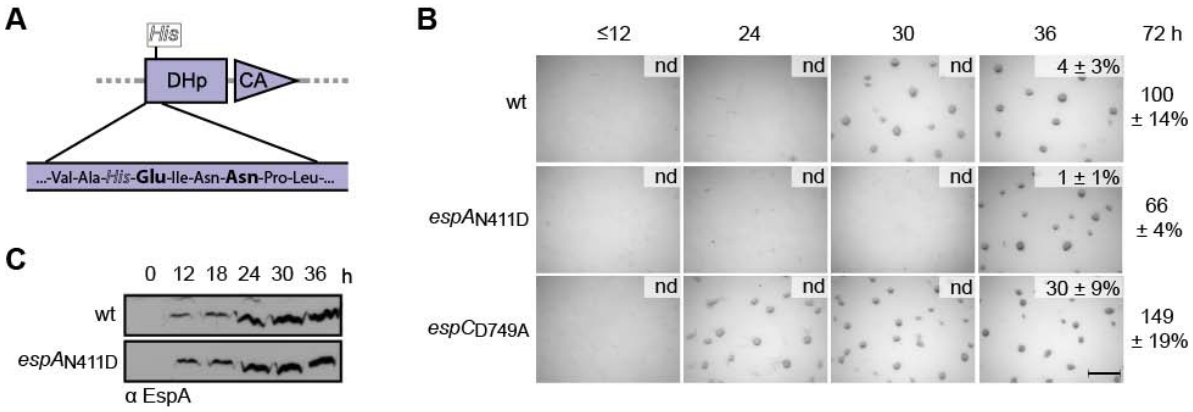

Figure 23 Disruption of the putative phosphatase motif in EspA effects developmental progression. *A, Putative phosphatase motif within the DHp domains of EspA.* The amino acid sequence surrounding the putative phosphatase motif $[H]^{E}/_{D}XX^{T}/_{N}$ [111] in EspA is displayed magnified from the scheme of a HK region. The invariant histidine residue is drawn italicized; the residues putatively mediating phosphatase activity are bold. *B, Developmental phenotypes of e*spA *phosphatase-motif mutants.* Wild type (wt; DZ2), *espC*$_{D749A}$ (PH1027), and *espA*$_{N411D}$ (PH1045) strains were developed under submerged culture in 24-well culture dishes, and pictures were recorded at the indicated hours of development. Heat and sonication resistant spores were isolated at the indicated time points and displayed as the percent of wild type spores at 72 h. Spore numbers are the average and associated standard deviation of three biological replicates. Scale bar = 0.5 mm; nd, not determined. *C EspA developmental protein accumulation pattern.* Anti-EspA immunoblot analysis of cell lysates prepared from the indicated strains developed for the indicated hours using a 16 ml submerged culture format.

Aggregation centers could be observed between 30 h and 36 h of development, approximately six hours later than observed for the wild type. Consistent with the delayed aggregation phenotype, the production of resistant spores was also reduced in the *espA*$_{N411D}$ strain. After 72 h of development the *espA*$_{N411D}$ strain only produced ~66 % of wild type spores. The EspA$_{N411D}$ protein accumulation pattern was indistinguishable from the wild type (**Figure 23C**, compare also section 2.2.1). Together with the *in vitro* phosphotransfer analysis (section 2.2.5) these data further support the assumption that EspA acts as a phosphatase to regulate the Esp system.

2.3.2 The EspC sensing domains might regulate the Esp system

As described in section 1.3, EspA and EspC both contain multiple sensing domains (**Figure 10** and **Figure 12**A). All the EspA sensing domains likely contribute to the developmental regulation mediated by the Esp system, because the *espA*$_{\Delta PAS1-2}$, *espA*$_{\Delta FHA}$ and the *espA*$_{\Delta FHA,\Delta PAS1-2}$ strains all displayed an early aggregation phenotype[11]. To gain a better understanding about the regulatory role of the EspC sensing domains, deletion mutations of the EspC sensing domains were generated and analyzed.

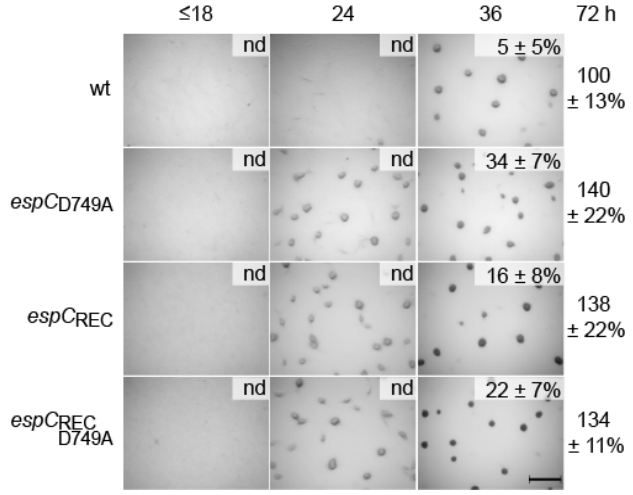

Figure 24 The EspC sensing domains might be involved in regulation the Esp system. *A, Developmental phenotypes of* espC *sensing domains mutants.* Wild type (wt; DZ2), *espC*$_{D749A}$ (PH1027), *espC*$_{REC}$ (PH1070) and *espC*$_{REC,\ D749A}$ (P1071) strains were developed under submerged culture in 24-well culture dishes, and pictures were recorded at the indicated hours of development. Heat and sonication resistant spores were isolated at the indicated time points and displayed as the percent of wild type spores at 72 h. Spore numbers are the average and associated standard deviation of three biological replicates. Scale bar = 0.5 mm; nd, not determined.

[11] P. Mann and P. I. Higgs, unpublished data

Since the genetic analysis suggested that the $EspC_{REC}$ was sufficient to mediate repression of developmental progression, the first attempt was to delete the entire region amino terminal to the receiver domain, resulting in the *espC*$_{REC}$ and the *espC*$_{REC\ D749A}$ strains. Both strains resulted in an early developmental phenotype which was indistinguishable from that of the Δ*espC* strain (**Figure 24**, also compare section 2.1.1). This observation could arise from three different possibilities: (a) the protein is not produced by the cells, (b) the protein interaction between $EspA_{HK}$ and $EspC_{REC}$ is perturbed such that EspA is no longer able to phosphorylate $EspC_{REC}$ or (c) the deleted sensing domains regulate the Esp system resulting in an early developmental phenotype. Unfortunately, the ~19 kDa $EspC_{REC}$ protein could not be detected by the anti-EspC immunoblot, because an intense cross reactive band was detected at its predicted molecular mass in the wild type and the *espC*$_{REC}$ lysates (data not shown). Thus, by means of this analysis it was not possible to clarify whether and how EspC's sensing domain interfere with the Esp signaling, resulting in an early developmental phenotype.

2.3.3 The EspC PAS domain regulates the output of the Esp system

Since the analysis of the *espC*$_{REC}$ and the *espC*$_{REC\ D749A}$ strains did not allow interpretation of the associated phenotype, I further generate a mutant lacking the EspC PAS domain (*espC*$_{\Delta PAS}$). The analysis of the *espC*$_{\Delta PAS}$ mutant strain revealed a developmental phenotype which was intermediate between the wild type and the Δ*espC* strain (**Figure 25**A). Aggregation could be observed at 27 h of development, approximately three hours earlier than the wild type and three hours later than the Δ*espC* strain. The production of resistant spores was also intermediate compared to the wild type and the Δ*espC* strain. By 36 h, a significantly higher number of resistant spores were produced compared to the wild type, but not as high as the number of spores produced by the *espC*$_{D749A}$ strain. The final number of resistant spores produced was ~100 %, ~149 % and ~175 % for the wild type, the *espC*$_{\Delta PAS}$ and the *espC*$_{D749A}$ strain, respectively. Importunely, in the *espC*$_{\Delta PAS,D749A}$ strain the early aggregation developmental phenotype was restored. At 36 h of development, the spore number produced by the *espC*$_{\Delta PAS,D749A}$ strain was slightly reduced (~28 %) compared to that of the *espC*$_{D749A}$ strain (~53 %). After 72 h of development the *espC*$_{\Delta PAS,\ D749A}$ strain produced as many heat and sonication resistant spores as the *espC*$_{D749A}$ strain (172 % and 175 %, respectively). The EspC protein accumulation pattern of the *espC*$_{\Delta PAS}$ strain revealed, that the protein level was at each time point lower than for

the wild type (**Figure 25** B). The earlier developmental phenotype of the *espC*$_{\Delta PAS}$ strain could therefore also arise from destabilized EspC. However, I consider this as unlikely, because the *espC*$_{\Delta PAS,\ D749A}$ strain produced as much EspC as the *espC*$_{D749A}$ strain, suggesting that the reduced protein level is likely the result of interfering with the EspC signaling. Together, these analyses demonstrate that the EspC PAS domain is modulating the output of the Esp regulatory system. Interestingly, the *espC*$_{\Delta PAS}$ mutant phenotype is reminiscent of the *espC*$_{H461Q}$ mutant phenotype, suggesting that the EspC PAS domain might be involved in regulating the phosphatase activity of EspC.

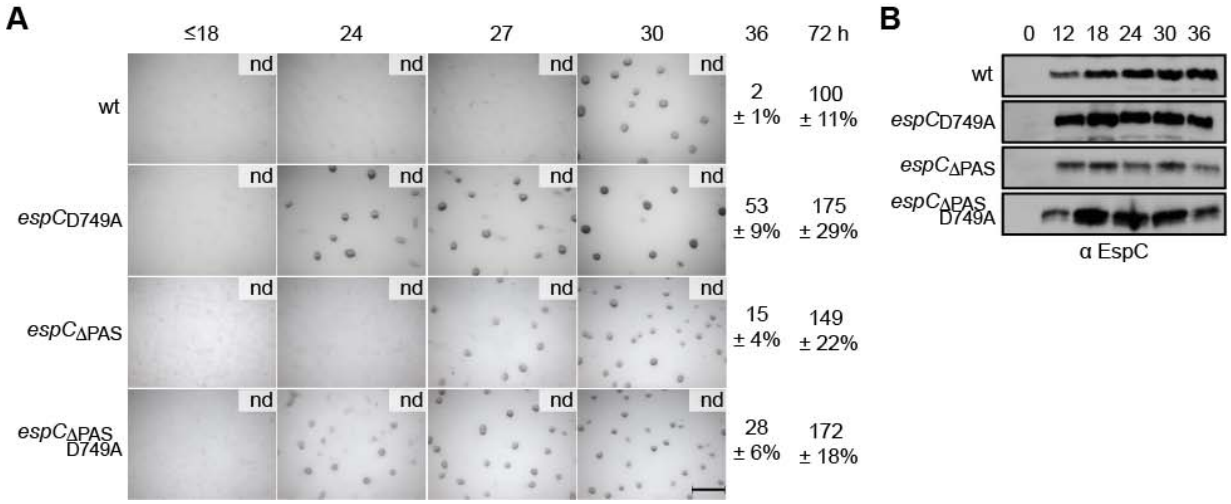

Figure 25 The EspC PAS domain is involved in developmental regulation. *A, Developmental phenotypes of* espC *PAS mutants.* Wild type (wt; DZ2), *espC*$_{D749A}$ (PH1027), *espC*$_{\Delta PAS}$ (PH1042) and *espC*$_{\Delta PAS,\ D749A}$ (PH1043) strains were developed under submerged culture in 24-well culture dishes, and pictures were recorded at the indicated hours of development. Heat and sonication resistant spores were isolated at the indicated time points and displayed as the percent of wild type spores at 72 h. Spore numbers are the average and associated standard deviation of three biological replicates. Scale bar = 0.5 mm; nd, not determined. *B, EspC developmental protein accumulation patterns of* espC *PAS domain mutants.* Anti-EspC immunoblot analysis of cell lysates prepared from the indicated strains developed for the indicated hours under 16 ml submerged culture format.

2.3.4 Differential expression of EspA and EspC might regulate cell fates

At 24 hours of development, EspA is three times more abundant than EspC

In many regulatory systems, the differential expression of regulatory proteins changes the signaling state of the system. To decipher the molar relationship between EspA and EspC, the signal intensities from a standard curve of the recombinant proteins Trx-EspA-His$_6$ and EspC$_{\Delta MASE1}$-His$_6$ were compared with different concentrations of lysates from wild type cells developed for 24 h (**Figure 26**, A and B, respectively). The titration of the purified, recombinant Trx-EspA-His$_6$ showed a linear increase of the signal intensity except for the 5

ng protein lane, in which the signal was saturated (**Figure 26**, A and C, black line). The titration of the purified, recombinant $EspC_{\Delta MASE1}$-His_6 also displayed a linear increase of the signal intensity (**Figure 26**, B and C, grey line). By comparing the signal intensities from EspA and EspC immunoblots from developmental lysates to the standard curves generated from the purified recombinant protein, the relative abundance of EspA and EspC could be calculated (**Figure 26**, D). These calculations (section 4.4.6) suggested that in one µg lysate, approximately 1.5 fmol EspA and 0.5 fmol EspC were detected. 10 µg lysate equal roughly the protein amount produced from $4x10^7$ cells developed for 24 h[12], therefore EspA is present at ~225 copies and EspC at ~75 copies per cell. These numbers of HPK molecules are in line with the abundance of other reported TCS signaling proteins; for example in exponentially growing *E. coli* cells EnvZ is present at ~100 copies per cell [117]. To our surprise, EspA was approximately three times more abundant than EspC, suggesting that EspA and EspC either do not interact in a 1:1 ratio, or that EspA and EspC are differentially produced in individual cell populations at 24 h of development.

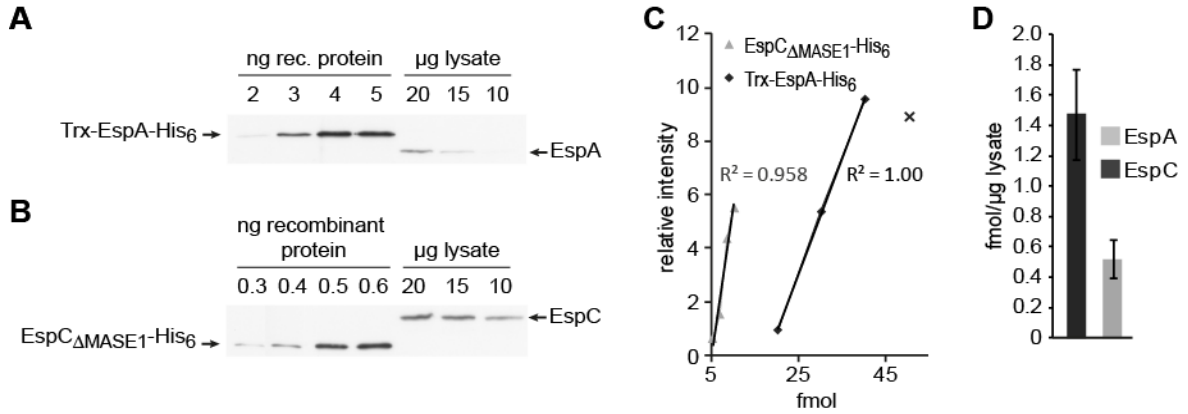

Figure 26 EspA is ~ 3 times more abundant that EspC in 24 h developed wt cells cells. *A, EspA protein titration experiment with whole population lysates from 24 h developed wild type cells.* Dilutions of recombinant produced Trx-EspA-His_6 and lysates from 24 h developed wild type (wt, DZ2) cells were subjected to anti-EspA immunoblot analysis. *B, EspC protein titration experiment of whole population lysates from 24 h developed wild type cells.* Dilutions of recombinant produced $EspC_{\Delta MASE1}$-His_6 and lysates from 24 h developed wild type (wt, DZ2) cells were subjected to anti-EspC immunoblot analysis. *C, Quantification of the titrated antigens for EspA and EspC from A and B, respectively.* The signal intensities from A and B were quantified and plotted against the different concentrations of the recombinant Trx-EspA-His_6 and $EspC_{\Delta MASE1}$-His_6 proteins. *D, Relative abundance of EspA and EspC in whole population lysates from 24 h developed wild type cells.* The signal intensities of the different lysate concentrations from the anti-EspA and anti-EspC immunoblots in A and B were quantified and compared to the signal intensities from the recombinant proteins in C.

[12] A 16 ml petri dish developed for 24h contains ~$1x10^{10}$ cells, which produce ~2.5 µg total protein

EspC is differentially produced in the two cell populations aggregated vs. non-aggregated cells

Since it was observed that EspA is three times more abundant than EspC in whole population lysates, I next wanted to further elucidate how EspA and EspC are expressed in the different cell populations aggregated and non-aggregated cells. Throughout the whole developmental program aggregated and non-aggregated cells can be separated using a low force centrifugation; at the early time points, the aggregated cell fraction is composed of cell clusters, later during development, also cells which transition into the cell clusters will be present in the aggregated cell fraction [124, 126, 173]. The separated cell fractions were subsequently analyzed by anti-EspA, anti-EspC and anti-FibA immunoblots. The extra cellular metalloprotease FibA served as a control protein for the separation, because it is reported to be exclusively produced by the aggregating cells [173] (**Figure 27**A, lower panel). Consistent with the whole population EspA immunoblot analysis (section 2.1.1), the protein level of EspA were upregulated throughout the early steps of the developmental program, but the protein levels appeared equally represented in the aggregated and non-aggregated fraction (**Figure 27**A, upper panel). Accordingly, the quantification of three independent separation experiments showed no significant difference between the two populations at each analyzed time point (**Figure 27**B).

In contrast, the EspC protein production was different between the aggregated and non-aggregated cells (**Figure 27**A, middle panel). At 18 h of development, EspC is highly enriched in the aggregated cell population (**Figure 27**B). Later, however, the distribution of EspC between the two populations changed; at 24 h of development, EspC was significantly enriched in the non-aggregated fraction, and this tendency remained visible at 30 h, although the significance level was not as reliable (P=0.12). Interestingly, the relative signal intensity of EspC remained constant in the aggregated cell population, suggesting that EspC is produced differentially in the non-aggregating fraction. The 66 kDa fragment of the control protein FibA (p66) was highly enrichment in the aggregated cell population at 18 h and 24 h of development; at 30 h a slight contamination of FibA containing cells was detected in the not-aggregated population. The average relative signal intensities of FibA at 18 h, 24 h and 30 h were highly significantly different between the two populations ($p = 0.018$, $p = 0.0008$ and $p = 0.025$, respectively; data not shown). The slight contamination of aggregated cells in the non-aggregated population at 30 h of development might explain the variability which was observed for the average relative EspC signal intensities at this time point (**Figure 27**B). Thus, this analysis revealed that EspC, but not

EspA is differentially produced in the two developmental subpopulations of aggregated cells and non-aggregated cells. Additionally, it suggests that the differential EspC production is exclusively controlled in the non-aggregated cell population.

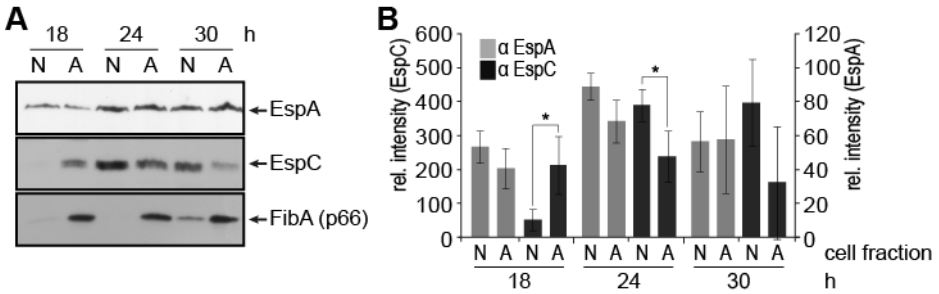

Figure 27 EspC is differentially regulated in non-aggregated and aggregated cells. *A, Developmental cell separation experiment.* The wild type (wt; DZ2) strain was developed under submerged culture in 16 ml culture dishes. At the indicated time points the cell populations were separated using a low force centrifugation (50 xG) into aggregated cells and non-aggregated cells. 20 µg of each fraction were resolved by SDS-PAGE and subjected to immunoblot analysis. EspC and EspA, hybrid histidine protein kinases; FibA (p66), 66 kDa fragment of the aggregating cell specific metallo-protease FibA. *B, Quantification of the EspA and EspC cell fraction specific distribution.* The average relative signal intensities together with the associated standard deviation of three independent developmental cell separation experiments are plotted. N, not-aggregated cells; A, aggregated cells, *; significantly different ($P<0.05$).

2.4 The Esp system regulates the protein level of MrpC by proteolysis

2.4.1 The half-life of MrpC is regulated by the Esp signaling system

MrpC is a transcription factor with an essential role in the developmental program, regulating both aggregation and sporulation [141]. Previous analyses revealed that in the Δ*espA* mutant, MrpC protein was produced earlier during the developmental program than in the wild type [158]. Since *mrpC* transcription was not affected in a signaling deficient $espA_{H407A}$ strain, it was proposed that EspA is involved in regulating the protein level of MrpC during developmental progression. As the results obtained in this study suggest that EspA and EspC act together in regulating developmental progression, I examined whether and how the different *espC* mutant strains (Δ*espC*, $espC_{H461A}$, $espC_{D749A}$ and $espC_{H461A,D749A}$) affect the protein level of MrpC (**Figure 28**A). In the wild type strain, MrpC protein was detected from the beginning of the developmental program (T = 0 h). The levels then first decreased (0 h – 12 h) followed by re-accumulation, peaking between 24 h and 30 h of development. The $espC_{H461A}$ strain, which displayed a developmental progression indistinguishable from the wild type strain (**Figure 15**A), also produced MrpC protein similar to the wild type, however, with reduced level of MrpC at 36 h of

development. Interestingly, all the early developing *espC* mutant strains (Δ*espC*, *espC*$_{D749A}$ and *espC*$_{H461A,D749A}$) showed a more rapid re-accumulation of MrpC with clearly increased protein levels at 18 h of development compared to the wild type. Together, these data suggest that early protein re-accumulation of MrpC correlates with early developmental phenotypes, resulting from mutations in *espC*. Since it was previously shown that a Δ*espA* strain does not affect *mrpC* transcription, we hypothesize that the Esp signaling system -consisting of EspA and EspC- either regulates translation or protein turnover of MrpC.

In order to distinguish between these two possibilities, the MrpC protein level was examined in cells which were starved for nine hours and then blocked for *de novo* protein synthesis by addition of chloramphenicol (**Figure 28**B). As a control for nonspecific degradation I also followed the protein level of an elongation factor involved in mRNA translation (EF-TU). The EF-TU protein level remained constant and therefore EF-TU was not subjected to non specific proteolytic degradation in the wild type strain (data not shown).

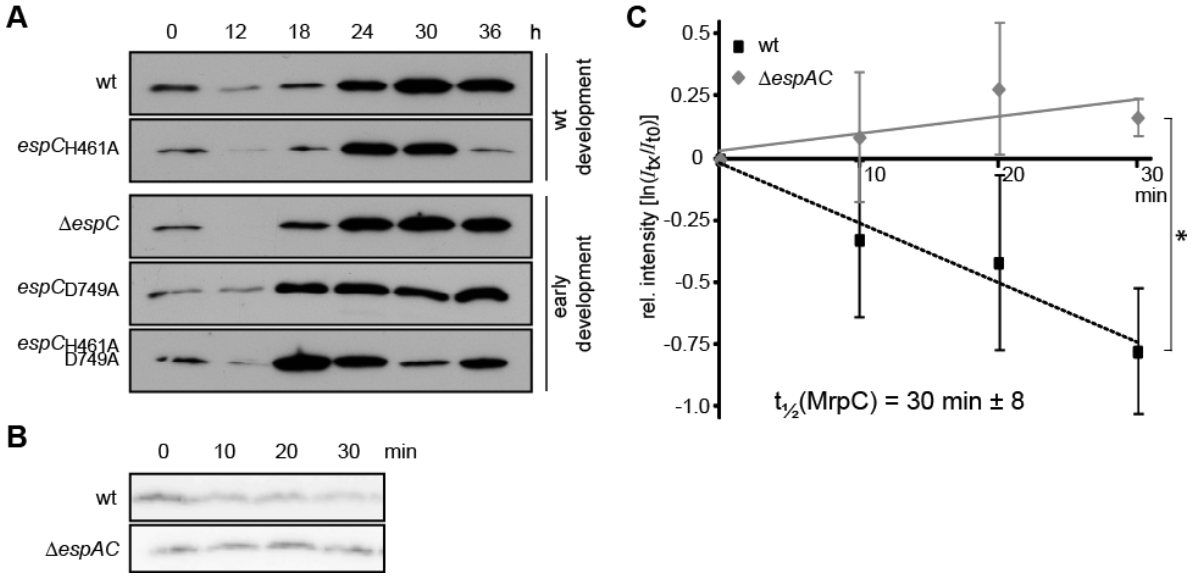

Figure 28 The Esp system negatively regulates MrpC protein stability. *A, MrpC developmental protein accumulation patterns.* MrpC protein pattern were analyzed in the wild type (DZ2, wt), Δ*espC* (PH1044), Δ*espA*Δ*espC* (PH1047), *espC*$_{H461A}$ (PH1026), *espC*$_{D749A}$ (PH1027) and *espC*$_{H461A,D749A}$ (PH1028) strains. 10 µg total protein lysates from cells developed for the indicated hours in the 16 ml submerged culture format were subject to anti-MrpC immunoblot. *B, Chloramphenicol chase of MrpC.* Wild type (wt) or Δ*espA*Δ*espC* (PH1047) cells were developed for nine hours as above and were subsequently treated with 34 ug ml^{-1} chloramphenicol for the indicated minutes. Equal proportions of the samples were subject to anti-MrpC immunoblot. *C, Calculation of the half-life (T½) of MrpC.* Triplicate biological replicates of wild type (DZ2, wt, black line) and Δ*espA*Δ*espC* (PH1047, gray line) chloramphenicol chase experiments represented in *B* were performed, and the MrpC band intensity for each time point was normalized to T=0 of the respective strain and averaged. The natural log of the average intensities was plotted vs. the minutes of chloramphenicol treatment. The slope of a linear fit of the data was used to calculate the MrpC T½ in wild type cells as described in the experimental procedures. *, average intensity values are significantly different (p=0.003).

In contrast, a gradual decrease of MrpC protein was observed over a time period of 30 minutes in the wild type strain, suggesting that MrpC was degraded. Interestingly, in the Δ*espA*Δ*espC* mutant strain the MrpC protein level remained unaffected. This data suggests that the degradation of MrpC is indeed regulated by the Esp signaling system. Quantification of three independent chloramphenicol chase experiments revealed a half-life of MrpC of approximately 30 minutes in the wild type strain (**Figure 28**C), whereas in the Δ*espA*Δ*espC* strain, MrpC did not appear to be turned over. The analysis of the MrpC level in the Δ*espA*Δ*espC* strain in fact showed a slight increase of the MrpC protein level, suggesting that the chloramphenicol did not fully block *de novo* protein synthesis during 30 minutes of treatment. Together, these analyses reveal that MrpC is subject to proteolytic degradation in the wild type strain, and that this degradation is directly or indirectly controlled by the Esp signaling system during development.

2.4.2 A serine protease mediates degradation of MrpC

The observation that the Esp system regulates the turnover of MrpC protein, prompted the identification of the protease which is degrading MrpC. The *M. xanthus* genome encodes for 263 predicted proteases (http://merops.sanger.ac.uk/index.shtml), therefore putative candidates were narrowed down using a proteases inhibitor screen ([148], **Figure 29**A). The protease inhibitors were applied to a MrpC chase experiment (section 2.4.1), and the MrpC protein level were determined by immunoblot after 0 min and 30 minutes of co-incubation (**Figure 29**B and **Figure 29**C). As observed before, chloramphenicol treatment lead to a reduction of the initial MrpC signal to ~ 37 % in the wild type (**Figure 29**B, lanes 1 and 2 and **Figure 29**C), but only to a minor reduction in the Δ*espA*Δ*espC* strain (**Figure 29**B, lanes 10 and 11 and **Figure 29**C). The application of different protease inhibitors (**Figure 29**B, lanes 3-9 and **Figure 29**C) resulted in three different pattern of MrpC degradation. First, aprotinine, benzamidine and E-64 did not significantly protect MrpC from degradation (**Figure 29**B, lanes 6-8), since the MrpC signal after 30 min of treatment was indistinguishable to that of the untreated control (**Figure 29**C). Second, EDTA treatment lead to a slight, but significant, reduction to ~62 % of the initial MrpC protein level (**Figure 29**B lane 4 and **Figure 29**C). Third, SMPI and PMSF resulted in a nearly complete block of the proteolytic activity on MrpC (**Figure 29**B lanes 3 and 5), because the signal intensity after 30 min was indistinguishable from the levels detected in the Δ*espA*Δ*espC* strain at 30 min (~89 % of the initial MrpC protein, **Figure 29**C). Since PMSF was dissolved in 99 % ethanol, I confirmed that ethanol did not influence the MrpC

protein level; after 30 min of ethanol treatment, the MrpC levels were indistinguishable from the wild type control (**Figure 29**B lane 9 and **Figure 29**C). Thus, as SMPI and PMSF block serine proteases, this protease inhibitor screen suggests that the protease that is responsible for the degradation of MrpC is a serine protease.

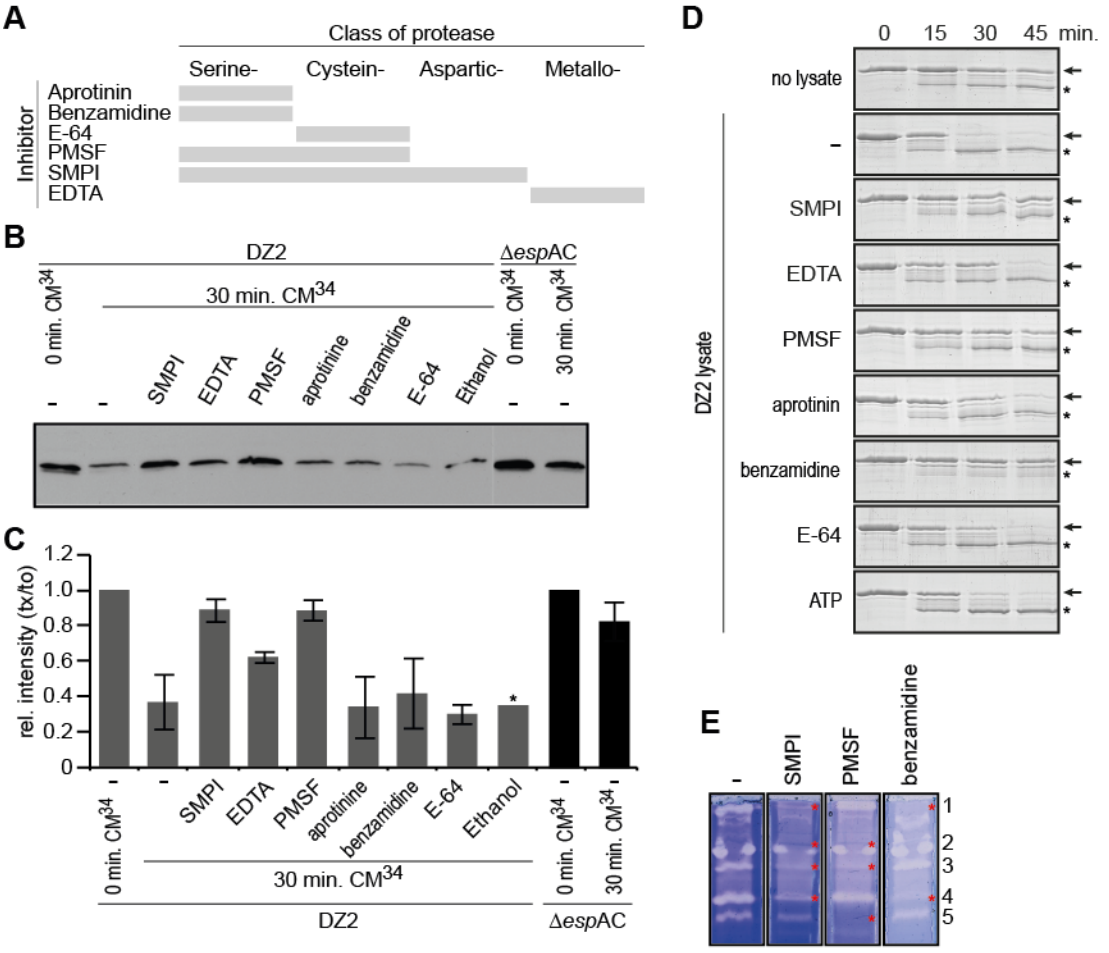

Figure 29 MrpC is likely degraded by a serine protease. *A, Schematic representation of the inhibitory spectrum of different protease inhibitors.* The inhibitory spectrum of six protease inhibitors (Aprotinin, Benzamidine, E-64, PMSF, EDTA, SMPI cocktail) is represented by vertical grey bars. *B,* in vivo *chloramphenicol chase of MrpC in the presence of different protease inhibitors.* Wild type (wt, DZ2) or Δ*espA* Δ*espC* (PH1047) cells were developed for nine hours in a 16 ml submerged culture format and treated with 34 ug ml^{-1} chloramphenicol with or without different protease inhibitors for 30 min. Equal proportions of the samples were subject to an anti-MrpC immunoblot. *C, Quantification of the inhibitory effect of the protease inhibitors*. The MrpC signal intensities of triplicate biological replicates of the chloramphenicol chase experiments in *B* were quantified and normalized to T=0 of the respective strain and averaged. The error bars represent the SD. *, data from only one experiment. *D,* in vitro *MrpC turnover experiment.* 2 µg purified recombinant His_6-MrpC were co-incubated with different protease inhibitors and 5 µg of 12 h developmental lysates from either the wild type (wt, DZ2) or the Δ*espA* Δ*espC* (PH1047) strains for the indicated minutes at 32°C. *; putative cleavage product formed, ←, MrpC. *E,* In gel *MrpC turnover experiment.* 150 µg ml^{-1} recombinant purified His_6-MrpC was co-polymerized in a 11 % SDS-PAG and 7.5 µg of 12 h developmental lysates were resolved in this modified zymogram gel. Proteins were refolded and incubated for 22 h in activity buffer at 32 °C. The gel was stained using Coomassie G250, zones of proteolysis appeared as cleared spots. *, indicate cleared zones which were absent in the reaction with a specific protease inhibitor.

To account for the problem that certain protease inhibitors might not be able to diffuse into the intact cells, I next examined whether MrpC proteolysis can be reconstituted *in vitro* (**Figure 29**D). Therefore, purified recombinant His_6-MrpC was incubated with wild type developmental lysates in either the presence or absence of protease inhibitors. Even if no lysate was added to the His_6-MrpC protein preparation, a slight decrease of the recombinant MrpC was detected. Simultaneously, a putative degradation product appeared (asterisk) and increase gradually, suggesting that the recombinant MrpC preparation contained a co-purified *E. coli* protease. However, when developmental wild type lysate was added to the reaction, a significantly higher rate of MrpC degradation was detected. After 30 min of co-incubation, almost all the recombinant MrpC was degraded, and simultaneously the putative degradation product increased until 30 min and then stayed constant. The application of the different protease inhibitors resulted in two different patterns of protection from MrpC degradation. First, the application of SMPI, PMSF and benzamidine resulted in a MrpC degradation pattern indistinguishable from the no lysate control, indicating that these three protease inhibitors blocked the MrpC degradation. Second, the addition of EDTA, aprotinine and E-64 resulted in a slight reduction in the MrpC degradation, but after 45 min of incubation, the recombinant His_6-MrpC was nearly completely degraded. In the *in vivo* MrpC turnover experiments (**Figure 28**B and **Figure 29**B), MrpC was completely degraded and no cleavage product could be detected by immunoblot analysis. In contrast, in the *in vitro* MrpC turnover experiment, a smaller product appeared which increased during the experimental time period (**Figure 29**D, asterisk).

One possible explanation for this discrepancy is that this degradation product might be further degraded by an ATP-dependent proteasomal reaction *in vivo* and that ATP might be the limiting factor for the further degradation *in vitro*. To test whether the addition of ATP could trigger further degradation of this smaller product, 10µM ATP was added to the *in vitro* MrpC turnover experiment. However, the addition of ATP did not result in an enhanced proteolysis of MrpC, suggesting that this putative degradation product cannot be degraded further under these experimental *in vitro* conditions. Together, these results suggest that MrpC degradation could be efficiently blocked by the addition of SMPI and PMSF *in vivo* and SMPI, PMSF and benzamidine *in vitro*, suggesting that the protease which degrades MrpC is a serine protease.

To sum up, the protease inhibitor screen was successful to narrow putative proteases down. Unfortunately, 149 of the 263 predicted proteases in the *M. xanthus* genome are serine

proteases which belong to 19 different families (http://merops.sanger.ac.uk/index.shtml). Thus, a modified zymogram approach was used as an initial attempt to identify the specific serine protease mediating MrpC degradation. Developmental cell lysates were resolved in a SDS-PAGE containing co-polymerized MrpC (Z-PAG). After resolving the cell lysates, the proteins were refolded within the Z-PAG and subsequently incubated either with or without protease inhibitors, to allow for *in gel* protease activity. Proteolytically digested MrpC appeared as cleared spots in the Z-PAG and regions which were no longer cleared after addition of protease inhibitors represented an inhibited protease (protection zone) (**Figure 29**E). The addition of the different protease inhibitors (SMPI, PMSF and benzamidine) resulted in a differential MrpC clearing pattern (asterisk); however, the three different serine protease inhibitors did not show a consistent pattern. SMPI and PMSF share the protected zones 2 and 3, while SMPI and benzamidine share the protected zones 1 and 4. PMSF and benzamidine did not share any protected zone, the zone 5 could only be observed using PMSF. As an attempt to identify a specific MrpC degrading protease, the protected zone 1 from the Z-PAG was analyzed by nano-LC-MS-MS. Unfortunately, no putative protease could be identified by this preliminary analysis. Thus, the serine protease mediating MrpC degradation remains to be elucidated.

3. DISCUSSION

Histidine-aspartate signaling systems have been studied for approximately four decades. Clearly, our view of these signaling systems changed over this period of research away from simple, linear and mono functional two component systems, towards highly sophisticated, modular and "networking" signaling modules. The challenge in His-Asp signaling research today is to understand the relationships and the wiring of this highly complex signaling proteins as well as the variety of unorthodox signaling mechanism of such systems. One of the biggest challenges is the identification of His-Asp signaling system pairs out of orphan gene organizations.

M. xanthus is a premier organism to study such complex signaling systems, as its genome encodes for a large repertoire of 251 non chemosensory His-Asp signaling proteins [122]. Interestingly, from these 251 genes only 29 % are organized as paired genes which is the most common organization in model organism like e.g. *E. coli* (72 %), *P. aeroginosa* (57 %) or *B. subtilis* (86 %). Instead, the majority is organized in either complex gene clusters (16 %) or as orphan genes (55 %). This unorthodox genetic organization of this large number of His-Asp signaling genes suggests a rather complex relationship of the encoded signaling proteins.

In the presented thesis I assigned the orphan HyHPK, EspC into the EspA/EspC/PktA5/PktB8 signaling system which negatively regulates developmental progression of *M. xanthus* (**Figure 30)**. In this Esp signaling system, the two HyHPK EspA and EspC form a complex and novel signal transduction module**.** I was able to show that the combined phosphorylation of both $EspA_{REC}$ and $EspC_{REC}$ is absolutely required for the repression of developmental progression and that the phosphorylation of both receiver domains is surprisingly achieved only by the $EspA_{HK}$, via inter- and intraprotein phosphorylation. The combined phosphorylation of $EspA_{REC}$ and $EspC_{REC}$ then drives the proteolytic degradation of the central transcription factor, MrpC, via an as yet unknown serine protease. Further, I gained initial evidence that the Esp system is likely regulated by phosphatase activity from both EspA and EspC. Additionally, there is growing evidence, that the Esp system is involved in cell fate determination processes in the *M. xanthus* developmental program.

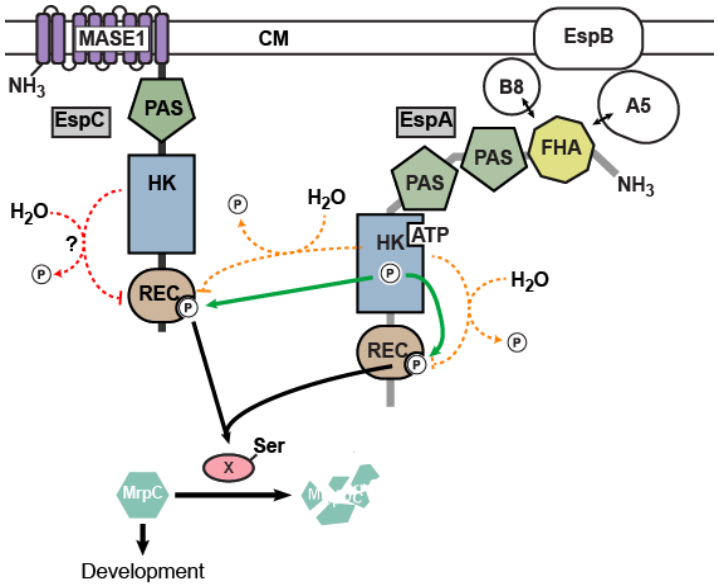

Figure 30 The Esp regulatory system utilizes inter- and intraprotein phosphorylation as a novel signaling mechanism. Two hybrid histidine kinases EspC (left) and EspA (right) regulate the accumulation rate of an important developmental regulator, MrpC (teal), in order to ensure appropriate and coordinated progression through the *M. xanthus* developmental program. EspC is anchored in the cytoplasmic membrane (CM) by a MASE1 sensing domain of unknown function [55]. The combined phosphorylation of the EspA and EspC receiver domains (REC) presumably activates an unknown serine protease (X) to stimulate MrpC turnover (black arrows). The EspA histidine kinase region (HK) autophosphorylates and donates a phosphoryl group to both its own and the EspC receiver domains (green arrows). Autophosphorylation of the EspC histidine kinase domain is not required for system output. Activity of EspA is controlled by the PktA5 (A5), PktB8 (B8) and EspB signaling module [157, 163]. The two serine/threonine kinases are thought to interact with the forkhead associated domain (FHA) in EspA [163]. Two Per-Arnt-Sim (PAS) domains in EspA and one in EspC are presumably involved in sensing of internal or membrane associated stimuli [53, 69]. EspA likely acts as a phosphatase towards its own REC [158] and the EspC REC (orange dashed lines). EspC might act as a phosphatase, thereby the EspC PAS domain might be involved in regulating the EspC phosphatase activity. The array of signaling domains may allow cell fate specific accumulation of MrpC within the developmental program.

3.1 Two orphan HyHPK, EspA and EspC, build one intimate signaling system

The genetically orphan HyHPK, EspC, was discovered in a screen that aimed for the identification of the signal output for the EspA/EspB/PktA5/PktB8 signaling module[13] [157-159, 163]. To test the relationships between EspA and EspC, genetic epistasis analysis was used. If EspC and EspA participate in one signaling pathway, the principle of a genetic epistasis analysis would suggest that Δ*espA* and Δ*espC* strains display the same developmental phenotypes (reviewed in [174]). Consistently, the analysis of the Δ*espA*, Δ*espC* and Δ*espAC* strains revealed exactly the same developmental phenotype, indicating that EspA and EspC likely participate in one signaling pathway (**Figure 11**). In line with

[13] K. Cho, unpublished data

this assumption, EspA and EspC transcription is similarly regulated during development[14]. Both genes are up-regulated upon induction of development; showing peak expression at ~12 h of development and share a nearly identical expression pattern over 36 h of development (**Figure 10**). Additional support for the hypothesis that EspA and EspC build one signaling system came from the bioinformatic analysis (**Figure 12**). This analysis revealed that EspA, EspC, MXAN_0095, MXAN_0195 and MXAN_2386 are closely related homologs. Interestingly, however, only EspA, EspC and MXAN_0195 show 100 % preservation in the closely related genomes. This indicates that EspA and EspC are functionally related. Although MXAN_0195 showed preservation in the cystobacterineae, microarray analysis revealed that, in contrast to EspA and EspC, MXAN_0195 is not regulated during development [122]. Therefore I do not consider it likely that MXAN_0195 also participates in the Esp signaling system. Generally, it is thought that new His-Asp phosphorelay systems evolve either by horizontal gene transfer (HGT) or linage specific expansion (LSE) [5]. Since I was unable to find EspA or EspC orthologs in other genomes outside of the cystobacterineae, it seems likely that EspA and EspC (and the additional three homolog HyHPK) evolved by LSE within this suborder of myxobacteria.

The hypothesis that EspA and EspC participate in one single signaling complex consequently suggests interaction between EspA and EspC; either as a higher order complex build out of EspA dimmers and EspC dimers or as an EspA-EspC heterodimer. A first example of heterodimer formation in bacteria was reported for the two HyHPKs RetS and GacS which are involved in regulating biofilm formation in *P. aeruginosa* [17]. However, heterodimer formation between EspA and EspC is unlikely, because: (a) both recombinant $EspA_{HK}$-His_6 and $EspC_{HK}$-His_6 readily autophosphorylate *in vitro* (**Figure 16**) and (b) we were unable to detect interaction between the $EspC_{HK}$ and the $EspA_{HK}$ by yeast two hybrid analysis[15]. Instead, self-interaction of $EspA_{HK}$ or $EspC_{HK}$ could be detected, suggesting homodimer formation of both HPKs. Moreover, in the just mentioned yeast two hybrid analysis interaction between full length EspA and $EspC_{\Delta MASE1}$ could be detected which further suggests that EspA and EspC homodimers interact in higher order oligomers. The protein fractionation experiments performed in this study further supported interaction between EspA and EspC, because the EspA membrane association was perturbed at 18 h of development in a Δ*espC* strain (**Figure 14**). Thus, EspA and EspC likely interact during the developmental program, and this interaction is not due to heterodimer formation of EspA

[14] B. Lee, PhD thesis
[15] T. Jeganathan and A. Schramm, unpublished data

and EspC, rather EspA and EspC homodimers interact in a higher molecular complex with each other.

The Esp system requires combined phosphorylation of $EspA_{REC}$ and $EspC_{REC}$, but the EspC invariant histidine is dispensable for signal transduction

In order to understand how EspA and EspC function within one signaling system, single substitution mutant strains of the invariant phospho-accepting residues in EspC were analyzed. This genetic analysis revealed that EspA and EspC both have to be phosphorylated simultaneously in order to mediate repression of developmental progression, since substitution of either the $EspA_{D696}$ or substitution of the $EspC_{D749}$ lead to exactly same early developmental phenotype (**Figure 15**A). The observation that the EspC invariant histidine residues have no effect on developmental progression, however, also indicates that the $EspC_{REC}$ does not accept phosphoryl groups from the $EspC_{HK}$. This is controversial to the paradigm of how a HyHPK functions; the internal REC of a HyHPK accepts phosphoryl groups from its own HK (**Figure 31**A (1), review in [2, 6]). This unusual finding was additionally supported by the analysis of a mutant lacking the entire CA domain. The phenotype of an $EspC_{\Delta CA}$ strain was reminiscent of that of the $EspC_{H461A}$ strain (**Figure 15** and **Figure 20**). Together, these genetic analyses strongly suggest that the EspC HK activity has no effect on regulation of development under our experimental conditions *in vivo*.

Controversially, the autophosphorylation experiments of truncated recombinant $EspC_{HK}$-His_6 protein revealed an *in vitro* autophosphorylation (**Figure 16**). However, a plausible explanation for this discrepancy is, that the $EspC_{REC}$ inhibits EspC's autophosphorylation *in vivo*. In line with this, it has recently, it has been reported for the *M. xanthus* HyHPK FrzE that the REC domain inhibits the autophosphorylation of the FrzE HK [99]. *In vitro* autophosphorylation of FrzE could only be observed if the FrzE REC was deleted or the invariant aspartate was substituted. In our genetic analysis the substitution of the invariant aspartate 749 resulted in an early developmental phenotype (**Figure 15**A); this phenotype could also be interpreted in a way that the autokinase inhibition by the $EspC_{REC}$ is released in this mutant. However, this alternate scenario had to be discarded, because an $EspC_{HK-REC}$-His_6 recombinant protein also autophosphorylated in the *in vitro* experiments (**Figure 16**). Thus, this analysis revealed that, at least under *in vitro* conditions, the internal $EspC_{REC}$ does not inhibit EspC autophosphorylation activity.

Finally, it remains to be elucidated if EspC also autophosphorylates *in vivo.* An elegant way to test the EspC autophosphorylation *in vivo* would be the analysis of developmental lysates

from the wild type and the *espC*$_{H461A}$ strain using Phos-tag™ PAGE followed by an anti-EspC immunoblot. Phos-tag™ is a chemical compound that can be co-polymerized within SDS-PAG and specifically interacts with phosphoryl groups of phosphorylated proteins and thus increases their retention time during the electrophoresis procedure [175]. If EspC autophosphorylates *in vivo*, the phosphorylated form of EspC should appear as an higher molecular mass band in the wild type but not in the *espC*$_{H461A}$ lysates.

Despite the uncertainties of the EspC$_{HK}$ autophosphorylation *in vivo*; substitution of the phosphor-accepting histidine 461 as well as the deletion of the entire EspC CA domain had no effect on developmental progression. Importantly, this indicates that the phosphorylation of the EspC$_{REC}$, which was indispensable for proper development, needs to be mediated by something different than the EspC$_{HK}$.

Inter- and intraprotein phosphorylation is a novel HyHPK signaling mechanism

Since EspC$_{HK}$ does not mediate phosphorylation of the EspC$_{REC,}$ there are two alternate possibilities of how the EspC$_{REC}$ might become phosphorylated: Either a small organic phosphoryl donor molecule such as acetyl phosphate [39] or an alternate histidine protein kinase donates phosphoryl groups to the EspC$_{REC}$, instead. I consider the former as unlikely, as it was not possible to detect EspC$_{REC}$ phosphorylation from acetyl phosphate *in vitro* (data not shown). Together with the notion that EspA and EspC likely form an intimate signaling system, I predicted EspA to be responsible for the EspC$_{REC}$ phosphorylation. Indeed, the biochemical phosphotransfer analysis confirmed this hypothesis that the EspA$_{HK}$-His$_6$ is able to donate phosphoryl groups to the EspC$_{REC}$-His$_6$ (**Figure 19**). Additionally, the analysis determined that the EspC$_{HK}$ is incapable of phosphorylating the EspC$_{REC}$ (**Figure 17**).

Generally, the phosphoryl group transfer in a HyHPK happens by a three step phosphorelay: (1) The phosphoryl group from the phosphorylated, invariant histidine residue in the HK is transferred to the internal REC. (2,3) Subsequently the phosphoryl group is shuttled via an HPT protein (2) to the terminal RR (3) (reviewed in [6]; **Figure 31**A). It has been thought so far that the only alternative to this paradigm is, that the HyHPK can transfer phosphoryl groups directly to a terminal RR, as shown for the CbbSR/CbbRR1/CbbRR2 system of *Rhodopseudomonas palustris* and the SgmT/DigR system of *Myxococcus xanthus* [176-178]; **Figure 31**B).

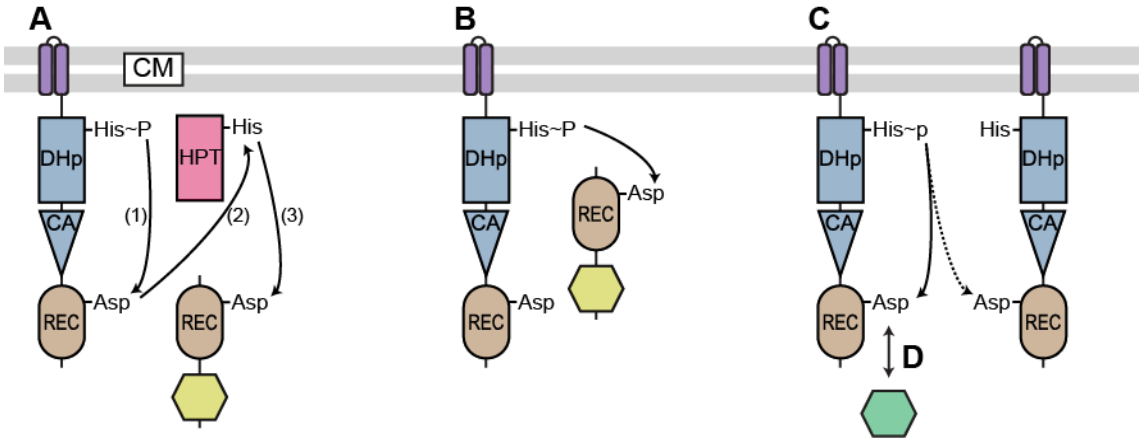

Figure 31 Functional properties of HyHPK signaling system. *A*, The prototypical phosphorelay system involving a HyHPK, a HPT protein and the terminal RR. *B*, HyHPKs can directly phosphorylate a RR without involving a HPT protein. *C*, Novel signaling mechanism involving inter- and intraprotein phosphorylation between two HyHPK. Details see Text. *D*, Proposed model of a HyHPK mediating signaling output directly via protein-protein interaction.

Further, this direct phosphorylation of the terminal RR by a HyHPK could be observed *in vitro* for the ArcA/ArcB system of *E. coli* [90, 96, 97], however, this seems not to play a significant role *in vivo* [179]. Thus, the observed interprotein phosphorylation from $EspA_{HK}$ to $EspC_{REC}$ displays a novel signaling mechanism of His-Asp signaling systems (**Figure 31**C).

It has been reported previously that receiver domains can either inhibit [99] or activate [82] cognate kinase activity. These two possibilities have to be disfavored for the Esp system, because if either of the two REC domains would inhibit the EspA kinase activity, the Δ*espC* (this study) or the $espA_{\Delta REC}$ strain [158] should not lead to exactly the same early developmental phenotype than the $espA_{D696A}$ and $espC_{D749A}$ strains (**Figure 15**). I also discarded a model in which a EspA phosphorylated REC domain is the sole output, and $EspA_{HK}$ dependent phosphorylation of the EspC receiver is needed to stimulate the EspA kinase because EspA efficiently phosphorylates its own receiver *in vitro* [158]. Finally, I disfavor a model in which the $EspC_{REC}$ domain is the sole output, and phosphorylation of the $EspA_{REC}$ is only necessary to stimulate phosphorylation of the $EspC_{REC}$. In this last scenario, I predict that in $espA_{D696A}$ and $espA_{\Delta REC}$ strains a low level of $EspA_{HK}$ phosphotransfer to EspC REC domain would produce an intermediate phenotype rather than the null phenotypes observed in the respective mutants (**Figure 11** and **Figure 15**, [158]). The biochemical experiments together with the genetic characterization of the *esp* mutants Δ*espA*, $espA_{\Delta REC}$, Δ*espC*, Δ*espAC*, $espA_{D696A}$ and $espC_{D749A}$, demonstrating that they all share exactly the same developmental phenotype (**Figure 15** and [158]), indicate

that the combined phosphorylation of both REC domains is absolutely required for developmental regulation by the Esp system.

This unique and novel phosphorylation relationship of the two Esp HyHPKs is also supported by the bioinformatic SDR analysis (section 2.2.4). For classical TCS systems, amino acid residues have been described that mediate the specificity between cognate HK and RR pairs [120, 121]. For HyHPKs, however, it is proposed that these residues do not underlie the same evolutionary pressure to be preserved, because of the spatial proximity of the HK and the REC domain within a HyHPK [179]. In spite of this proposal from Capra *et al*, I never the less went for the prediction of SDR residues for the Esp system, taking into consideration that the HyHPK EspA does not only phosphorylate its 'internal' $EspA_{REC}$ domain, but also the 'external' $EspC_{REC}$ domain. In fact, the analysis of the SDR residues in the EspA and EspC REC domains revealed conserved amino acids that might be responsible for the specificity determination (**Figure 18**). Interestingly, the SDR analysis of the HK regions in EspA and EspC gave additional information about the observation that the $EspC_{HK}$ had no effect on the developmental regulation by the Esp system, as the residues which were identified in the HK regions that putatively determine specificity in the EspC system did likely not underlie strong evolutionary pressure in the $EspC_{HK}$ region. Already, the closely related ortholog $EspC_{HK}$ protein sequences showed non-conservative substitutions in this putative SDR region. I propose that this drift of the putative SDR residues in the $EspC_{HK}$ was possible, because the $EspC_{HK}$ is dispensable for the signal output of the Esp system. Together, this bioinformatic analysis is in line with our biochemical analysis and additionally supports the unique inter- and intraprotein phosphorylation in the Esp system. In contrast to what was stated by Capra *et al*, this analysis revealed that SDR residues in certain HyHPK signaling systems (*i.e.* EspA), depending on their system design, also underlie evolutionary pressure.

3.2 The Esp system is bifunctionally regulated

Phosphatase activity is a widespread regulatory strategy in His-Asp signaling systems; it is proposed to (a) diminish unwanted *in vivo* crosstalk between non-related two component systems [180, 181] and (b) participate in the regulation of the signal output of a signaling system [106, 107, 169, 182-186]. As most RECs possess auto-dephosphorylation activity [36], consequently, the HPK mediated phosphates activity only becomes significant importance when the REC displays a low auto-dephosphorylation rate. Interestingly, the

auto-dephosphorylation rates of REC domains vary over five orders of magnitude. Here, the general trend is that chemosensory REC domains have a short half-life, presumably because they have to rapidly respond to changes in the environment, and REC that mediate transcriptional regulation having a longer half-life, likely to ensure efficient transcription of the target genes [187]. In many of the systems in which the REC has a long phosphorylation half-live, the corresponding HPK possesses phosphatase activity.

It is proposed that, the length of the REC domains phosphorylation half-life is mediated by a set of amino acid residues which lie in near spatial proximity to the invariant aspartate residues in the REC structure [187]. For $EspA_{REC}$ and $EspC_{REC}$ the phosphorylation half-lifes have not been experimentally determined yet. Therefore, I predicted their half-lifes, based on the relevant amino acids which revealed that both likely have an intermediate or long phosphorylation half live (data not shown). As a control, I likewise predicted the phosphorylation half-life of the sdRR RedF from *M. xanthus*, for which a long phosphorylation half-life has already been experimentally determined [104]. This analysis also revealed a long phosphorylation half live for RedF (data not shown), demonstrating that the bioinformatic analysis can lead to valuable assumptions about the phosphorylation half-life of REC domains. Thus, under the assumption that $EspA_{REC}$~ph and $EspC_{REC}$~ph have a long half-life, I propose that the Esp system likely would benefit from phosphatase activity for regulation of the signal output.

Accordingly, EspA indeed contains a proposed phosphatase motif [111, 172], and previous biochemical phosphotransfer experiments already suggested phosphatase activity of EspA, because they revealed that the phosphorylated form of an $EspA_{KR}$ construct was very short lived [158]. Based on my model that phosphorylation of the $EspA_{REC}$ and the $EspC_{REC}$ mediate repression of development, I predicted a delayed developmental phenotype for a mutant which lacks phosphatase activity. In line with this hypothesis, a substitution in the proposed phosphatase motif in EspA led to a delayed developmental phenotype (**Figure 23**). The *in vitro* phosphotransfer analysis from $EspA_{HK}$ to $EspC_{REC}$ additionally supported, that EspA possesses phosphatase activity, because upon addition of the $EspC_{REC}$ to $EspA_{HK}$ the label intensity on the $EspA_{HK}$ strongly decreased (**Figure 19**). Importantly, this label decrease was stronger than the simultaneous label increase on the $EspC_{REC}$, indicating that the phosphorylated $EspC_{REC}$ is constantly turned over. This effect was further enhanced after elongated incubation of the $EspA_{HK}$ with the $EspC_{REC}$ which is generally thought to indicate phosphatase activity of a bifunctional HK [188]. Together, these observations indicate that EspA likely acts as a phosphatase on its own REC, and also on the $EspC_{REC}$.

The proposed phosphatase motif was also identified in EspC, however, the genetic analyses elucidating the putative EspC phosphatase activity were much more difficult to interpret. Substitution mutations of the proposed phosphatase motif in EspC did not result in a phenotype different from the wild type (**Figure 20**). Since several recent reports showed that different substitutions in the phosphatase motif resulted in variable inhibition of the associated phosphatase activity [108-111], I analyzed a variety of substitutions that are reported to influence HPK phosphatase activity. All tested substitutions led to a phenotype indistinguishable from that of the wild type (**Figure 21**). These analyses suggest (a) that phosphatase activity might not play a crucial role in regulating developmental progression, (b) its effect was to minor to be detected by the analysis or (c) the conditions during our genetic analysis did not trigger phosphatase activity in EspC.

To further elucidate whether EspC also has phosphatase activity, I next focused on substitution mutants in the invariant histidine residue, since the invariant histidine residue of bifunctional HPK was shown to also participate in the phosphatase activity [107, 108, 110, 111, 169]. For VanS and NarX it is reported that a histidine to glutamine substitutions enhanced phosphatase activity [107, 111]. In line with these reports, a histidine to glutamine substitution in EspC led to a earlier phenotype which can be explained by enhanced transmitter phosphatase activity of EspC (**Figure 22**). As the simultaneous substitution of the phospho-accepting aspartate residue fully restored the early developmental phenotype, I propose that the effect observed for the histidine to glutamine substitution is due to affecting the phosphatase activity of the Esp system rather than to an unknown secondary effect. In summary, the genetic analysis of the EspC phosphatase activity revealed two contradictory results: Substitution mutations in the EspC phosphatase motif did not alter the developmental phenotype, but the putative phosphatase enhancing mutation $H_{461}Q$ showed the predicted effect on developmental progression. A plausible explanation for these results is that the EspC phosphatase activity is ‘off’ under the experimental conditions used for the developmental analysis. Consequently, this suggests that the EspC phosphatase activity has to be activated upon for example appropriate environmental ques. Correlating with this hypothesis, a deletion of the EspC PAS sensing domain resulted in a phenotype which was reminiscent of the phenotype observed for the *espC*$_{H461Q}$ mutant strain (**Figure 25**), suggesting that the EspC PAS domain might be responsible for regulating the EspC phosphatase activity.

There is a growing body of evidence showing that PAS domains might be important to regulate phosphatase activity of HPKs. The phosphatase activity of the HPK ResE from *B.*

subtilis is decreased upon anaerobic conditions, and the PAS domain of ResE is proposed to participate in this regulation of phosphatase activity [189, 190]. In the HPK ThkA from *T. maritima*, deletion of the PAS domain strongly impaired the phosphatase activity of the HPK [191]. Similarly, it was shown for WalK from *S. pneumoniae* that a PAS domain regulates the phosphatase activity, but not the kinase activity of WalK [76]. Together with this notion, a plausible explanation for the $espC_{H461Q}$ and the $espC_{\Delta PAS}$ phenotypes is, that EspC is locked in a phosphatase 'off' state by its PAS domain. A yet unknown signal sensed by the PAS domain would therefore be able to turn the EspC phosphatase activity 'on'. The generation of mutants combining a putative phosphatase 'on' phenotype ($espC_{H461Q}$ and the $espC_{\Delta PAS}$) with disruption of the phosphatase motif would help to further decipher this proposed phosphatase activity of EspC and its regulation. Additionally, *in vitro* phosphatase experiments with purified versions of the EspC (*e.g.* $EspC_{HK\ H461Q}$ or $EspC_{HK\ H461Q,\ N465Y}$) would greatly contribute to the understanding of the EspC phosphatase activity.

3.3 The Esp system might mediate the signal output via direct protein-protein interaction

The genetic analysis indicated that both REC domains, $EspA_{REC}$ and $EspC_{REC}$, have to be phosphorylated for proper developmental regulation. As already mentioned, a classical His-Asp phosphorelay system generally utilizes a HPT protein to shuttle the phosphoryl group from the internal REC of the HyHPK to the terminal RR (**Figure 31**A). Additionally, one can envision a scenario were the internal REC within the HyHPK, when phosphorylated, modulates an accessory protein via direct interaction (**Figure 31**D). Even though there are, to my knowledge, no reports of protein-protein interaction mediated signal output by HyHPKs, there are reasons which indicate that this mode of signaling output must exist. First, similar protein-protein interaction-mediated signal outputs are already reported for single domain response regulators like CheY, CpdR or PhyR. Here, the phosphorylation of the single domain response regulator changes its affinity to the target proteins FliM, ClpXP and the anti-sigma factor NepR, respectively [40, 192, 193]. Second, generally the abundance of HPT proteins compared to the number of HyHPK is low. *M. xanthus* encodes for 31 HyHPKs but only two HPT proteins [122]. Similarly, the slime mold *Dyctiostelium discoideum* encodes for 16 HyHPKs and the filamentous fungy *Cochliobolus heterostrophus* encodes for 21 HyHPKs, both, however, encode only for one HPT protein

[4, 194]. This low ratio of HPT proteins per HyHPK suggests either strong signal integration on the level of the HPT proteins, or that alternative signal transduction mechanism, like for example protein-protein interactions between the HyHPK REC and an output protein, must exist. Third, a genome survey by Wuichet *et al.* revealed that out of 899 analyzed bacterial genomes, 561 contained genes encoding for HyHPKs, but only 220 of these 561 organism also encoded for HPT proteins [4], suggesting that the other ~60 % of the HyHPKs containing organisms utilize other signal output mechanisms [89]. Together, all these observations point into the direction that besides the paradigm His-Asp phosphorelay system that utilizes HPT proteins for the signal transfer, alternative signal transduction mechanisms like protein-protein mediated signal output likely exist.

Generally, classical HyHPKs phosphorelay systems are thought to act through a RR with DNA binding domain, thus on the level of transcription [50, 77]. All of the *E. coli* phosphorelay systems (EvgA/EvgS, TorS/TorR, ArcB/ArcA, RcsC/RcsD/RcsE and BarA/UvrY) utilize RR that contain a DNA binding domain (http://mistdb.com/) and terminate in the modulation of transcription [94, 195-200]. Higgs *et al.* showed that deletion of *espA* enhanced the accumulation of MrpC without affecting the transcription of the *mrpC* gene [158]. In line with this observation, the early developing *espC* point mutants ($espC_{D749A}$ and $espC_{H461A,\ D749A}$) also showed early accumulation of MrpC (**Figure 28**A). In this study, I was able to demonstrate that the MrpC protein accumulation is regulated on the level of MrpC protein stability (section 2.4.1), thus these results showed that the Esp system acts at the post translational level, and I propose that the Esp system rather does not involve a HPT protein, instead it likely acts in a way that involves direct protein-protein interaction.

Proteolysis as an output for His-Asp signaling systems

Proteolysis is a posttranslational regulatory mechanism that enables the cell to rapidly and immediately control physiological processes. Several examples exist where proteolysis and His-Asp signaling mechanisms merge in order to ensure an appropriate regulation of key cellular processes. In *C. crescentus*, the central cell cycle regulator CtrA is regulated on many different levels, one of which is its directed proteolysis in the stalked cells shortly prior to cell division [201]. Interestingly, this directed proteolysis event is regulated temporarily and spatially by the same sophisticated His-Asp phosphorelay system that also activates CtrA itself [192, 202]. This regulatory system composed of the HyHPK, CckA, and HPT protein, ChpT which together can phosphorylate both RRs, CpdR and CtrA. CpdR, however, periodically localizes to the stalked pole and in its unphosphorylated state

recruits the protease ClpXP and also the RR CtrA, and thus mediates CtrA degradation. This regulatory mechanism shares several facets with the regulated proteolysis of MrpC (**Figure 28**). As for CtrA in *C. crescentus* the key regulatory protein in *M. xanthus*, MrpC, is subject of directed proteolysis during the developmental program, and this proteolysis is also regulated by a His-Asp signaling system, the Esp. In *C. crescentus*, the CpdR phosphorylation state mediates the localization of the ClpXP protease and CtrA at the stalk pole; however, it remains to be elucidated if the Esp system actively recruits MrpC and the putative degrading protease to the cytoplasmic membrane, where EspC and likely also EspA are located (**Figure 13**, **Figure 14**).

One other interesting question in this context is: Why does the Esp system rely on a combined phosphorylation of the two REC domains in EspA and EspC? One possible explanation could be that the Esp system mediates the localization of MrpC and the putative protease ,and at the same time serves as a adaptor protein to mediate the accessibility of MrpC to the protease. A similar scenario is reported for the directed proteolysis of the *E. coli* sigma factor RpoS. RpoS is degraded during exponential growth by the ClpXP protease [203]. Interestingly, RpoS is not directly degraded by the ClpXP protease upon binding, instead the RpoS degradation is dependent on the phosphorylation of an orphan RR called RssB which serves as an adapter protein [204-206]. One difference to the Esp system is that RssB contains an additional C-terminal extension which shares structural homology to a Ser/Thr phosphatase domain [207]. Until now, it is controversially discussed whether this C-terminal extension is absolutely required to mediate the degradation of RpoS by ClpXP [206, 208]. However, one can find other examples where the phosphorylation of a stand-alone response regulator changes the binding affinity of its REC to its partner protein. For example the *E. coli* chemosensory protein CheY can bind to FliM (and CheX) preferentially in its phosphorylated state [209, 210]. I envision a scenario were both a putative MrpC degrading protease and MrpC are recruited to the cytoplasmic membrane by the non-phosphorylated Esp system which then leads to the degradation of MrpC. To further understand this mechanism it would be crucial to examine if MrpC interacts with EspA and/or EspC. An elegant experiment to verify this putative interaction would be co-immuno precipitation of $EspA_{HK\text{-}REC}$, $EspC_{HK\text{-}REC}$ and MrpC protein mixtures using either one of the Esp proteins or MrpC as the bait protein.

Another very obvious question is: Which protease is degrading MrpC in an Esp-dependent manner? Protease inhibitor screens can be a useful tool to narrow down putative candidate proteases. Such a screen was already successfully used in *M. xanthus* to identify the

protease which is mediating the proteolytic activation of p25 to p17 [148, 149]. The *in vitro* and *in vivo* protease screening analysis applied in this study suggested that the protease which is important for the degradation of MrpC likely is a serine protease (**Figure 29**). Interestingly, a LonA-type protease, which belongs to the family of serine proteases, is already proposed to be involved in processing MrpC during developmental regulation [143, 144]. *M. xanthus* encodes for two LonA type peptidases (Merops family S16; http://merops.sanger.ac.uk/index.shtml), one of which is important for vegetative growth (LonV) and one of which is important for development (LonD) [211, 212]. LonD was reported to be responsible to process MrpC to its shorter, more active isoform, MrpC2 [143, 144]. LonA peptidases utilize a catalytic Ser residue [213] and can be inhibited by serine protease inhibitors. LonA peptidase activity depends on ATP, however, ADP acts as an inhibitor [214, 215]. The addition of ATP to the *in vitro* MrpC turnover assay did not result in any increase, and the addition of EDTA only resulted in a slight decrease of MrpC degradation, therefore I suggest that ATP dependent proteases are likely not important for the MrpC degradation (**Figure 29**D). Thus, the major question of which protease degrades MrpC, still remains to be elucidated. The next attempt towards answering this question was the modified Zymogram approach which is a useful tool to detect, quantify and characterize proteases [216-218]. Such zymogram approaches have also successfully been used to identify specific proteins by subsequent mass spectrometry from the zymogram gels [219]. Unfortunately, the present zymogram approach did not result in the identification of the protease which degrades MrpC. The addition of the protease inhibitors that showed inhibition in the above protease inhibitor screen (SMPI, PMSF, benzamidine) did not result in comparable pattern of protected zones in the zymogram (**Figure 29**E). The protease inhibitors display different preferences for serine protease families; aprotinine mainly inhibits proteases of family S1A and S7, benzamidine manly inhibits proteases of the family S1A. PMSF has a broader spectrum of inhibition throughout the serine proteases [220]. These differential inhibitory properties might explain the different protection zone pattern observed in the zymogram. Consistent with these differences in the inhibitory spectra, the strongest effect in all experiments could be observed after the addition of PMSF; also in the zymogram, the addition of PMSF resulted in the most zones of protection from MrpC degradation. Together with this observation that the PMSF addition showed the most robust effect in the *in vivo* MrpC turnover experiment, the analysis of the four protected zones after PMSF addition to the Zymogram by mass spectrometry might display the most promising approach to identify a small number of putative MrpC

degrading proteases. A subsequent more detailed candidate approach, for example by deleting candidate proteases that might be identified by the mass spectrometry analysis should enable the identification of the MrpC degrading protease.

3.4 Does the Esp system contribute to the cell fate decisions during development?

During a complex developmental process, the expenses of expressing many different developmental features are often split up between different members of a bacterial community. This division of labor by having different cell fates in a developmental process is therefore thought to be an evolutionary advantage [221, 222]. Such bimodal regulatory strategies are often regulated by master regulators. In line with this, in *B. subtilis* are at least three different master regulators Spo0A, DegU and ComA which regulate the developmental programs that result in three distinct cell fates, sporulation/biofilm formation, formation of miners and competence, respectively [223]. Another example of such bimodal regulation is the function of the master regulator CtrA in *C. crescentus*. CtrA is involved in the control of initiation of DNA replication, cell division and flagella biogenesis [224]. Thus, CtrA phosphorylation and its cellular localization are crucial for its differential function in the stalked- and the swarmer cells (discussed above).

The *M. xanthus* development is a very complex physiological process which similarly involves the formation of different cell fates as part of the developmental program. At least three different cell fates are known to be part of the developmental program: Cells that aggregate and later sporulate within multicellular fruiting bodies (reviewed in [123]), cells that do not contribute to the formation of fruiting bodies resembling a persister like state (peripheral rods) [126-128], and cells that lyse during development [124, 125, 225]. These different cell types can be separated by differential centrifugation into cells that already aggregated (aggregated cells) and cells that are not aggregated yet (non-aggregated cells). It should be noted however, that the distribution between aggregated and non-aggregated cells at a certain analyzed time point displays a snapshot, as for example cells that are found in the non-aggregated cell fraction at 12 h of development can lyse, remain in the non-aggregated cells or transition into the aggregated cell fraction until the next analyzed time point.

MrpC is a key player in the core regulatory network and is proposed to determine the formation of the different cell types. MrpC is not only absolutely required for aggregation

and sporulation [141, 226], it is further proposed that MrpC is involved in regulating the cell lysis [124, 125], and together with the accumulation of other key developmental regulators it is likely also involved in the determination of peripheral rods [124]. In fact, the MrpC protein shows a very specific accumulation pattern in the two cell populations, aggregating and non-aggregating cells. In the early time points during development, MrpC is enriched in the non-aggregating cells and degraded in the aggregated cell fraction; and in later time points, MrpC preferentially accumulates in the aggregating cells, presumably due to the transition of non-aggregated cells into the aggregating cell fraction [124]. In the same study, an additional fourth cell type is described, the cell clusters. Cell clusters are a cell population that can be found in the aggregated cell fraction already very early in the developmental program; at the onset of the developmental program they already account for ~25 % of the initial cell population. Until now it remains to be elucidated how exactly this latter cell population contributes to the developmental program, if they finally end up as cells in fruiting bodies or if they remain as an independent cell population. Interestingly, the MrpC protein accumulation profile within the cell clusters is significantly different from the non-aggregated cells at the early time points during development, suggesting that MrpC might also be involved in the determination of the cell cluster population.

Interestingly, the EspC protein accumulation pattern was opposite to the reported MrpC protein accumulation pattern of separated cell fractions (**Figure 27**). Early in the developmental program, EspC was exclusively detected in the aggregated cell fraction (which at this point represents the cell clusters), and later the EspC accumulation pattern changed and was then highly enriched in the non-aggregated cell population. This initial cell fate analysis suggests that the Esp system contributes to the cell fate decisions that are made during the developmental program. The Esp system presumably quenches the MrpC levels in the cell cluster fraction at early stages and thus probably prevents the induction of the developmental program in the cell cluster. Later during development, MrpC is allowed to accumulate, as after 48 h of development MrpC is exclusively produced by the aggregating cells. Interestingly, in these later stages of the developmental program, EspC accumulated in the non-aggregated cell fraction which might regulate the gradual increase of MrpC in some of the non-aggregated to ensure appropriate aggregation and subsequent sporulation in these cells. Importantly, it should be considered in this context that between 18 h and 30 h of development, cells presumably constantly transition from the non-aggregating into the aggregating cell fraction. Thus, the EspC protein level detected in the non-aggregating cell samples at later time points might be artificially enhanced, because

cells that do not have EspC, likely have high levels of MrpC and thus transition into the aggregating cell fraction. Therefore, it seems likely that the effect of EspC in the non-aggregated cell fraction happens earlier than the initial detection of EspC in this cell population suggests.

Correlating with the hypothesis that the Esp system prevents premature accumulation of high MrpC levels is that the deletion of EspA results in inappropriate formation of spores outside of fruiting bodies [157] accompanied with an earlier and more sharp accumulation of MrpC protein [158]. At this time it is not clear if and how the Esp system regulates the differentiation of cell clusters, non-aggregating cells or both. Single cell analysis with fluorescently marked EspA, EspC and MrpC would contribute greatly to the understanding of this cell fate differentiation processes. But clearly, it cannot be the only function of the Esp system to prevent sporulation outside of fruiting bodies, because deletion of *espA* or *espC* also leads to a sever timing defect in the developmental program, as aggregation is observe earlier in these mutants. This early developmental phenotype additionally suggests that the Esp system is also acting in the cells that transition into the aggregation centers. Currently, I envision a scenario in which the relative protein level of EspC versus EspA in one cell determines the output of the Esp system. On the whole population level, I showed that at 24 h of development, EspA is approximately three times more abundant then EspC (**Figure 26**). This analysis, however, did not reveal detailed information about the molar relationships between EspA and EspC in the different cell fractions. One can envision, that for example in the cell clusters high levels of EspC lead to an enhancement of the overall signal output of the Esp system, because multiple $EspC_{REC}$ domains become phosphorylated by one $EspA_{HK}$ in this cells. In contrast, in cells that are going to become peripheral rods, for example an one to one molar relationship between EspA and EspC might mediate an intermediate signal output, whereas in the cells that transition into the aggregation center and later sporulate, low amounts of EspC might mediate a very weak Esp signal output thus allowing for more MrpC accumulation in these cells.

Interestingly, cumulative deletions of other negative regulators in the developmental regulatory network in *M. xanthus* (Δ*espA*, Δ*espA*Δ*red*, Δ*espA*Δ*espC*Δ*red*, *todK*$^-$) leads to progressively higher amounts of spores formed outside of fruiting bodies[16]. This observation suggests that these negative regulators together are important to regulate the cell type differentiation processes. Eventually, they are specifically quenching the positive amplification loops present in the developmental regulatory network. Accordingly, the Esp

[16] B. Lee, PhD thesis

system seems also to be subject of auto-regulation, as the early developing *esp* mutant strains (Δ*espA*, Δ*espC*, $espC_{D749A}$, $espC_{H461A, D749A}$) displayed early production of EspA or EspC relative to the wild type strain (**Figure 11**, **Figure 15**). The auto-regulation of this negative regulatory system might help to fine tune the effect of the Esp system to ensure appropriate regulation of MrpC protein levels. Currently, it is not clear how this auto-regulation is mediated and regulated. One striking hypothesis is that the Esp protein production additionally influenced by MrpC. In line with this, the MrpC protein levels were higher and production started earlier in the early developing *esp* mutant strains. Therefore, the Esp system might together with MrpC display a negative regulatory circuit. The hypothesis that MrpC regulates the expression of EspA and EspC implies that it binds to the promoters of these genes. MrpC binding sequences, however, could not be identified by bioinformatic analysis in the relevant genomic regions. To elucidate whether MrpC binds to the promoter regions of *espA* and/or *espC*, I next perform electro mobility shift assays (EMSA).

3.5 Conclusion

With the analysis of the Esp-signaling system, this manuscript provides first evidence for a novel signaling mechanism of His-Asp signaling systems that utilizes direct inter- and intraprotein phosphorylation without involving an HPT protein. Additionally, this study further expanded the knowledge about the complexity and flexibility of such signaling systems and gives further insights into the regulation of a global physiological behavior, the regulation of development in *Myxococcus xanthus*. It is evident that in *M. xanthus* the 'unorthodox' signaling systems that utilize complex and 'unusual' signaling mechanism seem to play a much more important role than in other organisms. This is also reflected in the number of complex signaling systems that were discovered in *Myxococcus xanthus* e.g. the Red four component system [104, 162], the atypical HyHPK RodK [227, 228], the SgmT/DigR signaling system [178] and finally, the Esp signaling system [157, 158, 160]. Together with the fact that unorthodox signaling systems involving HyHPK can be found in all three domains of life, it is double noteworthy that the identification, characterization and detailed analysis of such novel signaling mechanism is indispensable for the detailed understanding of how organism sense and respond to their natural environments.

4. EXPERIMENTAL PROCEDURES

4.1 Chemicals and equipment

Media components and pure chemicals were purchased from Carl Roth (Karlsruhe), Merck (Darmstadt), Sigma-Aldrich (München) and Difco (Heidelberg). PCR purification, plasmid isolation and gel extraction kits were purchased from Quiagen (Hilden) or Zymo research (Freiburg). Protein BCA™ Protein Assay Kit from Thermo Scientific (Schwerte) were used for the determination of protein concentrations. Size standards for SDS-PAGE (Page Ruler Prestained Protein Ladder Plus) as well as for agarose gel electrophoresis (MassRuler DNA Ladder, Mix) were purchased from Thermo Scientific (Schwerte). DNA modifying enzymes (restriction endonucleases, T_4 DNA ligase, antarctic phosphatase) used in this study were from Thermo Scientific (Schwerte) or New England Biolabs (Frankfurt a.M.). The Platinum® Pfx DNA polymerase for PCR was delivered from Invitrogen Darmstadt), Phusion® High-Fidelity DNA polymerase was purchased by New England Biolabs (Frankfurt a.M.). Oligonucleotides were synthesized by Sigma-Aldrich (München). BigDye® Terminator v3.1 cycle mix and BigDye® XTerminator™ Purification Kit necessary for DNA sequencing were purchased from Applied Biosystems (Darmstadt), commercial DNA sequencing was perfomed by Eurofins MWG Operon (Ebersberg). Antibodies (anti-His_6, anti-T_7, anti-GST, goat-anti-rabbit/mouse-HRP) were purchased from Thermo Scientific (Schwerte), α-EspC polyclonal rabbit antisera were purchased from Eurogentec (Belgium, Serain). His-trap FF affinity columns were purchased from GE Healthcare (Freiburg) and Bio-Scale™ Mini Profinity™ IMAC cartridges were purchased from Bio-Rad (München). [γ^{32}P]-ATP was purchased by Hartmann analytic (Braunschweig). The preparation of all solutions was performed using demineralised and autoclaved water (daH_2O), unless otherwise described.

4.1.1 Instruments

All instruments and software that were used in this study are listed in **Table 2** and **Table 3**, respectively. Modifications or setting of the instruments and software will be described in detail in the relevant section.

Table 2 Instruments

APPLICATION	DEVICE	MANUFACTURER
Centrifugation	RC 5B plus Ultra Pro 80 Multifuge 1 S-R Biofuge fresco	Sorvall / Thermo scientific (Dreieich) Heraeus / Thermo scientific (Dreieich)
	L 90 K Optima Max XP	Beckman Coulter (Krefeld)
PCR	Mastercycler personal Mastercycler epgradient	Eppendorf (Hamburg)
DNA sequencing	3130 Genetic analyzer	Applied Biosystems (Darmstadt)
Cell disintegration	French® pressure cell press	SLM instruments (Urbana, IL)
Ultrasound sonification	Branson sonifier 250	Heinemann (Schwäbisch Gmünd)
FPLC protein purification	Äkta™ Purifier	Amersham Bioscience (München)
	Profinia™ purification system	Bio-Rad (München)
Protein electrophoresis	Mini-PROTEAN® 3 Cell PROTEAN® II XI Cell	Bio-Rad (München)
Western blotting	PerfectBlue Semi-Dry Elektroblotter	PEQLAB Biotechnologie (Erlangen)
	TE42 Protein transfer tank TE77 ECL semidry transfer unit	Amersham Bioscience (München)
Chemiluminescence detection	LAS-4000 luminescent image analyzer	Fujifilm Europe (Düsseldorf)
Microscopy	MZ 8 stereo microscope DME light microscope	Leica microsystems (Wetzlar)
Phosphor autoradiography	StormTM 840 imager Storage phosphor screen	GE Healthcare Life science (München)
Electroporation	Gene pulser Xcell	Bio-Rad (München)
Spectrometry	Ultrospec 2100 pro	Amersham Bioscience (München)
	Nanodrop ND-1000 UV-Vis spec.	Nanodrop (Wilmington, USA)
DNA illumination and documentation	UVT 20 LE UV table	Herolab (Wiesloch)
	2 UV Transilluminator	UVP BioDoc-IT-System (Upland, USA)
	Universal Hood II	Bio-Rad (München)
Reaction incubation	Thermomixer comfort	Eppendorf (Hamburg)
Incubation of cell cultures	Innova-4000® -44® orbital incubator	New Bronswick Scientific (Nürtingen)
	B6420 incubator	Heraeus (Langenselbold)

Table 3 Software and web-based programs

APPLICATION	PROGRAM NAME	MANUFACTURER
Microscopy imaging	Leica Application Suite	Leica microsystems (Wetzlar)
In silico cloning	Vector NTI Advanced™ 11	Invitrogen (Karlsruhe)
Predicition of protein parameters	ProtParam (Web based)	SIB (Genève, Schweiz); http://web.expasy.org/protparam/
Homology modeling	SWISS-MODEL (Web based)	SIB (Genève, Schweiz); http://swissmodel.expasy.org/
	PyMOL 0.99rc6	Schrödinger (Portland, USA)
Sequence alignment	Clustal X 2.0	SFI (Ireland)
	Bioedit 7.0.5.3	Ibis Bioscience (Carlsbad, USA)
Äkta system management	UNICORN	GE Healthcare Life science (München)
Phosphor autoradiography	Image Quant 3 and 5.2	GE Healthcare Life science (München)
Quantification of 1D Gel	Image J	NIH (Maryland, USA)
	Image Quant TL	Amersham Bioscience (München)
Statistical analysis	Excell 2007	Microsoft® (Redmond, USA)
	Origin 6.1	Origin Lab (Northampton, USA)
Ortholog identification	ACT: Artemis Comparison Tool	Wellcome Trust Sanger Institute (Hinxton, UK); http://www.sanger.ac.uk/

4.1.2 Buffers and solutions

Table 4 Media, buffer and solutions

NAME	COMPOSITION
Media	
CYE	0.1 % (w/v) Bacto™ Casitone, 0.5 % (w/v) yeast extract, 10 mM morpholinepropanesulphonic acid (MOPS) pH 7.6, 8 mM $MgSO_4$
LB	0.1 % (w/v) tryptone, 0.5 % (w/v) yeast extract, 0.5 % (w/v) NaCl
TSS medium	1 % (w/v) trypton, 0.5 % (w/v) yeast extract, 1 % (w/v) NaCl, 10 % (w/v) PEG 3350, 5 % (v/v) DMSO, 50 mM $MgCl_2$ pH 6,5
general buffer	
PBS	8 mM Na_2HPO_4, 2 mM KH_2PO_4 pH 7.4, 135 mM NaCl, 3.5 mM KCl
TBS	20 mM Tris pH 7.4, 500 mM NaCl
TBS-T	20 mM Tris pH 7.4, 500 mM NaCl, 0.05 % (v/v) Tween-20
TAE	40 mM Tris pH 8.0, 1 mM EDTA
MMC	10 mM MOPS pH 7.6, 4 mM $MgSO_4$, 2 mM $CaCl_2$
TE	10 mM Tris pH 8.0, 1 mM EDTA
CTAB/NaCl solution	275 mM cetyl trimethyl ammonium bromide, 700 mM NaCl
buffer for protein purification, refolding and activity assays	
lysis buffer H	10 mM HEPES pH 7.2, 150 mM NaCl
lysis buffer T	50 mM Tris pH 7.6, 150 mM NaCl, 140 mM galactose, 1 mM EDTA, 1 % Sigma mammalian protease inhibitor
binding buffer	50 mM HEPES pH 7.4, 0.5 M NaCl, 20 mM imidazole
elution buffer	50 mM HEPES pH 7.4, 0.5 M NaCl, 500 mM imidazole
TND	50 mM Tris-HCl pH 8.0, 150 mM NaCl, 1 mM DTT
TGND	50 mM Tris-HCl pH 8.0, 150 mM NaCl, 1 mM DTT, 10 % (v/v) glycerol
ZSB (2x)	125 mM Tris pH 6.8, 2 % (w/v) SDS, 20 % (v/v) glycerol, 0.01 % (w/v) bromphenolblue
zymo refolding buffer	100 mM MOPS pH 7.6, 2 % (v/v) Triton X-100
zymo activity buffer	100 mM MOPS pH 7.6, 1 % (v/v) Triton X-100, 0.63 µM ATP, 2 mM $MgCl_2$
buffer for western blotting and protein identification	
LSB (2x)	125 mM Tris-HCl pH 6.8, 20 % (v/v) glycerol, 4 % (w/v) SDS 10 % (v/v) β-mercaptoethanol, 0.02 % (w/v) bromphenolblue
cLSB	62.5 mM Tris-HCl pH 6.8, 10 % (v/v) glycerol, 2 % (w/v) SDS
acidic glycine buffer	100 mM glycine pH 2.5
tris-glycin-SDS	25 mM Tris, 190 mM glycine, 0,1% (w/v) SDS
resolving buffer (4x)	1.5 M Tris-HCl pH 8.8, 0.4 % (w/v) SDS
stacking buffer (4x)	500 mM Tris-HCl pH 6.8, 0.4 % (w/v) SDS
anode buffer I	300 mM Tris pH 10.4, 10 % (v/v) methanol
anode buffer II	25 mM Tris pH 10.4, 10 % (v/v) methanol
cathode buffer	25 mM Tris pH 9.4, 40 mM glycine, 10 % (v/v) methanol
Stains	
Ponceaus S	0.1 % (w/v) Ponceaus S, 5 % glacial acedic acid
Coomassie stain	0.2 % (w/v) Coomassie Brilliant Blue R250, 50 % (v/v) methanol, 7 % (v/v) glacial acidic acid
destain	50 % (v/v) methanol, 7 % (v/v) glacial acidic acid
6x Loading Dye	0.2 % (w/v) bromophenolblue, 0.2 % (w/v) xylencyanol, 50 % (v/v) glycerol

4.2 Microbiological methods

4.2.1 Bacterial strains and growth conditions

M. xanthus growth conditions

M. xanthus strains were grown under vegetative conditions on casitone yeast extract (CYE)-broth, -agar plates or -top agar (CYE-broth supplemented with 1.5 % or 0.75 % (w/v) agar agar, respectively) [229] in an orbital shaker at 32 °C in the dark. CYE media were supplemented with 2.5 % (w/v) galactose, 100 µg ml^{-1} kanamycin or 34 µg ml^{-1} chloramphenicol, if necessary. The optical density of *M. xanthus* suspensions was measured at 550 nm (A_{550}) using a cuvette with 1 cm path length. *M. xanthus* cultures were stored for a maximum of four weeks at 18 °C on CYE agar plates in the dark. For the long term storage of stock cultures 25 ml cell suspension of an overnight culture were mixed with 900 µl of a dimethyl sulfoxide solution (DMSO; 99.5 %) to induce sporulation. After incubation for 24 h at 32 °C the cultures were confirm to be free of contamination by light microscopy, centrifuged at 4 600 xG at RT for 15 min (Multifuge 1 S-R). Cell pellets were resuspended in 4 ml CYE broth and 1 ml of the cell suspension was mixed with 250 µl DMSO for storage at -80 °C.

Preparation and transformation of electro competent *M. xanthus*

Electro competent *M. xanthus* cells were prepared as described by Lee *et al* [230]. The respective *M. Xanthus* strain was incubated in 100 ml CYE-broth at 32 °C and grown to an optical density of approximately 0.3 – 0.4 A_{550}. The cell suspension was centrifuged at 4600 xG, RT for 15 min (Multifuge 1 S-R), washed twice by subsequent resuspension in 25 ml daH_2O and centrifuged as before. Finally, the cells were resuspended in 150 µl daH_2O, alliquoted (50 µl) and stored at -80 °C after flash freezing.

For the electroporation, 1 µg plasmid DNA was added to 50 µl electro competent cells and transferred to a 0.1 mm electroporation cuvette (BioRad). Electroporation was performed at 0.65 kV, 25 µF and 400 Ω, and afterwards the cells were recovered in 1 ml of CYE medium and incubated for 5 h at 32 °C. 100, 300 and 500 µl of the cells were mixed with molten CYE top agar (the temperature should be <55 °C) and plated on CYE agar plates supplemented with 100 µg ml^{-1} kanamycin. The plates were incubated at 32 °C for 5 to 14 days until swarming colonies became visible.

Generation of deletion and substitution mutant strains in *M. xanthus*

In-frame deletions and site-specific point mutations were generated by homologous recombination of the relevant suicide plasmids followed by *galK*-mediated counter selection on galactose [231], as previously described in detail [230]. Briefly, the plasmid relevant for the introduction of a point mutation or deletion of a gene/domain contains ~ 500 bp of the 5' and 3' sequences surrounding the region of interest. The plasmid was introduced by electroporation into *M. xanthus* cells, and single recombination through either the 5' or 3' fragment was selected by resistance to kanamycin. Resulting colonies are confirmed for plasmid integration at the expected region by colony PCR, performed using a plasmid-specific and a genome-specific oligonucleotide (E, Table 6). Positive colonies were incubated over night in CYE-broth and cells in which the plasmid was excised via homologous recombination, were selected by plating on CYE-agar plates containing galactose. Resulting kanamycin sensitive, galactose resistant colonies were screened by colony PCR to discriminate between colonies in which plasmid excision had generated the wild type versus the desired deletion/substitution. Importantly, one of the oligonucleotides (F, Table 6) used for this screening must align outside of the region used for the cloning procedure. For the PCR diagnosis of base pair substitutions, two gene-specific oligonucleotides were designed. One oligonucleotide had the wt base (E_{wt}) and one had the mutated base (E_{mut}) at the very 3' end of the oligonucleotide (Table 6). *M. xanthus* cells can accumulate random mutations during prolonged manipulation. To be sure that any observed phenotype results from the desired deletion/point mutation at least three independent mutant colonies had to analyzed. The strains that were generated and used in this study and the relevant plasmids which were used to generate these *M. xanthus* mutant strains are listed in **Table 5**.

The strain PH1068 was generated by electroporation and recombination of the plasmid pAS036 in the DZ2 background strain. The strain PH1069 was generated by electroporation and recombination of the pasmid pAS004 into the PH1068 background strain. The strain PH1070 was generated by electroporation and recombination of the plasmid pAS037 in the DZ2 background strain. The strain PH1071 was generated by electroporation and recombination of the pasmid pAS004 into the PH1070 background strain. The strain PH1072 was generated by electroporation and recombination of the plasmid pAS038 in the DZ2 background strain. The strain PH1073 was generated by electroporation and recombination of the pasmid pAS004 into the PH1072 background strain.

Table 5 *M. xanthus* strains and mutagenesis plasmids

STRAIN/PLASMID	GENOTYPE	SOURCE
M. xanthus strains		
DZ2	wild type	Campos & Zusman 1975
DZ4227	DZ2 Δ*espA*	Cho & Zusman 1999
PH1008	DZ2 $espA_{H407A}$	Higgs *et al.* 2008
PH1009	DZ2 $espA_{D696A}$	Higgs *et al.* 2008
PH1029	PH1009 $espA_{H407A}$	Schramm *et al.* 2012
PH1044	DZ2 Δ*espC*	Schramm *et al.* 2012
PH1026	DZ2 $espC_{H461A}$	Schramm *et al.* 2012
PH1027	DZ2 $espC_{D749A}$	Schramm *et al.* 2012
PH1028	PH1026 $espC_{D749A}$	Schramm *et al.* 2012
PH1047	DZ4227 Δ*espC*	Schramm *et al.* 2012
PH1032	DZ2 $espC_{\Delta CA}$	Schramm *et al.* 2012
PH1033	PH1027 $espC_{\Delta CA}$	Schramm *et al.* 2012
PH1034	DZ2 $espC_{N465Y}$	Schramm *et al.* 2012
PH1035	PH1027 $espC_{N465Y}$	Schramm *et al.* 2012
PH1036	DZ2 $espC_{N465E}$	Schramm *et al.* 2012
PH1037	PH1027 $espC_{N465E}$	Schramm *et al.* 2012
PH1038	DZ2 $espC_{N465R}$	Schramm *et al.* 2012
PH1039	PH1027 $espC_{N465R}$	Schramm *et al.* 2012
PH1040	DZ2 $espC_{N465C}$	Schramm *et al.* 2012
PH1041	PH1027 $espC_{N465C}$	Schramm *et al.* 2012
PH1042	DZ2 $espC_{E462A}$	Schramm *et al.* 2012
PH1043	PH1027 $espC_{E462A}$	Schramm *et al.* 2012
PH1045	DZ2 $espA_{D411N}$	Schramm *et al.* 2012
PH1068	DZ2 $espC_{H461Q}$	This study
PH1069	PH1068 $espC_{D749A}$	This study
PH1070	DZ2 $espC_{REC}$	This study
PH1071	DZ2 $espC_{REC\ D749A}$	This study
PH1072	DZ2 $espC_{\Delta PAS}$	This study
PH1073	DZ2 $espC_{\Delta PAS\ D749A}$	This study
mutagenesis plasmids		
pBJ114	suicide plasmid with Km^R and *galK*	Julien *et al.* 2000
pBS131	pBJ114 *espC* Δcodons44-797	Schramm *et al.* 2012
pPH150	pBJ114 $espA_{H407A}$	Higgs *et al.* 2008
pAS001	pBJ114 $espC_{H461A}$	Schramm *et al.* 2012
pAS004	pBJ114 $espC_{D749A}$	Schramm *et al.* 2012
pAS029	pBJ114 $espC_{\Delta CA}$	Schramm *et al.* 2012
pAS030	pBJ114 $espC_{N465E}$	Schramm *et al.* 2012
pAS031	pBJ114 $espC_{N465Y}$	Schramm *et al.* 2012
pAS032	pBJ114 $espC_{N465R}$	Schramm *et al.* 2012
pAS033	pBJ114 $espC_{N465C}$	Schramm *et al.* 2012
pAS034	pBJ114 $espC_{E462A}$	Schramm *et al.* 2012
pAS036	pBJ114 $espA_{D411N}$	Schramm *et al.* 2012
pAS037	pBJ114 $espC_{H461Q}$	This study
pAS038	pBJ114 $espC_{REC}$	This study
pAS039	pBJ114 $espC_{\Delta PAS}$	This study

E. coli growth conditions

E. coli cultures were grown in an orbital shaker at 37 °C in lysogeny broth (LB) medium [232]. The culture media was supplemented with 100 μg ml^{-1} ampicillin or 50 μg ml^{-1} kanamycin if necessary. The optical density of *E. coli* suspensions was measured at 550 nm (A_{550}) with a photometer using a cuvette with a 1 cm path length. Strains were stored for a

maximum of four weeks at 4 °C on LB agar plates. For long term storage of stock cultures, 680 µl suspensions of an overnight culture were mixed with 320 µl of 50 % (v/v) glycerol and stored at -80 °C.

Preparation and transformation of electro competent *E. coli*

Electro competent E. coli cells were generated based on the protocol from Inoue *et al.* [233]. For the preparation, *E. coli* Top10 cells were grown to an optical density of 0,7 A_{550} in a 1 L LB liquid culture at 37 °C. The cells were washed four times by subsequent resuspension in 10 % (v/v) sterile glycerol solution (1000 ml, 500 ml, 250 ml, 40 ml) followed by centrifugation at 4 600 xG, 4 °C for 30 min (Multifuge 1 S-R). Finally, the cells were resuspended in 2 ml of 10 % (v/v) glycerol, aliquoted (50 µl) and stored at -80 °C after flash freezing.

To transform the electro competent cells, 2 – 5 µl ligation reaction was added to 50 µl electro competent cells and transferred into a 0.1 mm electroporation cuvette (BioRad). The cuvette was assembled in the GenePulser (BioRad) and the electroporation was performed at 1.25 kV, 25 µF and 200 Ω. Afterwards, the process the cells were recovered in 1 ml LB medium and incubated at 37 °C for 1 h. Then 100 µl and 900 µl of the cell suspension were plated on a LB agar plate with an appropriate antibiotic for selection, and incubated at 37 °C over night.

Preparation and transformation of chemical competent *E. coli*

Chemical competent *E. coli* cells were prepeared as described by Chung *et al*, 1998 [234]. The respective *E. coli* strain was incubated at 37 °C in 25 ml LB-broth until the culture reached an optical density of 0.7 A_{550}. The cell suspension was centrifuged at 4 600 xG, 4 °C for 10 min (Multifuge 1 S-R) resuspended in 0.1 x volume of sterile, ice cold TSS, aliquoted (100 µl) and stored at -80 °C after flash freezing.

For the transformation, 50 – 100 ng plasmid DNA were added to 100 µl of the competent cells, incubated for 30 min on ice and then incubated for 2 min at 37 °C. After this heat shock, the cells were recovered in 500 µl LB medium and incubated for 1 h at 37 °C. Finally, 100 µl and 400 µl of the cell suspension was plated on a LB agar plates with an appropriate antibiotic for selection and incubated at 37 °C over night.

4.2.2 Development assays

M. xanthus development was induced under submerged culture conditions in eithera 16 or 0.5 ml format as described previously [158, 230]. Briefly, exponentially growing cells were diluted to an optical density of 0.035 A550 in CYE medium. 16 or 0.5 ml of the diluted culture were seeded in 85 mm petri dishes or 24-well plates (Sarstedt), respectively. The plates were incubated at 32 °C (without shaking) for 24 h, and the rich medium was replaced by an equivalent volume of MMC starvation buffer to induce development. To enumerate developmental spores, cells were harvested from 1 well of 24-well plates in triplicate, heated to 50 °C for 60 min, sonicated (output 3, 30 % duty 2 times 20 pulses, Branson Sonifier 250), and then enumerated using a Helber bacterial counting chamber (Hawksley, UK). Pictures were recorded at the indicated time points with a Leica MZ8 stereomicroscope with attached Leica DFC320 camera.

4.2.3 Cell separation analysis

Cells were induced to develop under submerged culture as described before. For subpopulation segregation analysis, the developing cells were harvested using a 20 ml pipette to flush the cell lawn off the surface of the petri dish. The entire 16 ml volume was then transferred to a 50 ml falcon tube, and the cell lawn was dispersed by vigorously pipetting up and down 30 times. Cells in aggregates were then sedimented by centrifugation at 50 xG (Heraeus Multifuge 1 S-R) for 5 min at RT. The supernatant fraction was carefully removed and transferred to a 50 ml Falcon tube, and the pellet (sedimented cell fraction) was resuspended in an equivalent volume (16 ml) of MMC starvation medium. Cells in the supernatant fraction were present as single cells or in clusters of 1 to 4 cells, whereas resuspended cells in the sedimented fraction were detected as very large clusters. Both fractions were dispersed at least three times at 5 M/s for 45 sec in a FastPrep 24 cell and tissue homogenizer (MP Biomedicals) at 4 °C. After dispersal, both the supernatant and sedimented cell fractions were detected as single cells. The cell suspensions were pelleted at 4 600 xG, 4 °C for 10 min and the cellpellets were resuspendet in cLSB. The protein concentration of the resulting protein samples was determined using the BCA™ Protein Assay Kit (Thermo Scientific).

4.3 Molecular biological methodes

4.3.1 Isolation of genomic DNA from *Myxococcus xanthus*

For the isolation of genomic DNA from *M. xanthus* DZ2, cells were grown in 25 ml of CYE broth at 32 °C overnight, harvested by centrifugation for 10 min at 4 600 xG at RT (Multifuge 1 S-R) and concentrated to an A_{550} of 7.0 in TE buffer. The cell suspension subsequently was mixed with 5 % (w/v) SDS, 100 µg ml^{-1} proteinase K and 50 µg ml^{-1} DNAse-free RNase A and incubated at 37 °C for 60 min. Then the suspension was mixed with 0.167 x volumes of 5 M NaCl and 0.114 x volumes of CTAB/NaCl solution and incubated for 10 min at 65 °C. Afterwards, the solution was mixed with 975 µl of a phenol:chloroform:isoamyl solution in a 25:24:1 ratio. The samples were centrifuged for 2 min (Biofuge) at 17 000 xG at RT. The aqueous layer was transferred into a fresh tube and mixed with an equal volume of a chloroform:isoamyl solution at a ratio of 24:1. After centrifugation, the aqueous layer was again transferred into a fresh tube and 0.6 volumes of isopropanol were added and the solution was inverted until the genomic DNA precipitated. The DNA was transferred into a fresh tube containing 1 ml of 70 % (v/v) ethanol and centrifuged for 4 min at 17 000 xG at RT (Biofuge). The supernatant was removed and 1 ml of 70 % (v/v) ethanol was added and centrifuged again. After this final washing step, the supernatant was removed, dryed and the pellet was resuspended in 50 µl daH_2O.

4.3.2 Isolation of plasmid DNA from *E. coli*

Isolation of plasmid DNA was performed using the alkaline lysis method [235]. *E. coli* cells were cultivated as described in section 4.2.1. For the isolation of the plasmid DNA from these cultures, the QIAprep Spin Miniprep Kit was used as recommended by the supplier (QIAquick® Spin Handbook, 03/2008).

4.3.3 Amplification of DNA fragments by PCR

The *in vitro* amplification of specific DNA fragments was performed by polymerase chain reaction [236] using the Platinum® Pfx DNA-polymerase (Life Technologies), Phusion DNA polymerase (NEB), Phu DNA polimerase or Taq DNA polymerase. Phusion DNA polymerase was used along with the supplied 5x phusion HF buffer. Pfx, Phu and Taq

DNA polymerase were used along with BufferJ (Bioline). The composition of a PCR reaction was performed as recommended by the manufacturer. Generally a 25µl PCR reaction contained:

0.2 – 0.5 µl	DNA polymerase
10 – 100 ng	template DNA
0.5 µM	primer (each)
0.2 µM	dNTP's (Buffer J already contains dNTP's)
KCl and $MgCl_2$ in different concentrations	

The PCR program had to be adjusted according to the primer (x), polymerase (y) and template (z) used. Generally, the PCR program was as follows:

Initial denaturation	98 °C	2 min
Cycle denaturation	98 °C	15 sec
Annealing	x °C	15 – 20 sec
Elongation	y °C	z min
Final elongation	y °C	5 min

As a rule of thumb, the melting temperature of the primer were calculated using NetPrimer (http://www.premierbiosoft.com/netprimer/index.html) and ~ 4°C were substracted from the calculated melting temperature and used as the annealing temperature (x). The elongation temperature (y) and elongation time (z) was used as recommended by the manufacturer of the respective polymerase. Generally 25 – 35 cycles of amplification were used for the PCR reaction. All PCR products were purified using the QIAquick PCR Purification Kit or the QIAquick Gel Extraction Kit according to supplier's instructions (QIAquick® Spin Handbook, 03/2008).

4.3.4 Restriction digestion, dephosphorylation and ligation of DNA

DNA PCR fragments (200-500 ng) or plasmid DNA (~1 µg) were digested using 0.5 - 1 µl FastDigest® endonucleases (Fermentas) or standart restriction endonucleases (NEB) in a total volume of either 20 µl 1x FastDigest® reactionbuffer or 20 µl 1x NEB reactionbuffer 1-4, respectively for 0.5 – 2 h at 37 °C. If dephosphorylation of a digested plasmid was

desired, 1 – 2 µl antarctic phosphatase (NEB) were added to the reaction which was further supplemented with 5 µl 10 x antarctic phosphates buffer and adjusted with daH_2O to a final reaction volume of 50 µl and incubated for 0.5 - 1 h at 37 °C. After digestion and/or dephosphorylation the reaction was purified using the QIAquick PCR Purification Kit according to the supplier's instructions (QIAquick® Spin Handbook, 03/2008).
DNA fragments were ligated by incubation with 1 µl T4-DNA ligase in a total volume of 20 µl of 1 x T4-DNA ligase buffer over night at 16 °C. Generally 5 – 15 fmol insert DNA were ligated together with 2 – 5 fmol linerarized plasmid DNA. After the ligation, 2 - 5 µl of the reaction were used directly for transformation in electro competent *E. coli* cells.

4.3.5 DNA gel electrophoresis

Gel electrophoresis of DNA was performed using 0.8 – 1.5 % (w/v) TAE agarose gels with 1 µg ml^{-1} ethidium bromide [237]. The DNA samples were mixed with 6x Loading Dye and the gels were run for ~30 min at 150 V. A *BstEII* digested λ phage DNA (Thermo Scientific) was used as a standard for fragment size. For DNA visualization, gels were exposed to a UV-transilluminator at a wavelength of 365 nm and documented with a video printer device.

4.3.6 Sequencing of DNA

PCR amplified DNA fragments or plasmid DNA was sequenced by MWG Operon (Ebersberg) and digital raw data was analyzed by VectorNTI™ contic express (Invitrogen).

4.3.7 Construction of Plasmids

For the construction of *M. xanthus* mutagenesis plasmids (**Table 5**), overlapping fragments matching ~ 500 bp up- and downstream of the nucleotides that should be mutated or the region that should be deleted were amplified from genomic DNA using the respective A,B or C,D oligonucleotide, listed in **(Table 6)**. After purification of the fragments, a second PCR was performed using 40 ng of both fragments as template and the respective A,D primer combination to fuse the fragments to a ~1 kb DNA double strand with the base substitution/deletion in the center. This DNA was cloned into the multiple cloning sites of the plasmid pBJ114. For the construction of over production plasmids (**Table 7**), the gene

or domain to be overproduced was amplified using gene/domain specific oligonucleotides (**Table 6**). The resulting fragments were subsequently cloned in the multiple cloning site of the desired overproduction plasmid, and confirmed to be error free by sequencing using plasmid specific primer. The detailed description for the generation of the published plasmids/mutant strains can be obtained from the original publications.

Table 6 Oligonucleotide

PLASMID	NAME	DESCRIPTION[a]	SEQUENCE (5'-3')[b]
pAS037	oPH561	*espC*$_{H461Q}$ A	cggaattcgtcaccgggctgctgctg
	oPH645	*espC*$_{H461Q}$ B	ttc**ctg**cccacaccggccgcgagc
	oPH646	*espC*$_{H461Q}$ C	ggg**cag**gaaatcaacaacccgctgg
	oPH539	*espC*$_{H461Q}$ D	gcggatccacttggtggtgtagaagg
	oPH647	*espC*$_{H461Q}$ E$_{mut}$	agcgggttgttgatttc**ctg**
	oPH547	*espC*$_{H461Q}$ E$_{wt}$	cgggttgttgatttc**gtg**
	oPH549	*espC*$_{H461Q}$ F	ttcgccacggatgacctg
pAS038	oPH1035	*espC*$_{REC}$ A	gcgaattcgtcgtcgtgggcggctcg
	oPH1036	*espC*$_{REC}$ B	ggatgcctgcacccgcccgccgaccc
	oPH1037	*espC*$_{REC}$ C	gggcgggtgcaggcatccacgccgc
	oPH 803	*espC*$_{REC}$ D	gcggatccgccgcacgccgcca
pAS039	oPH1040	*espC*$_{\Delta REC}$ A	cggaattcggtttcgacaaggggctggag
	oPH1041	*espC*$_{\Delta REC}$ B	ctccttggtcagttggagctggccgatg
	oPH1042	*espC*$_{\Delta REC}$ C	ctccaactgaccaaggagctccaggccc
	oPH1043	*espC*$_{\Delta REC}$ D	cgggatccgcgcacctcgttcatggatg
pAS024	oPH345	*espC*$_{HK-REC}$ for	gacgaattcgcggtggggacgctcgcg
	oPH348	*espC*$_{HK-REC}$ rev	gacctcgagcactgccgtcagggccgc
pPH155	oPH160	*espA*$_{-ss}$ for	cggaattctgcctcatcctcatcagcacc
	oPH163	*espA*$_{-ss}$ rev	cggaattctcatcgccccgcctcggcggagc
pPH158	oPH485	*mrpC* for	catggatcccacggtttcaaccgccccctc
	oPH486	*mrpC* rev	ggctcgagctacttctccttgccggcgatc
(pBJ114)	oPH553	M13 for	ttcgctattacgccagctgg
	oPH554	M13 rev	ttagctcactcattaggcacc
(pET24a,28a,32b)	oPH566	T7 for	taatacgactcactataggg
	oPH567	T7 term/rev	gctagttattgctcagcgg

[a] Primers labeled as A, B, C, D, E or F represent the primers used for the overlapping fragment fusion PCR. Primers are otherwise labeled as forward (for) or reverse (rev).

[b] Bolded sequences indicate the mutated codon. Underlined sequences indicate restriction sites used for cloning. Outlined sequences indicate the overlap for the fusion PCR step.

pAS037

The mutagenesis plasmid pAS037 was generated by cloning a homolog fragment reaching from the bp 895-1894 in *espC* of DZ2 genomic DNA, but harboring a one base pair substitution in the codon 461, CAC (his) to CAG (glu). The fragment was cloned in the multiple cloning site of pBJ114 using the EcoRI and BamHI restriction sites. The resulting plasmid was confirmed to be error free by sequencing using the M13for and M13rev primer. After integration into the genome of *M. xanthus*, the transformants were screened by colony PCR. After identification of positive colonies, multiple clones were confirmed to

display the same developmental phenotype. Candidate colonies were additionally confirmed to be error free by sequencing ~ 1000 bp around the generated substitution.

pAS038

The deletion plasmid pAS038 was generated by fusing and cloning the two homolog fragments reaching from bp -500 - 30 and 2044 - 2524 leading to the deletion of the *espC* codons 10 – 681. The fragment was cloned in the multiple cloning site of pBJ1114 using the EcoRI and BamHI restriction sites. The remaining cloning procedure was performed as per pAS0037.

pAS039

The deletion plasmid pAS039 was generated by fusing and cloning the two homolog fragments reaching from bp 476 - 951 and 1315 - 1779 leading to the deletion of the *espC* codons 317 – 438. The fragment was cloned in the multiple cloning site of pBJ1114 using the EcoRI and BamHI restriction sites. The remaining cloning procedure was performed as per pAS0037.

pAS024

The overproduction plasmid pAS024 ($EspC_{HK\text{-}REC}$-His_6) encodes the HK and REC of EspC with a C-terminal His_6 affinity tag and was constructed by PCR amplifying *espC* (MXAN_6855) codons 451-819 from DZ2 genomic DNA. The resulting fragment was cloned into the EcoRI and XhoI sites of pET24a+. The construct was sequenced to confirm absence of PCR generated errors using T7term and T7for primer.

pPH155

The overproduction plasmid pPH155 (Trx-His_6-$EspA_{-SS}$-His_6) encodes for *espA* lacking the first 38 amino acids. The construct has a Trx- and a His_6 affinity tag at the N-terminus and a His_6 affinity tag at the C-terminus and was constructed by amplifying the *espA* (MXAN_0931) codons 39-769 from DZ2 genomic DNA. The resulting fragment was cloned into the EcoRI site of pET32B+. The construct was sequenced to confirm absence of PCR generated errors using T7term and T7for primer.

pPH158

The overproduction plasmid pPH158 (His_6-MrpC) encodes for *mrpC* from codon 2 to codon 249 with a N-terminal His_6 affinity tag. It was constructed by subcloning from pPH153 which contains the *mrpC* codons 2 – 249 in the multiple cloning site of pZERO-2. The *mrpC* codon were excised from the BamHI and XhoI restriction sites of pPH153 and subsequently ligated into the same restriction sites of pET28a+.

4.4 Biochemical methodes

4.4.1 SDS-PAGE

To analyze proteins under denaturing conditions, discontinuative sodium dodecyl sulphate polyacrylamide gel electrophoresis (SDS-PAGE) was performed [238]. The resolving gel of the SDS-PAG was composed of X % Rotipphorese® NR-Acrylamide/Bisacrylamide (29:1) solution, 0.35 mM ammoniumperoxodisulfat (APS) and 0.06 % (v/v) N,N,N,N-Tetramethylethylenediamine (TEMED) in 1x resolving buffer. The desired concentration of acrylamide/bisacrylamide (X) was adjusted depending on the protein size to be analyzed and is stated in the relevant sections. The stacking gel of the SDS-PAG was composed of 5 % Rotiphorese® NR-Acrylamide/Bisacrylamide (29:1) solution, 0.44 mM APS and 0.076 % (v/v) TEMED in 1x stacking buffer. The electrophoresis was performed using the BioRad electrophoresis chambers and a Tris-Glycin-SDS buffer at a constant voltage of 100 - 150 V until the dye front reached the bottom of the resolving gel. To determine the molecular mass of the resolved proteins PageRuler™ Prestained Protein Ladder (Thermo Scientific) was used as a molecular mass standard. After the electrophoresis the SDS-PAG was stained with coomassie stain or an immunoblot to a PVDF membrane was performed.

4.4.2 Immunoblot analysis

For immunoblot analysis, samples containing 5 - 20 µg of protein were resolved by denaturing SDS-PAGE in 8 % (anti-EspA and -EspC immunoblots), 12 % (anti-MrpC, -PilC, -EFTU and FibA immunoblots) PAGs. Proteins were transferred to PVDF membrane at 100mA per minigel using a semi-dry transfer apparatus (PeqLab). Briefly, two pieces of thin Whatman® paper were soaked in anode buffer I and placed on the anode of the blotter, one Whatman® paper soaked in anode buffer II was placed above these two sheets. A

PVDF membrane activated in methanol and washed in daH_2O was placed on top of these three Whatman® paper and the SDS-PAG was positioned on the PVDF membrane. Three Whatman® papers soaked in cathode buffer were placed on the gel and the semi dry apparatus was closed and connected to the power supply. After 75 min of the transfer, the PVDF membrane was dried, rehydrated by incubation in 100 % methanol followed by incubation in daH_2O. Then, the membrane was blocked in 5 % (w/v) dry-milk in 1 x PBS for either 30 min at RT or over night at 4 °C. After blocking, primary antibodies were incubated for 2 h at RT. The antibodies were diluted in blocking solution as follows: Anti-EspC (this study) at 1:200, anti-EspA [239] at 1:1 000, anti-MrpC [240] at 1:2 000, anti-PilC [167] at 1:10 000, anti-EFTU (Hycolt® Biotech, Netherlands) at 1:8 000 and anti-FibA [241] at 1:2 000. After the primary antibody incubation the membrane was washed three times for 5 min with blocking solution, then secondary antibody was added and incubated for 1 – 2 h at RT. Secondary antibodies goat α-rabbit or α-mouse IgG conjugated to horseradish peroxidase (HRP) (Thermo Scientific) were used at a dilution of 1:20 000 and signals were detected with enhanced chemiluminescence substrate (Thermo Scientific) followed by exposure to autoradiography film (Thermo scientific) or detection by the LAS-4000 luminescent image analyzer (GE Healthcare).

Protein sample preparation

Protein lysates for immunoblot analyses were prepared from developmental cells grown in 16 ml submerged culture format. At the indicated time points, the MMC buffer was removed, and the cells were resuspended in 1 ml ice cold MMC buffer, incubated with an equivalent volume of 26 % ice cold trichloroacetic acid for 15 min on ice, pelleted at 17 000 xG for 5 min at 4 °C (Biofuge), and washed twice with acetone. The pellet was resuspended in 100 µl of 100 mM Tris buffer (pH 7.6), diluted with 300 µl cLSB and heated for 1 min at 94 °C. The protein concentration of each sample was determined using a BCA™ Protein Assay Kit (Thermo Scientific). Then, samples were further diluted in 2 x LSB to 2 µg μl^{-1}, and stored at -20 °C.

Delipidification of proteins samples

To deplete contaminating lipids from the protein samples of the *M. xanthus* developmental cell cultures, the samples were delipidified using a mixture of acetone and methanol in the ratio 8:1 [242]. For this purpose the cells which were harvested from 16 ml submerged cultures were resuspended in 500 µl of MMC buffer supplemented with 5 % (v/v) of Sigma

Mammalian Protease Inhibitor Cocktail and disrupted by a FastPrep® 24 cell and tissue homogenizer for 5-7 times at 6.5 M/s for 45 seconds at 4 °C together with 700 mg of 0.1 mm zirconia beads (Roth). After the disintegration the cell lysate was recovered without disturbing the beads. The beads were washed with 300 µl of MMC buffer/PI and the supernatant from the washing step was added to the cell lysate. The cell lysate was then mixed with 1 ml of the solvent solution and incubated for 90 min at 4°C. After the incubation the proteins where precipitated by centrifugation (Biofuge) at 2 800 xG for 15 min at 4 °C. The pellet was subsequently flushed, first with acetone and then methanol, followed by air drying in the fume hood. The proteins were resolved in 100 µl cLSB by incubation at 37 °C for 15 min.

Determination of the concentration of protein samples

To determine the concentration of protein samples the BCA™ Protein Assay Kit (Thermo Scientific) was used as recommended by the supplier, exept that only 50 µl of the analyte and 950 µl of the 'developing solution' was used. If glycerol was part of the protein solution, the samples were diluted 1:20 in daH_2O to prevent interference of glycerol with the BCA™ Assay Kit.

4.4.3 Generation and affinity purification of anti-EspC rabbit polyclonal antisera

Antigen production for immunization

For antigen production, $EspC_{\Delta MASE1}$-His_6 (*espC* codons 311-833) was overproduced as inclusion body (IB) protein from 800 ml BL21(λDE3) cultures using pAS002 induced with 1 mM IPTG at an optical density of approx. 0.7 A_{550}. After incubation at 37 °C for 2 h in an orbital shaker, the cells were pelleted at 4 600 xG at 4 °C for 30 min (Multifuge 1 S-R), resuspended in 32 ml lysis buffer H, and lysed by passageing through a French Press (SLM-AMINCO/Spectronic) three times at approximately 18 000 psi. The IBs were pelleted at 600 xG at 4 °C for 30 min (Multifuge 1 S-R), resuspended in 32 ml ice cold lysis buffer H supplemented with 1 % (v/v) Triton X-100. The solution then was incubated for 15 min at RT, and the IBs were harvested as described above. The IB pellet was resuspended in 1x cLSB, heated for 5 min at 94 °C and the protein concentration was determined using a BCA™ Protein Assay Kit (Thermo Scientific). 500 µg of sample was resolved on a 10 % preparative SDS-PAG, and the relevant band was excised from gels stained with 0.1 % Coomassie dye in water. Polyclonal rabbit anti-$EspC_{\Delta MAES1}$ antibodies were generated against the emulsified gel slices by Eurogentec (Serain, Belgium).

Affinity purification of antibodies

To immobilize antigen for antisera purification, 1 mg of recombinant $EspC_{\Delta MASE1}$-His_6 was resolved using a 1.5 mm thick SDS-PAG, blotted to PVDF membrane, and stained with Ponceaus S. The region of the membrane containing the antigen was excised, washed in acidic glycine buffer for 5 min, washed in TBS-T buffer two times for 2 min, and then blocked with TBS-T buffer supplemented with 3 % BSA (Pentax fraction V) for 1 h at RT. The membrane was then rinsed twice with TBS-T, incubated with 10 ml of a 1:5 dilution of anti-EspC serum for 3 h at 4 °C, washed twice in TBS-T for 5 min and twice in PBS for 5 min. To elute the bound antibody, the membrane was incubated twice with 1 ml of acidic glycine buffer for 10 min at RT, and the eluates were combined and was neutralized with 25 – 50 µl of a 1 M Tris buffer (pH 8.0).

4.4.4 Overproduction and purification of recombinant proteins

The plasmids that encode for the recombinant proteins described below are listed in **Table 7**. The overproduction of $EspC_{\Delta MASE1}$-His_6 is described in section 4.4.3.

Table 7 Strains and plasmids for cloning and protein overproduction

STRAIN/PLASMID	GENOTYPE	SOURCE
***E. coli* strains**		
Top10	F⁻ *endA1 recA1 galE15 galK16 nupG rpsL* Δ*lacX74* Φ80*lacZ*ΔM15 *araD139* Δ(ara, leu)7697 *mcrA* Δ(*mrr-hsdRMS-mcrBC*) λ⁻	Life Technologies
BL21λDE3	F⁻ *ompT gal dcm lon hsdS$_B$*(r_B^- m_B^-) λ(DE3 [*lacI lacUV5*-T7 gene 1 *ind1 sam7 nin5*])	Novagen
overexpression plasmids		
pET24a+	T7-Promoter, His_6-Tag (C-terminal), *kan*	Novagen
pET28a+	T7-Promoter, His_6-Tag (N- and C-terminal), *kan*	Novagen
pET32b+	T7-Promoter, His_6-Tag, Trx-Tag (N-terminal), His_6-Tag (C-terminal), *bla*	Novagen
pAS002	pET24a+ *espC*$_{\Delta MASE1}$ (aa 311-833)	Schramm *et al.* 2012
pBS122	pET24a+ *espC*$_{REC}$ (aa 690-819)	Schramm *et al.* 2012
pAS019	pET24a+ *espC*$_{REC\ D749A}$ (aa 690-819)	Schramm *et al.* 2012
pBS121	pET24a+ *espC*$_{HK}$ (aa 451-679)	Schramm *et al.* 2012
pAS021	pET24a+ *espC*$_{HK\ H461A}$ (aa 451-679)	Schramm *et al.* 2012
pAS022	pET24a+ *espA*$_{HK}$ (aa 390-646)	Schramm *et al.* 2012
pAS023	pET24a+ *espA*$_{HK\ H407A}$ (aa 390-646)	Schramm *et al.* 2012
pAS024	pET24a+ *espC*$_{HK\text{-}REC}$ (aa 451-819)	This study
pPH155	pET32b+ *espA*$_{-SS}$ (aa 39-769)	P. Higgs (unpublished)
pPH158	pET28a+ *mrpC* (aa 2-249)	P. Higgs (unpublished)

$EspA_{HK}$-His_6, $EspA_{HK\ H407A}$-His_6, $EspC_{HK}$-His_6, $EspC_{HK\ H461A}$-His_6 or $EspC_{HK\text{-}REC}$-His_6 were each produced as inclusion bodies (IBs) from 1 L *E. coli* BL21(λDE3) cultures. Protein over production was induced with 0.5 mM IPTG at an optical density of ~ 0.7 A_{550} for 3 h at 37 °C, from the over production plasmids pBS121, pAS012, pAS022, pAS023 and pAS024. To isolate IBs, the respective cell cultures were harvested by centrifugation (4 600 xG, 4 °C, Multifuge 1 S-R), resuspended in 25 ml TND buffer and lysed by passageing through a French Press (SLM-AMINCO/Spectronic) three times at approximately 18 000 psi. IBs were collected by centrifugation at 4 600 xG, 4 °C for 30 min (Multifuge 1 S-R), resuspended in 25 ml TND buffer, and treated by French Press as above. To remove contaminating proteins, IBs were pelleted as described above and resuspended in 20 ml TND buffer supplemented with 1 M Guanidine HCl (GuHCl), and the solution was incubated for 2 h at RT with gentle rotation. Purified IBs were pelleted as above, washed in TND buffer, and then solubelized in 15 ml TND buffer supplemented with 6 M GuHCl by vortexing. The protein solution then was clarified by centrifugation at 100 000 xG, for 30 min at RT (L 90 K, T 865). The solution was diluted with TND buffer to achieve a final GuHCl concentration of 2 M and a protein concentration of approximately 0.1 mM which was determined by the absorbance at 280 nm (A_{280})[$\varepsilon_{280}(EspA_{HK}\text{-}His_6)$ = 1 490; $\varepsilon_{280}(EspC_{HK}\text{-}His_6)$ = 2 980]. For refolding of the proteins, the solution was dialyzed in TGND buffer for 2 h at 4 °C two times, followed by dialysis in fresh buffer over night. The resulting protein preparation was clarified by centrifugation at 17 000 xG, 4 °C for 5 min (Biofuge) and concentrated using a 10 molecular weight cut off Amicon Ultra column (Millipore). The refolded proteins were stored at -20 °C for further assays.

$EspC_{REC}$-His_6 and $EspC_{REC\ D749A}$-His_6 were overproduced as soluble proteins from 0.5 L of an *E. coli* strain BL21(λDE3) culture by induction with 1 mM IPTG at an optical density of ~ 0.7 A_{550} for 2 h at 37 °C, from pBS122 and pAS019, respectively. For purification of the recombinant proteins, the cell cultures were harvested by centrifugation (4 600 xG, 4 °C, Multifuge 1 S-R), resuspended in binding buffer and lysed by French Press as described above. The lysate was clarified by centrifugation at 100 000 xG, 4 °C for 1 hour (L 90 K, T 865), and the supernatant was subjected to purification by nickel affinity chromatography at 4 °C (ÄKTApurifier, GE Healthcare) using a 1 ml His trap FF1 nickel affinity column (GE Healthcare). The proteins were eluted using a 30 ml linear gradient of 20-500 mM imidazole in elution buffer. A portion of each eluted fraction was analyzed by SDS-PAGE,

elution fractions containing the peak levels of purified protein were pooled, dialyzed and stored as described above.

Trx-His_6-$EspA_{-ss}$-His_6 and His_6-MrpC were overproduced as soluble proteins in the *E. coli* strain BL21(λDE3) by induction with 0.5 mM IPTG at an optical density of ~ 0.7 A_{550} for 2 h at 37 °C, from pPH155 and pPH158, respectively. For purification of the recombinant proteins, the cell cultures were harvested by centrifugation (4 600 xG, 4 °C, Multifuge 1 S-R), resuspended in IMAC lysis buffer (BioRad), supplemented with 10 mM EDTA and 1 mg ml^{-1} lysozyme and lysed by French Press as described above. After the lysis, 100mM $MgSO_4$ and 20 U ml^{-1} benzonase® (Merck) were added to the lysate and incubated for 30 min on ice. Subsequently, the recombinant protein was purified using the Profinia™ protein purification systm (Bio-Rad) as recommended by the supplier. Purity was examined using SDS-PAGE and the eluted protein was dialyzed and stored as described above.

4.4.5 Protein fractionation

For protein fractionation, cells from the DZ2 and Δ*espC* strains were grown in developmental 16 ml submerged culture format. At the indicated time points, the MMC buffer was removed, and the cells were resuspended in 1 ml ice cold lysis buffer T, harvested and the plates were flushed again with 1 ml lysis buffer T and the fractions were combined. The cell suspension then was sonicated (output 3, 30 % duty 3 times 20 sec, Branson Sonifier 250) and centrifuged at 6 900 xG for 8 min at 4 °C (Biofuge). The supernatant was removed and a 300 µl sample was kept for further analysis (whole cell, wc). The remaining supernatant was centrifuged at 60 000 xG for 50 min at 4 °C (Optima Max XP, MLA 130). Afterwards the supernatant was removed (soluble protein, sol) and the pellet was carefully resuspended in 1 ml lysis buffer T (membrane proteins, mem). The proteins from all fractions (wc, sol, mem) were precipitated by addition of an equivalent volume of ice cold 23 % TCA and prepared as described previously (section 4.4.2). 10 µl of the samples were analyzed by immunoblot analysis with the antibodies MrpC, PilC, EspA and EspC.

4.4.6 Determination of the EspA and EspC protein production ration

To determine the relative rations of EspA and EspC in developmental cells, standards of recombinant Trx-His_6-$EspA_{-ss}$-His_6 and $EspC_{\Delta MASE1}$-His_6 were used to compare the

signals from immunoblot analysis of developmental cell lysates. For this porpose, the protein concentration of both recombinant proteins was determined using the BCA™ Protein Assay Kit (Thermo Scientific) as described before. A series of dilutions of both proteins was resolved in a 8 % SDS-PAG and subsequently probed by an EspA or an EspC immunoblot. The series of dilution reached from 0.5 – 5 ng per lane for EspA and 0.1 – 0.6 ng per lane for EspC. The signal intensities were quantified using ImageJ 1.43U [243] and plotted versus the calculated number of EspA and EspC molecules. The number of molecules was determined as follows:

- 1 Da = $1.66 \cdot 10e^{-24}$ g
- 1 mol = $6 \cdot 10e^{23}$ molecules
- MW(Trx-His_6-$EspA_{-ss}$-His_6) = 98 kDa
- MW($EspC_{\Delta MASE1}$-His_6) = 59 kDa

From the resulting plots, the slope of the intensity vs. the molecules of EspA (III) and EspC (IV) was determined using Microsoft Excel™.

To determine the ratio of EspA and EspC from developmental cell lysates, a protein sample from 24 h developing wild type cells was produced as described before. The protein concentration of the sample was determined via the BCA™ Protein Assay Kit (Thermo Scientific) and 5, 10 and 15 µg lysate were resolved in a 8 % SDS-PAG and subsequently probed by an EspA or an EspC immunoblot. The signal intensities were quantified using ImageJ 1.43U [243] and the molar concentrations (fmol μl^{-1}) of EspA and EspC were determined by using the equations (III) or (IV), respectively.

4.4.7 Radiolabeled *in vitro* autophosphorylation and phosphotransfer assays

In vitro autophosphorylation of 10 µM HK recombinant protein or 7 µM HK-REC recombinant protein was carried out in TGND buffer supplemented with 5 mM $MgCl_2$, 50 mM KCl. To initiate autophosphorylation, 0.5 mM ATP and 1.7 µM [γ^{32}P]-ATP (222 TBq $mmol^{-1}$; Hartmann Analytic, Braunschweig) were added and autophosphorylation was examined at intervals between 0 and 60 min. At each time point, 10 µl sample was withdrawn, quenched with 2 x LSB, and resolved using SDS-PAGE. Importantly, the samples were not heated prior loading and 15 % polyacrylamide gels were used to resolve radiolabeled proteins. The gels were exposed to a Storage Phosphor Screen (GE Healthcare) over night and analyzed using a Storm™ 800 imaging system (GE Healthcare). [^{32}P]-labeled HK signal intensities from three independent experiments were quantified by ImageJ 1.43U [243]; the average intensity and associated standard deviation was calculated using Microsoft Excel™.

Phosphotransfer reactions were performed by first autophosphorylating 15 µM of either $EspA_{HK}$-His_6 or $EspC_{HK}$-His_6 (or respective point mutants) for 60 min. 6.5 µl of the HK~P were then added to 3.5 µl of either phosphorylation buffer, 28 µM $EspC_{REC}$-His_6 or $EspC_{REC\ D749A}$-His_6, leading to an equivalent 10 µM final concentration for each reaction partner. The reactions were quenched after two or five min and analyzed as above, except 20 % polyacrylamide gels were used.

4.4.8 MrpC turnover assays

In vivo MrpC turnover

The *in vitro* turnover experiments were carried out with wild type (DZ2) or Δ*espA*Δ*espC* mutant (PH1047) strains, developed in 16 ml submerged culture format for 9 h and treated with 34 µg ml^{-1} chloramphenicol to block *de novo* protein synthesis [244]. At 0, 10, 20 or 30 min after addition of chloramphenicol, the cells were quickly harvested by scraping the cells from the petri dish, pelleted at 4 600 xG, 4 °C for 2 min (Multifuge 1 S-R), immediately resuspended in 400 µl hot (70 °C) LSB, heated for 5 min at 99 °C and stored at -20 °C for further analyses. 15 µl of protein samples were analyzed by immunoblot as described above. Band intensities from triplicate experiments were quantified with ImageJ 1.43U [243]. The MrpC half-life in wild type cells was calculated assuming a first order kinetic degradation reaction [245-247]. Briefly, each background-subtracted band intensity value was first normalized to the intensity at T=0 and the natural log of the resulting values was plotted versus time using Microsoft Excel™. The slope (k) of a linear fit of each graph

(equation V, VI, VII) was used to calculate the t½ using the equation t½ = ln(2)/-k [246]. The average and the associated standard deviation were calculated from the three individual half lives.

Protease inhibitor screen

For the protease inhibitor screens, protease inhibitors were used in the following concentrations: 2 % Sigma mammalian protease inhibitor cocktail (SMPI), 5 mM EDTA, 1 mM PMSF, 1.5 µM aprotinine, 5 mM benzamidine, 10 µM E-64. The *in vivo* protease inhibitor screen, was performed as the *in vivo* MrpC turnover experiments, except that the inhibitors were added shortly prior to the addition of chloramphenicol and samples were withdrawn at 0 min and 30 min after addition of chloramphenicol. The signal intensities of three independent biological replicates were quantified using ImageJ 1.43U [243] and the background subtracted intensities were normalized against the signal intensity of wt cells treated with chloramphenicol for 0 min.

Lysate production for *in vitro* and *in gel* turnover experiments

Lysates for protease activity assays were prepared from wild type (DZ2) or Δ*espA*Δ*espC* mutant (PH1047) strains, developed in 16 ml submerged culture. After 12 h of development, the MMC buffer was removed, the cells were resuspended in 2 ml ice cold 100 mM MOPS buffer at pH 7.6, sonicated (output 3, 30 % duty 3 times 20 sec, Branson Sonifier 250) and centrifuged at 6 900 xG for 8 min at 4 °C (Biofuge). The supernatant was removed, glycerol was added to a final concentration of 10 % (v/v) and the protein concentration was determined using the BCA™ Protein Assay Kit (Thermo Scientific) as described before. The cell lysates were stored at -20 °C until further analysis.

***In vitro* MrpC turnover**

In vitro turnover assays were performed using 2 µg His_6-MrpC and 5 µg of wild type (DZ2) lysate in a total volume of 20 µl 50 mM HEPES buffer at pH 7.6. The reactions were incubated at 32 °C, quenched at the desired time point by the addition of 20 µl LSB and

boiled for 5 min at 99 °C. 20 µl of the protein samples were resolved in a 12 % SDS-PAG and subsequently stained with Coomassie stain. Protease inhibitors were used at the same concentrations as for the *in vivo* protease inhibitor screen, and were pre-incubated with the wild type lysates for 5 min on ice prior to the addition of the recombinant His_6-MrpC. If necessary, ATP was likewise added to a final concentration of 10 mM.

In gel MrpC turnover

For the *in gel* MrpC turnover analysis, zymogram SDS-PAGs (Z-PAG) were prepared, containing 150 µg ml^{-1} recombinant His_6-MrpC which was co-polymerized in the resolving gel of a standard 11 % SDS-PAG. Per reaction, 7.5 µg wild type DZ2 lysate were pre-incubated in a total volume of 10 µl ZSB per reaction at 25 °C for 15 min. As multiple reactions were analysed, this step was carried out with a master mix. 10 µl of the reaction was loaded to each well of the Z-PAG and electrophoresis was performed with a voltage of 100 V at 4 °C using pre-cooled tris-glycin-SDS buffer as running buffer. After the run, the Z-PAG was incubated for 10 min at RT in zymo refolding buffer. Subsequently, the Z-PAG was cut at each well-boundary and the Z-PAG slices were incubated in a total volume of 5 ml zymo activity buffer for 22 h at 32 °C. Prior to this incubation, protease inhibitors were added to the zymo activity buffer. The protease inhibitors were used in the same concentrations as described before. After the incubation, the gel strips were stained with Coommasie staining solution and subsequently destained. The co-polymerized His_6-MrpC resulted in a blue background stain of the entire Z-PAG. Due to migration of the co-polymerized His_6-MrpC, the gel was stained darker at the bottom of the Z-PAG. In regions were proteases were active, His_6-MrpC was degraded, resulting in decreased background staining (cleared zones).

4.5 Bioinformatic analyses

4.5.1 Homolog identification

Homologs to EspA in the *M. xanthus* genome were identified using a BLASTp [164] analysis with EspA as query sequence. All results with a bitscore higher than the bitscore of EspC were used for the further analysis. Othologs for EspA, EspC and the other three identified homolog HyHPK within the publically available Myxococcales genomic sequences, were identified using reciprocal BLASTp [164] analysis as described by

Huntley *et al* [248]. Briefly, the protein sequence of either EspA or EspC was used as query in a BLASTp analysis against the public available protein database from *Stigmatella aurantiaca* DW4/3-1 (accession number CP002271) [248], *Myxococcus fulvus* HW-1 (accession CP002830) [249], *Corallococcus coralloides* DSM2259 (accession CP003389) [250], *Anaeromyxobacter dehalogenans* 2CP-C (accession CP000251.1) [251], *Haliangium ochraceum* SMP-2 (accession CP001804.1) [252], *Sorangium cellulosum* So ce 56 (accession AM746676) [253], and *Plesiocystis pacifica* SIR-1 (accession ABCS00000000). The protein with the best hit (highest bitscore) was then used as a query in a second BlastP analysis against the protein database from *Myxococcus xanthus* DK1622 (accession CP000113) [254]. If the highest scoring match was identical to the protein sequence originally used for the first BlastP analysis, the two proteins were considered orthologs [255, 256]. Additionally, the sequences were also analyzed in the unpublished genomes *M. macrospores* and *M. stipitatus*, provided by Stuart Huntley, using the Artemis Comparison Tool (Wellcome Trust Sanger Institute).

4.5.2 SDR analysis

In silico analysis of the putative SDR in EspA and EspC, were performed by ClustalX multiple sequence alignments [170] of the DHp and REC domains of EspA, EspC, their orthologs in *Stigmatella aurantiaca* (Sa_EspA: STIAU_9475 and Sa_EspC: STIAU _0700, respectively) and *Corallococcus coralloides* (Cc_EspA: COCOR_00882 and Cc_EspC; COCOR_07432, respectively), the *M. xanthus* control group sequences and the *E. coli* EnvZ/OmpR His-Asp signaling pair for which SDR residues have already been mapped [12, 120, 121]. The control group sequences were identified by a BLASTp [164] analysis using either the $EspA_{HK}$ or the $EspA_{REC}$ as query against the *M. xanthus* protein database. Hits with a bitscore higher than the bitscore of the respective domains in EspC were collected and used for the analysis. The DHp and REC of each protein was identified by SMART [48, 49], and aligned using the standart parameter of the ClustalX program. Later the alignments were manually trimmed to the same length. A substitution in the putative SDR region was considered conservative if it had a score in the PAM250 matrix greater than one [171] and were shaded green. For the homology modeling of the putative $EspA_{HK}$-$EspC_{REC}$ complex, the $EspA_{HK}$ region and the $EspC_{REC}$ domain were aligned on the *T. maritima* $(HK853CP)_2$-$(RR468)_2$ crystal structure complex (PDB: 3dge; [23]) using PyMol

(Schrödinger). The putative specificity determining regions were located in analogy to Capra *et al.* [121] and are highlighted as spheres.

REFERENCES

1 Galperin, M.Y., *et al.* (2010) Interplay of heritage and habitat in the distribution of bacterial signal transduction systems. *Mol Biosyst* 6, 721-728

2 Stock, A.M., *et al.* (2000) Two-component signal transduction. *Annu Rev Biochem* 69, 183-215

3 Galperin, M.Y. (2005) A census of membrane-bound and intracellular signal transduction proteins in bacteria: bacterial IQ, extroverts and introverts. *BMC Microbiol* 5, 35

4 Wuichet, K., *et al.* (2010) Evolution and phyletic distribution of two-component signal transduction systems. *Curr Opin Microbiol* 13, 219-225

5 Alm, E., *et al.* (2006) The evolution of two-component systems in bacteria reveals different strategies for niche adaptation. *PLoS Comput Biol* 2, e143

6 Appleby, J.L., *et al.* (1996) Signal transduction via the multi-step phosphorelay: not necessarily a road less traveled. *Cell* 86, 845-848

7 Park, H., *et al.* (1998) Two-domain reconstitution of a functional protein histidine kinase. *Proc Natl Acad Sci U S A* 95, 6728-6732

8 Stock, A., *et al.* (1985) Homologies between the *Salmonella typhimurium* CheY protein and proteins involved in the regulation of chemotaxis, membrane protein synthesis, and sporulation. *Proc Natl Acad Sci U S A* 82, 7989-7993

9 Tanaka, T., *et al.* (1998) NMR structure of the histidine kinase domain of the *E. coli* osmosensor EnvZ. *Nature* 396, 88-92

10 Tomomori, C., *et al.* (1999) Solution structure of the homodimeric core domain of *Escherichia coli* histidine kinase EnvZ. *Nat Struct Biol* 6, 729-734

11 Laub, M.T. and Goulian, M. (2007) Specificity in two-component signal transduction pathways. *Annu Rev Genet* 41, 121-145

12 Zapf, J., *et al.* (2000) A transient interaction between two phosphorelay proteins trapped in a crystal lattice reveals the mechanism of molecular recognition and phosphotransfer in signal transduction. *Structure* 8, 851-862

13 Ninfa, A.J. and Magasanik, B. (1986) Covalent modification of the glnG product, NRI, by the glnL product, NRII, regulates the transcription of the glnALG operon in *Escherichia coli*. *Proc Natl Acad Sci U S A* 83, 5909-5913

14 Weiss, V., *et al.* (2002) Mechanism of regulation of the bifunctional histidine kinase NtrB in *Escherichia coli*. *J Mol Microbiol Biotechnol* 4, 229-233

15 Hidaka, Y., *et al.* (1997) Demonstration of dimer formation of the cytoplasmic domain of a transmembrane osmosensor protein, EnvZ, of *Escherichia coli* using Ni-histidine tag affinity chromatography. *FEBS Lett* 400, 238-242

16 Marina, A., *et al.* (2005) Structure of the entire cytoplasmic portion of a sensor histidine-kinase protein. *EMBO J* 24, 4247-4259

17 Goodman, A.L., *et al.* (2009) Direct interaction between sensor kinase proteins mediates acute and chronic disease phenotypes in a bacterial pathogen. *Genes Dev* 23, 249-259

18 Gao, Z., *et al.* (2008) Heteromeric interactions among ethylene receptors mediate signaling in *Arabidopsis*. *J Biol Chem* 283, 23801-23810

19 Grefen, C., *et al.* (2008) Subcellular localization and in vivo interactions of the *Arabidopsis thaliana* ethylene receptor family members. *Mol Plant* 1, 308-320

20 Roberts, D.L., *et al.* (1994) Identification of the site of phosphorylation on the osmosensor, EnvZ, of *Escherichia coli*. *J Biol Chem* 269, 8728-8733

21 Wu, J., *et al.* (1999) A novel bacterial tyrosine kinase essential for cell division and differentiation. *Proc Natl Acad Sci U S A* 96, 13068-13073

22 Wolfe, A.J. and Stewart, R.C. (1993) The short form of the CheA protein restores kinase activity and chemotactic ability to kinase-deficient mutants. *Proc Natl Acad Sci U S A* 90, 1518-1522

23 Casino, P., *et al.* (2009) Structural Insight into Partner Specificity and Phosphoryl Transfer in Two-Component Signal Transduction. *Cell* 139, 325-336

24 Bilwes, A.M., *et al.* (1999) Structure of CheA, a signal-transducing histidine kinase. *Cell* 96, 131-141

25 Dutta, R. and Inouye, M. (2000) GHKL, an emergent ATPase/kinase superfamily. *Trends Biochem Sci* 25, 24-28

26 Polosina, Y.Y. and Cupples, C.G. (2010) Wot the 'L-Does MutL do? *Mutat Res* 705, 228-238

27 Krukenberg, K.A., *et al.* (2011) Conformational dynamics of the molecular chaperone Hsp90. *Q Rev Biophys* 44, 229-255

28 Huang, W.M. (1996) Bacterial diversity based on type II DNA topoisomerase genes. *Annu Rev Genet* 30, 79-107

29 Mushegian, A.R., *et al.* (1997) Positionally cloned human disease genes: patterns of evolutionary conservation and functional motifs. *Proc Natl Acad Sci U S A* 94, 5831-5836

30 Grebe, T.W. and Stock, J.B. (1999) The histidine protein kinase superfamily. *Adv Microb Physiol* 41, 139-227

31 Dago, A.E., *et al.* (2012) Structural basis of histidine kinase autophosphorylation deduced by integrating genomics, molecular dynamics, and mutagenesis. *Proc Natl Acad Sci U S A* 109, E1733-1742

32 Bick, M.J., *et al.* (2009) How to switch off a histidine kinase: crystal structure of *Geobacillus stearothermophilus* KinB with the inhibitor Sda. *J Mol Biol* 386, 163-177

33 Szurmant, H., *et al.* (2007) Sensor complexes regulating two-component signal transduction. *Curr Opin Struct Biol* 17, 706-715

34 Casino, P., *et al.* (2010) The mechanism of signal transduction by two-component systems. *Current Opinion in Structural Biology* 20, 763-771

35 Stock, A.M., *et al.* (1989) Three-dimensional structure of CheY, the response regulator of bacterial chemotaxis. *Nature* 337, 745-749

36 Hess, J.F., *et al.* (1988) Phosphorylation of three proteins in the signaling pathway of bacterial chemotaxis. *Cell* 53, 79-87

37 Hess, J.F., *et al.* (1987) Protein phosphorylation is involved in bacterial chemotaxis. *Proc Natl Acad Sci U S A* 84, 7609-7613

38 Oosawa, K., *et al.* (1988) Mutants defective in bacterial chemotaxis show modified protein phosphorylation. *Cell* 53, 89-96

39 Lukat, G.S., *et al.* (1992) Phosphorylation of bacterial response regulator proteins by low molecular weight phospho-donors. *Proc Natl Acad Sci U S A* 89, 718-722

40 Lee, S.Y., *et al.* (2001) Crystal structure of an activated response regulator bound to its target. *Nat Struct Biol* 8, 52-56

41 Gao, R. and Stock, A.M. (2010) Molecular strategies for phosphorylation-mediated regulation of response regulator activity. *Curr Opin Microbiol* 13, 160-167

42 Makino, K., *et al.* (1989) Signal transduction in the phosphate regulon of *Escherichia coli* involves phosphotransfer between PhoR and PhoB proteins. *J Mol Biol* 210, 551-559

43 Aiba, H., *et al.* (1989) Transfer of phosphoryl group between two regulatory proteins involved in osmoregulatory expression of the *ompF* and *ompC* genes in *Escherichia coli*. *J Biol Chem* 264, 8563-8567

44 Welch, M., *et al.* (1993) Phosphorylation-dependent binding of a signal molecule to the flagellar switch of bacteria. *Proc Natl Acad Sci U S A* 90, 8787-8791

45 Blat, Y. and Eisenbach, M. (1994) Phosphorylation-dependent binding of the chemotaxis signal molecule CheY to its phosphatase, CheZ. *Biochemistry* 33, 902-906

46 Fiedler, U. and Weiss, V. (1995) A common switch in activation of the response regulators NtrC and PhoB: phosphorylation induces dimerization of the receiver modules. *EMBO J* 14, 3696-3705

47 McCleary, W.R. (1996) The activation of PhoB by acetylphosphate. *Mol Microbiol* 20, 1155-1163

48 Letunic, I., *et al.* (2012) SMART 7: recent updates to the protein domain annotation resource. *Nucleic Acids Res* 40, D302-305

49 Schultz, J., *et al.* (1998) SMART, a simple modular architecture research tool: identification of signaling domains. *Proc Natl Acad Sci U S A* 95, 5857-5864

50 Galperin, M.Y. (2010) Diversity of structure and function of response regulator output domains. *Curr Opin Microbiol* 13, 150-159

51 Mascher, T., *et al.* (2006) Stimulus perception in bacterial signal-transducing histidine kinases. *Microbiol Mol Biol Rev* 70, 910-938

52 Ulrich, L.E. and Zhulin, I.B. (2010) The MiST2 database: a comprehensive genomics resource on microbial signal transduction. *Nucleic Acids Res* 38, D401-407

53 Henry, J.T. and Crosson, S. (2011) Ligand-binding PAS domains in a genomic, cellular, and structural context. *Annu Rev Microbiol* 65, 261-286

54 Clarke, D.J. (2010) The Rcs phosphorelay: more than just a two-component pathway. *Future Microbiol* 5, 1173-1184

55 Nikolskaya, A.N., *et al.* (2003) MASE1 and MASE2: two novel integral membrane sensory domains. *J Mol Microbiol Biotechnol* 5, 11-16

56 Punta, M., *et al.* (2012) The Pfam protein families database. *Nucleic Acids Res* 40, D290-301

57 Galperin, M.Y. (2004) Bacterial signal transduction network in a genomic perspective. *Environ Microbiol* 6, 552-567

58 Verhamme, D.T., *et al.* (2001) Glucose-6-phosphate-dependent phosphoryl flow through the Uhp two-component regulatory system. *Microbiology* 147, 3345-3352

59 Hofmann, K. and Bucher, P. (1995) The FHA domain: a putative nuclear signalling domain found in protein kinases and transcription factors. *Trends Biochem Sci* 20, 347-349

60 Li, J., *et al.* (1999) Kinase interaction domain of kinase-associated protein phosphatase, a phosphoprotein-binding domain. *Proc Natl Acad Sci U S A* 96, 7821-7826

61 Ding, Z., *et al.* (2007) Phosphoprotein and phosphopeptide interactions with the FHA domain from *Arabidopsis* kinase-associated protein phosphatase. *Biochemistry* 46, 2684-2696

62 Chevalier, D., *et al.* (2009) 14-3-3 and FHA domains mediate phosphoprotein interactions. *Annu Rev Plant Biol* 60, 67-91

63 Liao, H., *et al.* (1999) Structure and function of a new phosphopeptide-binding domain containing the FHA2 of Rad53. *J Mol Biol* 294, 1041-1049

64 Lee, G.I., *et al.* (2003) NMR structure of the forkhead-associated domain from the *Arabidopsis* receptor kinase-associated protein phosphatase. *Proc Natl Acad Sci U S A* 100, 11261-11266

65 Hoffman, E.C., *et al.* (1991) Cloning of a factor required for activity of the Ah (dioxin) receptor. *Science* 252, 954-958

66 Nambu, J.R., *et al.* (1991) The *Drosophila* single-minded gene encodes a helix-loop-helix protein that acts as a master regulator of CNS midline development. *Cell* 67, 1157-1167

67 Finn, R.D., *et al.* (2006) Pfam: clans, web tools and services. *Nucleic Acids Res* 34, D247-251

68 Moglich, A., *et al.* (2009) Structure and signaling mechanism of Per-ARNT-Sim domains. *Structure* 17, 1282-1294

69 Huang, Z.J., *et al.* (1993) PAS is a dimerization domain common to *Drosophila* period and several transcription factors. *Nature* 364, 259-262

70 Taylor, B.L. and Zhulin, I.B. (1999) PAS domains: internal sensors of oxygen, redox potential, and light. *Microbiol Mol Biol Rev* 63, 479-506

71 Pongratz, I., *et al.* (1998) Role of the PAS domain in regulation of dimerization and DNA binding specificity of the dioxin receptor. *Mol Cell Biol* 18, 4079-4088

72 Lee, J., *et al.* (2008) Changes at the KinA PAS-A dimerization interface influence histidine kinase function. *Biochemistry* 47, 4051-4064

73 Eswaramoorthy, P., *et al.* (2010) The threshold level of the sensor histidine kinase KinA governs entry into sporulation in *Bacillus subtilis*. *J Bacteriol* 192, 3870-3882

74 Eswaramoorthy, P., *et al.* (2009) *In vivo* domain-based functional analysis of the major sporulation sensor kinase, KinA, in *Bacillus subtilis*. *J Bacteriol* 191, 5358-5368

75 Strickland, D., *et al.* (2008) Light-activated DNA binding in a designed allosteric protein. *Proc Natl Acad Sci U S A* 105, 10709-10714

76 Gutu, A.D., *et al.* (2010) Kinetic characterization of the WalRKSpn (VicRK) two-component system of *Streptococcus pneumoniae*: dependence of WalKSpn (VicK) phosphatase activity on its PAS domain. *J Bacteriol* 192, 2346-2358

77 Galperin, M.Y. (2006) Structural classification of bacterial response regulators: diversity of output domains and domain combinations. *J Bacteriol* 188, 4169-4182

78 Jenal, U. and Galperin, M.Y. (2009) Single domain response regulators: molecular switches with emerging roles in cell organization and dynamics. *Curr Opin Microbiol* 12, 152-160

79 Hoch, J.A. and Varughese, K.I. (2001) Keeping signals straight in phosphorelay signal transduction. *J Bacteriol* 183, 4941-4949

80 Varughese, K.I. (2005) Conformational changes of Spo0F along the phosphotransfer pathway. *J Bacteriol* 187, 8221-8227

81 Sarkar, M.K., *et al.* (2010) Chemotaxis signaling protein CheY binds to the rotor protein FliN to control the direction of flagellar rotation in *Escherichia coli*. *Proc Natl Acad Sci U S A* 107, 9370-9375

82 Paul, R., *et al.* (2008) Allosteric regulation of histidine kinases by their cognate response regulator determines cell fate. *Cell* 133, 452-461

83 Burbulys, D., *et al.* (1991) Initiation of sporulation in *B. subtilis* is controlled by a multicomponent phosphorelay. *Cell* 64, 545-552

84 Jiang, M., *et al.* (2000) Multiple histidine kinases regulate entry into stationary phase and sporulation in *Bacillus subtilis*. *Mol Microbiol* 38, 535-542

85 Zhou, H., *et al.* (1995) NMR studies of the phosphotransfer domain of the histidine kinase CheA from *Escherichia coli*: assignments, secondary structure, general fold, and backbone dynamics. *Biochemistry* 34, 13858-13870

86 Kato, M., *et al.* (1997) Insights into multistep phosphorelay from the crystal structure of the C-terminal HPt domain of ArcB. *Cell* 88, 717-723

87 Varughese, K.I., *et al.* (1998) Formation of a novel four-helix bundle and molecular recognition sites by dimerization of a response regulator phosphotransferase. *Mol Cell* 2, 485-493

88 Rodrigue, A., *et al.* (2000) Two-component systems in *Pseudomonas aeruginosa*: why so many? *Trends Microbiol* 8, 498-504

89 Zhang, W. and Shi, L. (2005) Distribution and evolution of multiple-step phosphorelay in prokaryotes: lateral domain recruitment involved in the formation of hybrid-type histidine kinases. *Microbiology* 151, 2159-2173

90 Tsuzuki, M., *et al.* (1995) Phosphotransfer circuitry of the putative multi-signal transducer, ArcB, of *Escherichia coli*: in vitro studies with mutants. *Mol Microbiol* 18, 953-962

91 Goulian, M. (2010) Two-component signaling circuit structure and properties. *Curr Opin Microbiol* 13, 184-189

92 Qian, W., *et al.* (2008) Two-component signal transduction systems of *Xanthomonas* spp.: a lesson from genomics. *Mol Plant Microbe Interact* 21, 151-161

93 Iuchi, S., *et al.* (1989) A second global regulator gene (*arcB*) mediating repression of enzymes in aerobic pathways of *Escherichia coli*. *J Bacteriol* 171, 868-873

94 Iuchi, S. and Lin, E.C. (1988) *arcA* (*dye*), a global regulatory gene in *Escherichia coli* mediating repression of enzymes in aerobic pathways. *Proc Natl Acad Sci U S A* 85, 1888-1892

95 Salmon, K.A., *et al.* (2005) Global gene expression profiling in *Escherichia coli* K12: effects of oxygen availability and ArcA. *J Biol Chem* 280, 15084-15096

96 Georgellis, D., *et al.* (1997) In vitro phosphorylation study of the arc two-component signal transduction system of *Escherichia coli*. *J Bacteriol* 179, 5429-5435

97 Iuchi, S. and Lin, E.C. (1992) Mutational analysis of signal transduction by ArcB, a membrane sensor protein responsible for anaerobic repression of operons involved in the central aerobic pathways in *Escherichia coli*. *J Bacteriol* 174, 3972-3980

98 Ng, W.L. and Bassler, B.L. (2009) Bacterial quorum-sensing network architectures. *Annu Rev Genet* 43, 197-222

99 Inclan, Y.F., *et al.* (2008) The receiver domain of FrzE, a CheA-CheY fusion protein, regulates the CheA histidine kinase activity and downstream signalling to the A- and S-motility systems of *Myxococcus xanthus*. *Mol Microbiol* 68, 1328-1339

100 Inclan, Y.F., *et al.* (2007) FrzZ, a dual CheY-like response regulator, functions as an output for the Frz chemosensory pathway of *Myxococcus xanthus*. *Mol Microbiol* 65, 90-102

101 Bueno, R., *et al.* (1985) Role of Glnb and Glnd Gene-Products in Regulation of the Glnalg Operon of *Escherichia-Coli*. *Journal of Bacteriology* 164, 816-822

102 Wanner, B.L. (1996) Signal transduction in the control of phosphate-regulated genes of *Escherichia coli*. *Kidney Int* 49, 964-967

103 Zhu, Y., *et al.* (2000) Phosphatase activity of histidine kinase EnvZ without kinase catalytic domain. *Proc Natl Acad Sci U S A* 97, 7808-7813

104 Jagadeesan, S., *et al.* (2009) A Novel "Four-component" Two-component Signal Transduction Mechanism Regulates Developmental Progression in *Myxococcus xanthus*. *Journal of Biological Chemistry* 284, 21435-21445

105 Jiang, P., *et al.* (2000) Functional dissection of the dimerization and enzymatic activities of *Escherichia coli* nitrogen regulator II and their regulation by the PII protein. *Biochemistry* 39, 13433-13449

106 Fleischer, R., *et al.* (2007) Purification, reconstitution, and characterization of the CpxRAP envelope stress system of *Escherichia coli*. *J Biol Chem* 282, 8583-8593

107 Haldimann, A., *et al.* (1997) Transcriptional regulation of the *Enterococcus faecium* BM4147 vancomycin resistance gene cluster by the VanS-VanR two-component regulatory system in *Escherichia coli* K-12. *J Bacteriol* 179, 5903-5913

108 Hsing, W. and Silhavy, T.J. (1997) Function of conserved histidine-243 in phosphatase activity of EnvZ, the sensor for porin osmoregulation in *Escherichia coli*. *J Bacteriol* 179, 3729-3735

109 Dutta, R., *et al.* (2000) The critical role of the conserved Thr247 residue in the functioning of the osmosensor EnvZ, a histidine Kinase/Phosphatase, in *Escherichia coli*. *J Biol Chem* 275, 38645-38653

110 Chen, Y.E., *et al.* (2009) Dynamics of Two Phosphorelays Controlling Cell Cycle Progression in *Caulobacter crescentus*. *Journal of Bacteriology* 191, 7417-7429

111 Huynh, T.N., *et al.* (2010) Conserved mechanism for sensor phosphatase control of two-component signaling revealed in the nitrate sensor NarX. *Proc Natl Acad Sci U S A* 107, 21140-21145

112 Silversmith, R.E. (2010) Auxiliary phosphatases in two-component signal transduction. *Current Opinion in Microbiology* 13, 177-183

113 Fisher, S.L., *et al.* (1995) Cross-talk between the histidine protein kinase VanS and the response regulator PhoB. Characterization and identification of a VanS domain that inhibits activation of PhoB. *J Biol Chem* 270, 23143-23149

114 Silva, J.C., *et al.* (1998) *In vivo* characterization of the type A and B vancomycin-resistant *enterococci* (VRE) VanRS two-component systems in *Escherichia coli*: a nonpathogenic model for studying the VRE signal transduction pathways. *Proc Natl Acad Sci U S A* 95, 11951-11956

115 Siryaporn, A. and Goulian, M. (2008) Cross-talk suppression between the CpxA-CpxR and EnvZ-OmpR two-component systems in *E. coli*. *Mol Microbiol* 70, 494-506

116 Skerker, J.M., *et al.* (2005) Two-component signal transduction pathways regulating growth and cell cycle progression in a bacterium: a system-level analysis. *PLoS Biol* 3, e334

117 Cai, S.J. and Inouye, M. (2002) EnvZ-OmpR interaction and osmoregulation in *Escherichia coli*. *J Biol Chem* 277, 24155-24161

118 Batchelor, E. and Goulian, M. (2003) Robustness and the cycle of phosphorylation and dephosphorylation in a two-component regulatory system. *Proc Natl Acad Sci U S A* 100, 691-696

119 Ninfa, A.J., *et al.* (1988) Crosstalk between bacterial chemotaxis signal transduction proteins and regulators of transcription of the Ntr regulon: evidence that nitrogen assimilation and chemotaxis are controlled by a common phosphotransfer mechanism. *Proc Natl Acad Sci U S A* 85, 5492-5496

120 Skerker, J.M., *et al.* (2008) Rewiring the specificity of two-component signal transduction systems. *Cell* 133, 1043-1054

121 Capra, E.J., *et al.* (2010) Systematic dissection and trajectory-scanning mutagenesis of the molecular interface that ensures specificity of two-component signaling pathways. *PLoS Genet* 6, e1001220

122 Shi, X., *et al.* (2008) Bioinformatics and experimental analysis of proteins of two-component systems in *Myxococcus xanthus*. *J Bacteriol* 190, 613-624

123 Kroos, L. (2007) The *Bacillus* and *Myxococcus* developmental networks and their transcriptional regulators. *Annu Rev Genet* 41, 13-39

124 Lee, B., *et al.* (2012) *Myxococcus xanthus* developmental cell fate production: heterogeneous accumulation of developmental regulatory proteins and reexamination of the role of MazF in developmental lysis. *J Bacteriol* 194, 3058-3068

125 Nariya, H. and Inouye, M. (2008) MazF, an mRNA interferase, mediates programmed cell death during multicellular *Myxococcus* development. *Cell* 132, 55-66

126 O'Connor, K.A. and Zusman, D.R. (1991) Development in *Myxococcus xanthus* involves differentiation into two cell types, peripheral rods and spores. *J Bacteriol* 173, 3318-3333

127 O'Connor, K.A. and Zusman, D.R. (1991) Analysis of *Myxococcus xanthus* cell types by two-dimensional polyacrylamide gel electrophoresis. *J Bacteriol* 173, 3334-3341

128 O'Connor, K.A. and Zusman, D.R. (1991) Behavior of peripheral rods and their role in the life cycle of *Myxococcus xanthus*. *J Bacteriol* 173, 3342-3355

129 Harris, B.Z., *et al.* (1998) The guanosine nucleotide (p)ppGpp initiates development and A-factor production in *Myxococcus xanthus*. *Genes Dev* 12, 1022-1035

130 Singer, M. and Kaiser, D. (1995) Ectopic production of guanosine penta- and tetraphosphate can initiate early developmental gene expression in *Myxococcus xanthus*. *Genes Dev* 9, 1633-1644

131 Kaiser, D. (2004) Signaling in myxobacteria. *Annu Rev Microbiol* 58, 75-98

132 Kuspa, A., *et al.* (1992) Identification of heat-stable A-factor from *Myxococcus xanthus*. *J Bacteriol* 174, 3319-3326

133 Kuspa, A., *et al.* (1992) A-signalling and the cell density requirement for *Myxococcus xanthus* development. *J Bacteriol* 174, 7360-7369

134 Cho, K. and Zusman, D.R. (1999) AsgD, a new two-component regulator required for A-signalling and nutrient sensing during early development of *Myxococcus xanthus*. *Mol Microbiol* 34, 268-281

135 Garza, A.G., *et al.* (2000) The asgE locus is required for cell-cell signalling during *Myxococcus xanthus* development. *Mol Microbiol* 35, 812-824

136 Garza, A.G., *et al.* (2000) Control of asgE expression during growth and development of *Myxococcus xanthus*. *J Bacteriol* 182, 6622-6629

137 Kuspa, A. and Kaiser, D. (1989) Genes required for developmental signalling in *Myxococcus xanthus*: three *asg* loci. *J Bacteriol* 171, 2762-2772

138 Plamann, L., *et al.* (1995) The *Myxococcus xanthus asgA* gene encodes a novel signal transduction protein required for multicellular development. *J Bacteriol* 177, 2014-2020

139 Plamann, L., *et al.* (1994) Evidence that *asgB* encodes a DNA-binding protein essential for growth and development of *Myxococcus xanthus*. *J Bacteriol* 176, 2013-2020

140 Konovalova, A., *et al.* (2012) Two intercellular signals required for fruiting body formation in *Myxococcus xanthus* act sequentially but non-hierarchically. *Mol Microbiol* 86, 65-81

141 Sun, H. and Shi, W. (2001) Genetic studies of mrp, a locus essential for cellular aggregation and sporulation of *Myxococcus xanthus*. *J Bacteriol* 183, 4786-4795

142 Nariya, H. and Inouye, S. (2005) Identification of a protein Ser/Thr kinase cascade that regulates essential transcriptional activators in *Myxococcus xanthus* development. *Mol Microbiol* 58, 367-379

143 Nariya, H. and Inouye, S. (2006) A protein Ser/Thr kinase cascade negatively regulates the DNA-binding activity of MrpC, a smaller form of which may be necessary for the *Myxococcus xanthus* development. *Mol Microbiol* 60, 1205-1217

144 Ueki, T. and Inouye, S. (2003) Identification of an activator protein required for the induction of *fruA*, a gene essential for fruiting body development in *Myxococcus xanthus*. *Proc Natl Acad Sci U S A* 100, 8782-8787

145 Ellehauge, E., *et al.* (1998) The FruA signal transduction protein provides a checkpoint for the temporal co-ordination of intercellular signals in *Myxococcus xanthus* development. *Mol Microbiol* 30, 807-817

146 Ogawa, M., *et al.* (1996) FruA, a putative transcription factor essential for the development of *Myxococcus xanthus*. *Mol Microbiol* 22, 757-767

147 Kruse, T., *et al.* (2001) C-signal: a cell surface-associated morphogen that induces and co-ordinates multicellular fruiting body morphogenesis and sporulation in *Myxococcus xanthus*. *Mol Microbiol* 40, 156-168

148 Lobedanz, S. and Sogaard-Andersen, L. (2003) Identification of the C-signal, a contact-dependent morphogen coordinating multiple developmental responses in *Myxococcus xanthus*. *Genes Dev* 17, 2151-2161

149 Rolbetzki, A., *et al.* (2008) Regulated secretion of a protease activates intercellular signaling during fruiting body formation in *M. xanthus*. *Dev Cell* 15, 627-634

150 Sogaard-Andersen, L. and Kaiser, D. (1996) C factor, a cell-surface-associated intercellular signaling protein, stimulates the cytoplasmic Frz signal transduction system in *Myxococcus xanthus*. *Proc Natl Acad Sci U S A* 93, 2675-2679

151 Shi, W., *et al.* (1996) Cell density regulates cellular reversal frequency in *Myxococcus xanthus*. *Proc Natl Acad Sci U S A* 93, 4142-4146

152 Mittal, S. and Kroos, L. (2009) Combinatorial regulation by a novel arrangement of FruA and MrpC2 transcription factors during *Myxococcus xanthus* development. *J Bacteriol* 191, 2753-2763

153 Mittal, S. and Kroos, L. (2009) A combination of unusual transcription factors binds cooperatively to control *Myxococcus xanthus* developmental gene expression. *Proc Natl Acad Sci U S A* 106, 1965-1970

154 Viswanathan, P., *et al.* (2007) Combinatorial regulation of genes essential for *Myxococcus xanthus* development involves a response regulator and a LysR-type regulator. *Proc Natl Acad Sci U S A* 104, 7969-7974

155 Thony-Meyer, L. and Kaiser, D. (1993) devRS, an autoregulated and essential genetic locus for fruiting body development in *Myxococcus xanthus*. *J Bacteriol* 175, 7450-7462

156 Boysen, A., *et al.* (2002) The DevT protein stimulates synthesis of FruA, a signal transduction protein required for fruiting body morphogenesis in *Myxococcus xanthus*. *J Bacteriol* 184, 1540-1546

157 Cho, K. and Zusman, D.R. (1999) Sporulation timing in *Myxococcus xanthus* is controlled by the espAB locus. *Mol Microbiol* 34, 714-725

158 Higgs, P.I., *et al.* (2008) EspA, an orphan hybrid histidine protein kinase, regulates the timing of expression of key developmental proteins of *Myxococcus xanthus*. *J Bacteriol* 190, 4416-4426

159 Lee, B., *et al.* (2005) EspC is involved in controlling the timing of development in *Myxococcus xanthus*. *J Bacteriol* 187, 5029-5031

160 Schramm, A., *et al.* (2012) Intra- and Interprotein Phosphorylation between Two-hybrid Histidine Kinases Controls *Myxococcus xanthus* Developmental Progression. *J Biol Chem* 287, 25060-25072

161 Rasmussen, A.A. and Sogaard-Andersen, L. (2003) TodK, a putative histidine protein kinase, regulates timing of fruiting body morphogenesis in *Myxococcus xanthus*. *J Bacteriol* 185, 5452-5464

162 Higgs, P.I., *et al.* (2005) Four unusual two-component signal transduction homologs, RedC to RedF, are necessary for timely development in *Myxococcus xanthus*. *J Bacteriol* 187, 8191-8195

163 Stein, E.A., *et al.* (2006) Two Ser/Thr protein kinases essential for efficient aggregation and spore morphogenesis in *Myxococcus xanthus*. *Mol Microbiol* 60, 1414-1431

164 Altschul, S.F., *et al.* (1997) Gapped BLAST and PSI-BLAST: a new generation of protein database search programs. *Nucleic Acids Res* 25, 3389-3402

165 Yu, C.S., *et al.* (2006) Prediction of protein subcellular localization. *Proteins* 64, 643-651

166 Yu, C.S., *et al.* (2004) Predicting subcellular localization of proteins for Gram-negative bacteria by support vector machines based on n-peptide compositions. *Protein Sci* 13, 1402-1406

167 Bulyha, I., *et al.* (2009) Regulation of the type IV pili molecular machine by dynamic localization of two motor proteins. *Mol Microbiol* 74, 691-706

168 Willett, J.W. and Kirby, J.R. (2011) CrdS and CrdA comprise a two-component system that is cooperatively regulated by the Che3 chemosensory system in *Myxococcus xanthus*. *MBio* 2

169 Albanesi, D., *et al.* (2009) Structural plasticity and catalysis regulation of a thermosensor histidine kinase. *Proc Natl Acad Sci U S A* 106, 16185-16190

170 Larkin, M.A., *et al.* (2007) Clustal W and Clustal X version 2.0. *Bioinformatics* 23, 2947-2948

171 Gonnet, G.H., *et al.* (1992) Exhaustive matching of the entire protein sequence database. *Science* 256, 1443-1445

172 Pazy, Y., *et al.* (2010) Identical phosphatase mechanisms achieved through distinct modes of binding phosphoprotein substrate. *Proc Natl Acad Sci U S A* 107, 1924-1929

173 Lee, B., *et al.* (2011) The *Myxococcus xanthus* spore cuticula protein C is a fragment of FibA, an extracellular metalloprotease produced exclusively in aggregated cells. *PLoS One* 6, e28968

174 Avery, L. and Wasserman, S. (1992) Ordering gene function: the interpretation of epistasis in regulatory hierarchies. *Trends Genet* 8, 312-316

175 Kinoshita, E., *et al.* (2009) Separation and detection of large phosphoproteins using Phos-tag SDS-PAGE. *Nat Protoc* 4, 1513-1521

176 Romagnoli, S. and Tabita, F.R. (2006) A novel three-protein two-component system provides a regulatory twist on an established circuit to modulate expression of the *cbbI* region of *Rhodopseudomonas palustris* CGA010. *J Bacteriol* 188, 2780-2791

177 Romagnoli, S. and Tabita, F.R. (2007) Phosphotransfer reactions of the CbbRRS three-protein two- component system from *Rhodopseudomonas palustris* CGA010 appear to be controlled by an internal molecular switch on the sensor kinase. *J Bacteriol* 189, 325-335

178 Petters, T., *et al.* (2012) The orphan histidine protein kinase SgmT is a c-di-GMP receptor and regulates composition of the extracellular matrix together with the orphan DNA binding response regulator DigR in *Myxococcus xanthus*. *Mol Microbiol* 84, 147-165

179 Capra, E.J. and Laub, M.T. (2012) Evolution of Two-Component Signal Transduction Systems. *Annu Rev Microbiol*

180 Groban, E.S., *et al.* (2009) Kinetic buffering of cross talk between bacterial two-component sensors. *J Mol Biol* 390, 380-393

181 Alves, R. and Savageau, M.A. (2003) Comparative analysis of prototype two-component systems with either bifunctional or monofunctional sensors: differences in molecular structure and physiological function. *Molecular Microbiology* 48, 25-51

182 Raivio, T.L. and Silhavy, T.J. (1997) Transduction of envelope stress in *Escherichia coli* by the Cpx two-component system. *J Bacteriol* 179, 7724-7733

183 Dahl, M.K., *et al.* (1992) The phosphorylation state of the DegU response regulator acts as a molecular switch allowing either degradative enzyme synthesis or expression of genetic competence in *Bacillus subtilis*. *J Biol Chem* 267, 14509-14514

184 Igo, M.M., *et al.* (1989) Phosphorylation and dephosphorylation of a bacterial transcriptional activator by a transmembrane receptor. *Genes Dev* 3, 1725-1734

185 Walker, M.S. and DeMoss, J.A. (1993) Phosphorylation and dephosphorylation catalyzed in vitro by purified components of the nitrate sensing system, NarX and NarL. *J Biol Chem* 268, 8391-8393

186 Carmany, D.O., *et al.* (2003) Genetic and biochemical studies of phosphatase activity of PhoR. *J Bacteriol* 185, 1112-1115

187 Thomas, S.A., *et al.* (2008) Two variable active site residues modulate response regulator phosphoryl group stability. *Mol Microbiol* 69, 453-465

188 Laub, M.T., *et al.* (2007) Phosphotransfer profiling: systematic mapping of two-component signal transduction pathways and phosphorelays. *Methods Enzymol* 423, 531-548

189 Nakano, M.M. and Zhu, Y. (2001) Involvement of ResE phosphatase activity in down-regulation of ResD-controlled genes in *Bacillus subtilis* during aerobic growth. *J Bacteriol* 183, 1938-1944

190 Baruah, A., *et al.* (2004) Mutational analysis of the signal-sensing domain of ResE histidine kinase from *Bacillus subtilis*. *J Bacteriol* 186, 1694-1704

191 Yamada, S., *et al.* (2009) Structure of PAS-linked histidine kinase and the response regulator complex. *Structure* 17, 1333-1344

192 Iniesta, A.A., *et al.* (2006) A phospho-signaling pathway controls the localization and activity of a protease complex critical for bacterial cell cycle progression. *Proc Natl Acad Sci U S A* 103, 10935-10940

193 Francez-Charlot, A., *et al.* (2009) Sigma factor mimicry involved in regulation of general stress response. *Proc Natl Acad Sci U S A* 106, 3467-3472

194 Catlett, N.L., *et al.* (2003) Whole-genome analysis of two-component signal transduction genes in fungal pathogens. *Eukaryot Cell* 2, 1151-1161

195 Simon, G., *et al.* (1994) The *torR* gene of *Escherichia coli* encodes a response regulator protein involved in the expression of the trimethylamine N-oxide reductase genes. *J Bacteriol* 176, 5601-5606

196 Suzuki, K., *et al.* (2002) Regulatory circuitry of the CsrA/CsrB and BarA/UvrY systems of *Escherichia coli*. *J Bacteriol* 184, 5130-5140

197 Eguchi, Y., *et al.* (2003) Transcriptional regulation of drug efflux genes by EvgAS, a two-component system in *Escherichia coli*. *Microbiology* 149, 2819-2828

198 Ferrieres, L. and Clarke, D.J. (2003) The RcsC sensor kinase is required for normal biofilm formation in *Escherichia coli* K-12 and controls the expression of a regulon in response to growth on a solid surface. *Mol Microbiol* 50, 1665-1682

199 Hagiwara, D., *et al.* (2003) Genome-wide analyses revealing a signaling network of the RcsC-YojN-RcsB phosphorelay system in *Escherichia coli*. *J Bacteriol* 185, 5735-5746

200 Teplitski, M., *et al.* (2003) Pathways leading from BarA/SirA to motility and virulence gene expression in *Salmonella*. *J Bacteriol* 185, 7257-7265

201 Domian, I.J., *et al.* (1997) Cell type-specific phosphorylation and proteolysis of a transcriptional regulator controls the G1-to-S transition in a bacterial cell cycle. *Cell* 90, 415-424

202 Biondi, E.G., *et al.* (2006) Regulation of the bacterial cell cycle by an integrated genetic circuit. *Nature* 444, 899-904

203 Schweder, T., *et al.* (1996) Regulation of *Escherichia coli* starvation sigma factor (sigma s) by ClpXP protease. *J Bacteriol* 178, 470-476

204 Muffler, A., *et al.* (1996) The response regulator RssB controls stability of the sigma(S) subunit of RNA polymerase in *Escherichia coli*. *EMBO J* 15, 1333-1339

205 Zhou, Y., *et al.* (2001) The RssB response regulator directly targets sigma(S) for degradation by ClpXP. *Genes Dev* 15, 627-637

206 Klauck, E., *et al.* (2001) Role of the response regulator RssB in sigma recognition and initiation of sigma proteolysis in *Escherichia coli*. *Mol Microbiol* 40, 1381-1390

207 Studemann, A., *et al.* (2003) Sequential recognition of two distinct sites in sigma(S) by the proteolytic targeting factor RssB and ClpX. *EMBO J* 22, 4111-4120

208 Moreno, M., *et al.* (2000) Regulation of sigma S degradation in *Salmonella enterica* var typhimurium: in vivo interactions between sigma S, the response regulator MviA(RssB) and ClpX. *J Mol Microbiol Biotechnol* 2, 245-254

209 McEvoy, M.M., *et al.* (1999) Identification of the binding interfaces on CheY for two of its targets, the phosphatase CheZ and the flagellar switch protein fliM. *J Mol Biol* 289, 1423-1433

210 Bren, A. and Eisenbach, M. (1998) The N terminus of the flagellar switch protein, FliM, is the binding domain for the chemotactic response regulator, CheY. *J Mol Biol* 278, 507-514

211 Tojo, N., *et al.* (1993) The *lonD* gene is homologous to the *lon* gene encoding an ATP-dependent protease and is essential for the development of *Myxococcus xanthus*. *J Bacteriol* 175, 4545-4549

212 Tojo, N., *et al.* (1993) Cloning and nucleotide sequence of the *Myxococcus xanthus* lon gene: indispensability of *lon* for vegetative growth. *J Bacteriol* 175, 2271-2277

213 Amerik, A., *et al.* (1991) Site-directed mutagenesis of La protease. A catalytically active serine residue. *FEBS Lett* 287, 211-214

214 Menon, A.S. and Goldberg, A.L. (1987) Binding of nucleotides to the ATP-dependent protease La from *Escherichia coli*. *J Biol Chem* 262, 14921-14928

215 Swamy, K.H. and Goldberg, A.L. (1981) *E. coli* contains eight soluble proteolytic activities, one being ATP dependent. *Nature* 292, 652-654

216 Harcum, S.W. and Bentley, W.E. (1993) Detection, Quantification, and Characterization of Proteases in Recombinant *Escherichia coli*. *Biotechnology Techniques* 7, 441-447

217 Yadav, S.C., *et al.* (2011) Identification and characterization of cysteine proteinases of *Trypanosoma evansi*. *Parasitol Res* 109, 559-565

218 Sudha, V.T., *et al.* (2008) Identification of a serine protease as a major allergen (Per a 10) of *Periplaneta americana*. *Allergy* 63, 768-776

219 Peterson, R., *et al.* (2009) Fungal proteins with mannanase activity identified directly from a Congo Red stained zymogram by mass spectrometry. *J Microbiol Methods* 79, 374-377

220 Rawlings, N.D. (2010) Peptidase inhibitors in the MEROPS database. *Biochimie* 92, 1463-1483

221 Shapiro, J.A. (1998) Thinking about bacterial populations as multicellular organisms. *Annu Rev Microbiol* 52, 81-104

222 Kearns, D.B. and Losick, R. (2005) Cell population heterogeneity during growth of *Bacillus subtilis*. *Genes Dev* 19, 3083-3094

223 Lopez, D. and Kolter, R. (2010) Extracellular signals that define distinct and coexisting cell fates in *Bacillus subtilis*. *FEMS Microbiol Rev* 34, 134-149

224 Garcia Vescovi, E., *et al.* (2010) Two component systems in the spatial program of bacteria. *Curr Opin Microbiol* 13, 210-218

225 Wireman, J.W. and Dworkin, M. (1977) Developmentally induced autolysis during fruiting body formation by *Myxococcus xanthus*. *J Bacteriol* 129, 798-802

226 Sun, H. and Shi, W. (2001) Analyses of *mrp* genes during *Myxococcus xanthus* development. *J Bacteriol* 183, 6733-6739

227 Rasmussen, A.A., *et al.* (2006) Four signalling domains in the hybrid histidine protein kinase RodK of *Myxococcus xanthus* are required for activity. *Mol Microbiol* 60, 525-534

228 Wegener-Feldbrugge, S. and Sogaard-Andersen, L. (2009) The atypical hybrid histidine protein kinase RodK in *Myxococcus xanthus:* spatial proximity supersedes kinetic preference in phosphotransfer reactions. *J Bacteriol* 191, 1765-1776

229 Campos, J.M. and Zusman, D.R. (1975) Regulation of development in *Myxococcus xanthus*: effect of 3':5'-cyclic AMP, ADP, and nutrition. *Proc Natl Acad Sci U S A* 72, 518-522

230 Lee, B., *et al.* (2010) Two-component systems and regulation of developmental progression in *Myxococcus xanthus*. *Methods Enzymol* 471, 253-278

231 Ueki, T., *et al.* (1996) Positive-negative KG cassettes for construction of multi-gene deletions using a single drug marker. *Gene* 183, 153-157

232 Bertani, G. (1951) Studies on lysogenesis. I. The mode of phage liberation by lysogenic *Escherichia coli*. *J Bacteriol* 62, 293-300

233 Inoue, H., *et al.* (1990) High efficiency transformation of *Escherichia coli* with plasmids. *Gene* 96, 23-28

234 Chung, C.T., *et al.* (1989) One-step preparation of competent *Escherichia coli*: transformation and storage of bacterial cells in the same solution. *Proc Natl Acad Sci U S A* 86, 2172-2175

235 Birnboim, H.C. and Doly, J. (1979) A rapid alkaline extraction procedure for screening recombinant plasmid DNA. *Nucleic Acids Res* 7, 1513-1523

236 Mullis, K., *et al.* (1986) Specific enzymatic amplification of DNA in vitro: the polymerase chain reaction. *Cold Spring Harb Symp Quant Biol* 51 Pt 1, 263-273

237 Sambrook, J., *et al.* (1989) *Molecular cloning: a laboratory manual*. Cold Spring Harbor Laboratory Press, Cold Spring Harbor, N.Y

238 Laemmli, U.K. (1970) Cleavage of structural proteins during the assembly of the head of bacteriophage T4. *Nature* 227, 680-685

239 Cho, K., *et al.* (2000) Developmental aggregation of *Myxococcus xanthus* requires *frgA*, an *frz*-related gene. *J Bacteriol* 182, 6614-6621

240 Zusman, D.R., *et al.* (2007) Chemosensory pathways, motility and development in *Myxococcus xanthus*. *Nat Rev Microbiol* 5, 862-872

241 Kearns, D.B., *et al.* (2002) An extracellular matrix-associated zinc metalloprotease is required for dilauroyl phosphatidylethanolamine chemotactic excitation in *Myxococcus xanthus*. *J Bacteriol* 184, 1678-1684

242 Mastro, R. and Hall, M. (1999) Protein delipidation and precipitation by tri-n-butylphosphate, acetone, and methanol treatment for isoelectric focusing and two-dimensional gel electrophoresis. *Anal Biochem* 273, 313-315

243 Abramoff, M.D., Magalhaes, P.J., Ram, S.J. (2004) Image Processing with ImageJ. *Biophotonics International* 11, 7

244 Nath, K. and Koch, A.L. (1971) Protein degradation in *Escherichia coli*. II. Strain differences in the degradation of protein and nucleic acid resulting from starvation. *J Biol Chem* 246, 6956-6967

245 Arias, I.M., *et al.* (1969) Studies on the synthesis and degradation of proteins of the endoplasmic reticulum of rat liver. *J Biol Chem* 244, 3303-3315

246 Belle, A., *et al.* (2006) Quantification of protein half-lives in the budding yeast proteome. *Proc Natl Acad Sci U S A* 103, 13004-13009

247 Segal, H.L. and Kim, Y.S. (1963) Glucocorticoid Stimulation of the Biosynthesis of Glutamic-Alanine Transaminase. *Proc Natl Acad Sci U S A* 50, 912-918

248 Huntley, S., *et al.* (2011) Comparative genomic analysis of fruiting body formation in *Myxococcales*. *Mol Biol Evol* 28, 1083-1097

249 Li, Z.F., *et al.* (2011) Genome sequence of the halotolerant marine bacterium *Myxococcus fulvus* HW-1. *J Bacteriol* 193, 5015-5016

250 Huntley, S., *et al.* (2012) Complete genome sequence of the fruiting myxobacterium *Corallococcus coralloides* DSM 2259. *J Bacteriol* 194, 3012-3013

251 Thomas, S.H., *et al.* (2008) The mosaic genome of *Anaeromyxobacter dehalogenans* strain 2CP-C suggests an aerobic common ancestor to the delta-proteobacteria. *PLoS One* 3, e2103

252 Ivanova, N., *et al.* (2010) Complete genome sequence of *Haliangium ochraceum* type strain (SMP-2). *Stand Genomic Sci* 2, 96-106

253 Schneiker, S., *et al.* (2007) Complete genome sequence of the myxobacterium *Sorangium cellulosum*. *Nat Biotechnol* 25, 1281-1289

254 Goldman, B.S., *et al.* (2006) Evolution of sensory complexity recorded in a *myxobacterial* genome. *Proc Natl Acad Sci U S A* 103, 15200-15205

255 Fang, G., *et al.* (2010) Getting started in gene orthology and functional analysis. *PLoS Comput Biol* 6, e1000703

256 Overbeek, R., *et al.* (1999) The use of gene clusters to infer functional coupling. *Proc Natl Acad Sci U S A* 96, 2896-2901

ABBREVIATIONS

aa	amino acid
ATP	adenosintriphosphat
BLASTp	Basic Local Alignment Search Tool (proteins query mode)
CA	histidine kinase like ATPase domain
CELLO	Subcellular Localization Predictor
COCOR	*Corallococcus coralloides* gene annotation
DHp	dimerization and histidine phosphotransfer domain
DNA	deoxyribonucleic acid
FHA	forkhead associated domain
EDTA	ethylenediaminetetraacetic acid
GST	glutathion-S-transferase
His_6	hexa histidine (affinity tag)
HK	histidine kinase region
HGT	horizontal gene transfer
HPK	histidine protein kinase
HPT	histidine containing phosphotransfer protein/domain
HyHPK	hybrid histidine protein kinase
LILAB	*Myxococcus fulvus* gene annotation
LSE	lineage specific expansion
MASE1	membrane associated sensor
MIST2	The Microbial Signal Transduction database
MXAN	*Myxococcus xanthus* gene annotation
PAS	period arnt sim domain
PFAM	Protein Family database
PMSF	phenylmethylsulfonylfluorid
ppGpp	guanosine-3′,5′-bispyrophosphate
REC	receiver domain
RR	response regulator
SDR	specificity determining residues
sdRR	single domain response regulator
SMART	Simple Modular Architecture Research Tool
SMPI	sigma mammalian protease inhibitor cocktail
STAUR	*Stigmatella aurantiaca* gene annotation
Trx	thioredoxin
Y2H	yeast two hybrid

ACKNOWLEDGMENTS

The current page (acknowledgments) contains personal data, thus is not part of the electronic version of the thesis.

Diese Seite (Danksagung) enthält persönliche Daten. Sie ist deshalb nicht Bestandteil der Online-Veröffentlichung.

CURRICULUM VITAE

The current page (CV) contains personal data, thus is not part of the electronic version of the thesis.

Diese Seite (Lebenslauf) enthält persönliche Daten. Sie ist deshalb nicht Bestandteil der Online-Veröffentlichung.